CENTRO DE INVESTIGACIÓN Y DE ESTUDIOS AVANZADOS DEL INSTITUTO POLITÉCNICO NACIONAL

UNIDAD IRAPUATO

Unidad de Genómica Avanzada

“Transcriptómica de la regeneración de extremidad delantera en *Ambystoma mexicanum*”

TESIS

Que presenta

IBT Francisco Javier Falcón Chávez

Para obtener el grado de:

MAESTRO EN CIENCIAS

en la especialidad de Biología Integrativa

Directores de Tesis:

Dr. Luis Alfredo Cruz Ramírez

Dra. Selene Lizbeth Fernández Valverde

Irapuato, Guanajuato **Mayo, 2019**

CENTRO DE INVESTIGACIÓN Y DE ESTUDIOS AVANZADOS DEL INSTITUTO POLITÉCNICO NACIONAL

UNIDAD IRAPUATO

Unidad de Genómica Avanzada

"Transcriptomics of forelimb regeneration in *Ambystoma mexicanum*"

THESIS

Presents

IBT Francisco Javier Falcón Chávez

To obtain the grade of

Master of Sciences in Integrative Biology

Thesis Directors:

Dr. Luis Alfredo Cruz Ramírez

Dr. Selene Lizbeth Fernández Valverde

Irapuato, Guanajuato **May, 2019**

El presente trabajo fue realizado bajo la asesoría del Dr. Luis Alfredo Cruz Ramírez y la Dra. Selene Lizbeth Fernández Valverde en los laboratorios de Complejidad Molecular y del Desarrollo como en el Laboratorio de Genómica Funcional y Evolutiva de ARNs Regulatorios de en la Unidad de Genómica Avanzada de CINVESTAV Unidad Irapuato en Guanajuato, México.

Se agradece al Consejo Nacional de Ciencia y Tecnología, CONACYT por la beca con el número 435864 otorgada durante el periodo de realización del presente trabajo.

AGRADECIMIENTOS

Agradezco, antes que todos a mi Familia, quienes siempre han apoyado mis decisiones y me han ayudado en mis momentos de necesidad. Sin duda alguna, sin mis padres y mi hermano no sería la persona que soy ahora, y por eso les doy las gracias.

Agradezco al Dr. Alfredo Cruz, que desde mi tesis de licenciatura me acogió bajo su tutela y con quien he desempeñado la mayor parte de mi vida como científico. Sin duda alguna, un gran mentor y amigo del cual aprendí cosas que llevaré conmigo siempre.

Agradezco a la Dra. Selene Fernández, de quien recibí apoyo tanto en los momentos buenos como en los momentos difíciles. Sin duda alguna, sin su tutela no cabe duda de que este proyecto no sería posible. Una de las científicas más brillantes que he conocido, y una de las cuales solo puedo aspirar a convertirme.

Agradezco al Dr. Alfredo Herrera y al Dr. Octavio Martínez, quienes fueron parte de mi formación académica, cuyos comentarios y observaciones hicieron este trabajo posible.

Agradezco al Dr. Luis Brieba, al Dr. Cei, y a la Dra. Therese, quienes a pesar de no estar involucrados dentro del proyecto me brindaron su ayuda incondicional con el fin de lograr mi formación académica.

Agradezco a los miembros del Laboratorios de Complejidad Molecular y del Desarrollo, como también del Laboratorio de Genómica Funcional y Evolutiva de ARNs Regulatorios, cuyo apoyo y retroalimentación esta tesis no sería lo que es ahora. Y un agradecimiento especial a Hugo Varela, quien me acogió en su hogar a pesar de que no podía corresponder su gratitud en ese momento, por haberme apoyado cuando lo necesite.

Agradezco a mi generación de Biología Integrativa, de cada uno de ellos me llevo un pedazo. De Marcel me llevo todos aquellos datos y ademanes que tanto nos hacían reír. De Pablo me llevo tantas discusiones que tuvimos y nuestra buena amistad. De Eduardo Castro me llevo sus incesantes bromas y consejos. De Eduardo González me llevo todas las risas y situaciones que vivimos. Por confiarme su amistad durante este periodo, les agradezco infinitamente.

Agradezco a los miembros de clubes de ciencia Román, Diego, Manuel y Gil, porque gracias a ellos decidí perseguir una carrera científica. Y quisiera dar un agradecimiento especial a Gil que sin sus consejos y ayuda no estaría en donde estoy, y que su amistad de hace más de 15 años dure para toda la vida.

Agradezco a Araceli Fernández, que sin su tutela y paciencia probablemente MAZORKA no sería lo que es ahora, y quien nunca se reusó a ayudarnos para poder hacer uso del clúster.

Por último, agradezco al Consejo Nacional de Ciencia y Tecnología (CONACyT) por el apoyo de beca que me otorgaron durante la maestría durante el tiempo que realicé este proyecto.

Table of Contents

Table of Figures

Table of Tables

Glossary

AEC - **A**pical **E**pidermal **C**ap

MMP - **M**atrix **M**etallo**p**rotease

AER - **A**pical **E**ctodermal **R**idge

Dpa - **D**ays **p**ost **a**mputation

ECM - **E**xtra**c**ellular **M**atrix

GO - **G**ene **O**ntology

lncRNA - **l**ong **n**on-**c**oding **RNA**

cpm - **C**ounts **p**er **m**illion

ROS - **R**eactive **O**xygen **S**pecies

BBH - **B**est **B**i-directional **H**its

1 Abstract

Regeneration is the phenomenon in which an organism replaces a lost body part regaining both structure and function. This phenomenon is widely distributed across the tree of life, from unicellular organisms all the way up to vertebrates, nevertheless, the ability to regenerate seems to be limited in most vertebrates such as humans. However, amphibians seem to have their regenerative capabilities unhindered being able to regenerate a wide variety of structures such as limbs, spinal cord and heart. To gain more information about regeneration, we studied limb regeneration through an RNA-seq time course experiment. Using eight different time points, I generated a transcriptome assembly which was annotated identifying protein coding genes and long non-coding RNAs. I also performed a differential expression analysis to find genes that changed throughout the process of regeneration, along with GO term and KEGG term enrichment analyses to find groups of genes associated with a specific function. Altogether, I found genes that had already been described to be involved in regeneration, but also novel elements that have yet to be characterized.

Resumen

Regeneración es un fenómeno en el cual un organismo reemplaza una parte perdida de su cuerpo restaurando tanto estructura como función. Este fenómeno esta ampliamente distribuido en el árbol de la vida, desde organismos unicelulares hasta los vertebrados, sin embargo, la habilidad para regenerar parece ser limitada en la mayoría de los vertebrados como los humanos. No obstante, los anfibios no tienen tantas limitaciones, siendo así capaces de regenerar una gran variedad de estructuras como extremidades, médula espinal y corazón. Para obtener más información acerca de la regeneración, estudiamos la regeneración de extremidad usando un experimento de RNA-seq a lo largo del proceso. Usando ocho diferentes puntos de tiempo, generé un ensamblado de transcriptoma el cual fue anotado identificando tanto genes codificantes de proteínas como RNAs largos no codificantes. Además, hice un análisis de expresión diferencial para encontrar los genes que cambian a lo largo del proceso de regeneración, junto con el análisis de enriquecimiento de términos GO y KEGG que permitirían identificar genes asociados con una función en específico. En conjunto, encontré genes cuyo comportamiento ya había sido descrito en el proceso de regeneración, como también nuevos elementos que todavía necesitan caracterizarse.

2 Introduction

2.1 Definition of Regeneration

Regeneration could be broadly defined as the replacement of a lost part of an organism or an organism itself from a piece of a preceding one (Morgan, 1901). While this definition might be a little vague, it includes most, if not all, the regeneration processes regardless of the organism for which it has been described on. Regeneration is a developmental process widely distributed across the tree of life, being present in unicellular organisms like Stentor, or pluricellular organisms from the kingdoms of fungi, plantae and animalia (Hernández-Oñate & Herrera-Estrella, 2015).

This phenomenon has baffled humanity for several millennia. One of the most ancient references to regeneration dates to almost 3,000 years ago in Hesiod's Theogony, where he speaks of the titan Prometheus. Known for giving mortals the secret of fire that had been safekept by the gods as a punishment, Prometheus was chained to the side of the Caucasus Mountains by Zeus, the leader of the Olympian gods, where Prometheus would have his liver eaten by an eagle, however, his liver would regenerate overnight; thus, providing an endless supply of food for the eagle and torment for Prometheus (Chen & Chen, 1994).

Although the process of regeneration was interesting for humans since ancient times, it was not until the 18th century when this phenomenon began appearing in scientific studies. René-Antoine Ferchault de Réaumur started studying regeneration on crustaceans as early as 1710 by amputating their limbs and observing under which conditions regeneration was carried on (Ratcliff, 2005). Following Ferchaul de Réaumur's steps, his pupil Abraham Trembley discovered in 1744 that yet another type of animal can regenerate: The Hydra (Lenhoff & Lenhoff, 1984). In the 1760's, the Italian physiologist Lazzaro Spallanzani performed the first experiments in vertebrates by showing that salamanders can regenerate limbs, this with the intention of separating the term regeneration from reproduction (Tsonis & Fox, 2009).

Over a century later after Spallanzani's work, in 1901, Thomas H. Morgan would publish a book which laid down the bases of modern regeneration research. In this book, which he called "Regeneration", Morgan compiled the most relevant findings on the field, and offered insightful commentaries on various regeneration-related processes (Morgan, 1901).

From this point forward, research on regeneration has advanced at a steady pace, using different animal models to understand its basis such as planarian, hydra, fish, mice and a variety of salamander species.

2.1.1 Types of Regeneration

Like in many phenomena in biology, regeneration can be sub-classified based on different processes. A classification scheme for regeneration is presented in Carlson (2007), categorizing the regeneration phenomenon into six groups:

- Physiological regeneration: The process through which most multicellular organisms replace worn out cells depending on their physiological needs. A very notable example of this type of regeneration is the replacement of epidermal cells.
- Epimorphic regeneration: This type of regeneration involves the replacement of complex body parts through the formation of a blastema, which is a mass of undifferentiated cells that can proliferate and differentiate yet again into the lineages that were present in the lost structure. Clear examples of this regeneration are limb regeneration of several amphibians, as well as whole organism in some flatworms such as planarians.
- Tissue regeneration: This branch of regeneration englobes those processes that are in charge of damaged tissue replacement but, contrary to epimorphic regeneration, they perform this action without the presence of a blastema, such as the regeneration of muscle and bone after an injury in mammals.
- Cellular regeneration: Within this type of regeneration are the processes where the reconstitution of a damaged cell takes place. It can be observed in unicellular organisms such as the ones belonging to the *Stentor* genus as well as in other protozoans. Animals also exhibit this type of regeneration in cells from the neural system.
- Hypertrophy: This regenerative process involves either the increase in size of a paired organ whose counterpart has been lost, like in the case of the kidneys, or even the restoration of mass of a damaged organ such as the liver.
- Morphallaxis: Within this group are processes in which organisms reconstitute a structure by remodeling using existing body cells, with the chance of these going through differentiation in order to compensate for missing cells. Most studied organisms on this phenomenon are the one belonging to the *Hydra* genus.

In this work, we will mainly focus on epimorphic regeneration. The term epimorphic regeneration was first proposed by Morgan in 1901, along with the term morphallaxis, which he considered as antagonistic phenomena (Figure 1).

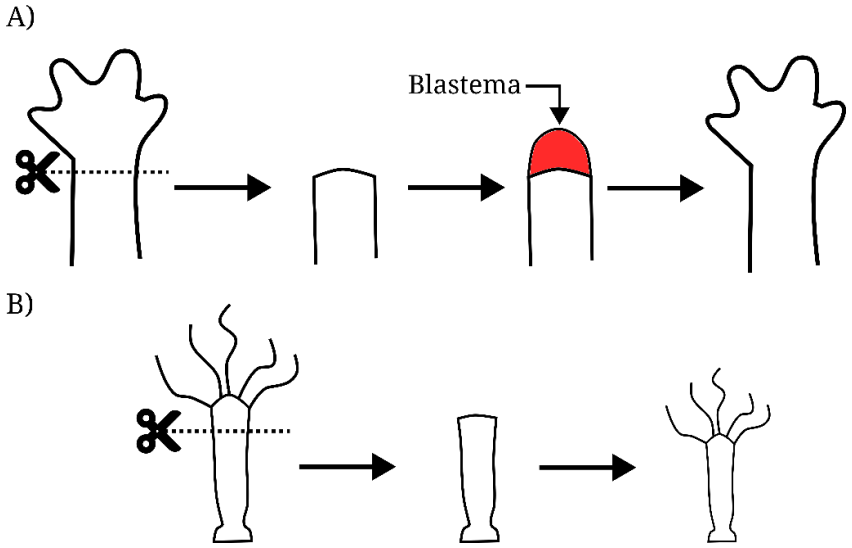

Figure 1 - Contrast between the different regeneration types in animals. A) epimorphic regeneration and B) morphallactic regeneration

2.2 Limb Regeneration in Salamanders

As mentioned before, salamanders have played an important role in the field of regeneration research. They are one of the few vertebrate groups that can perform epimorphic regeneration, making them of special interest for applied research. Among salamanders, there has been one that stands out and that is the Mexican axolotl (*Ambystoma mexicanum*).

The Mexican axolotl is an endemic species of the lakes of Xochimilco and Chalco, and is known to be a neotenic organism, meaning that it retains its larval features throughout adulthood. With more than 150 years as a research model organism (Reiß, Olsson, & Hoßfeld, 2015), a variety of different molecular biology tools have been developed on the axolotl, just like the generation of transgenic lines through techniques such as plasmid injection (Sobkow, Epperlein, Herklotz, Straube, & Tanaka, 2006) and CRISPR-Cas genome editing (Fei et al., 2017; Nowoshilow et al., 2018), which have furthered our knowledge of the regeneration phenomenon.

2.2.1 Overview of salamander limb regeneration

To better understand regeneration, scientist first wondered how cells behaved through the limb regeneration process, providing a series of descriptive studies detailing each stage of the phenomenon (Iten & Bryant, 1973; Schmidt, 1968; Tank, Carlson, & Connelly, 1976). Here I present the regeneration process divided into six major stages as described by Carlson (2007) (Figure 2):

Wound healing

Shortly after amputation, the wound surface is covered by a thin translucid epidermis sheet that is generated through migration of epidermal cells adjacent to the amputation site. There are also clear signs of trauma on the distal area denoted by necrotic spots across the end of the humerus, as well as moderate presence of inflammatory cells, however, not to an extent one would expect if an injury of the same magnitude was inflicted to a mammal (Figure 2A).

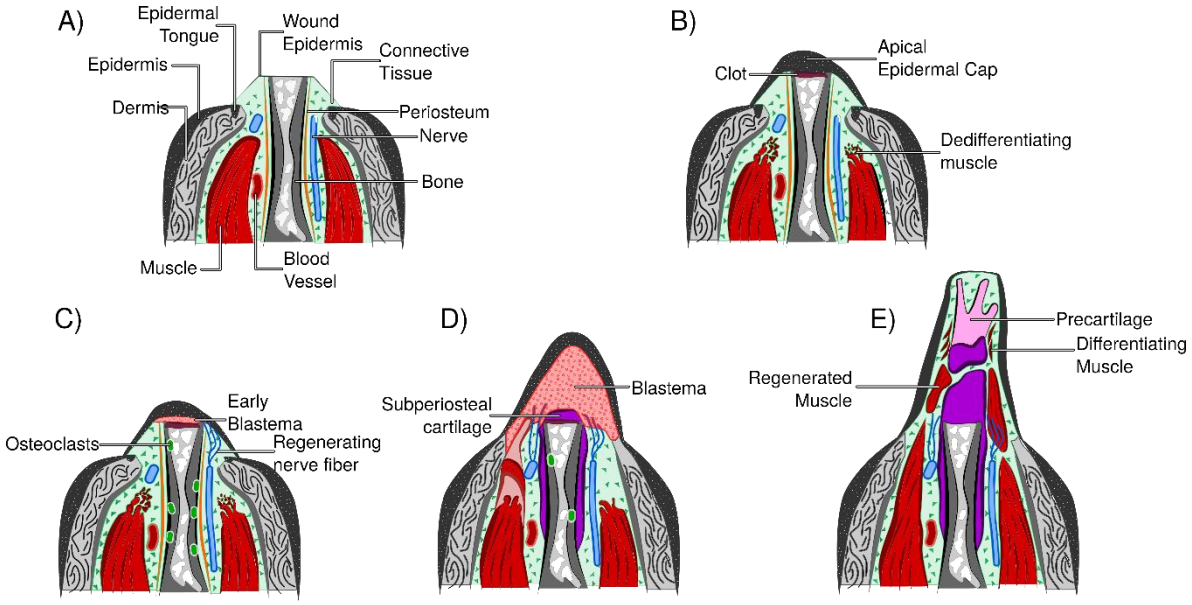

Figure 2 - General overview of the salamander limb regeneration process. A) *Wound healing stage*: after the amputation, the wound is covered by a thin layer of migrating epidermis **B)** *Phagocytosis and demolition stage*: during this stage, removal of damaged tissue begins, as well as a thickening of the wound epidermis, forming what is known as the Apical Epidermal Cap **C)** *Dedifferentiation stage*: the first stage where the blastema is distinguishable, regenerating nerve fibers have made their way to the AEC, and different tissues have begun dedifferentiation and migration **D)** *Blastema formation stage*: the blastema grows rapidly, as dedifferentiation continues **E)** *Morphogenesis*: tissues begin to differentiate, and patterns begin to form in order to give rise to the new limb. Based on Carlson (2007).

Phagocytosis and demolition

This stage could be considered as a phase of preparation for dedifferentiation, as several factors necessary for the regenerative process are taking place. Firstly, the wound epidermis begins to thicken and forms what is known as Apical Epithelial Cap (AEC), while macrophages remove sarcoplasm (cytoplasm from striated muscle) from damaged areas. It is important to highlight that apart from the start of removal of tissue debris, not much is known about this phase, and it could be considered as the least understood stage in terms of its underlying molecular processes (Figure 2B).

Dedifferentiation

This stage is the most distinctive of the regeneration process, in its cells that seem to have lost all histological traits and that resemble embryonic cells (blastema cells), are first visible across the regions of the connective tissue that have been loosen due to the remodeling of the extracellular matrix via metalloproteases. Numerous osteoclasts begin to appear, and bone erosion starts.

There are only signs of trauma at the distal area of the bone, and the inflammatory response begins to disappear. At the AEC, there is no evidence of cell layering, and it has now been penetrated by regenerating nerves.

As for muscle, cells begin to lose striation at the amputation site and now harbors immature looking cells that will later migrate to the blastema. Similar changes begin to happen to dermal fibroblasts (Figure 2C).

Blastema formation

In this stage, the blastemal cells now resemble the mesenchymal cells that are present on the embryonic limb bud. These are being accumulated rapidly and lack distinguishable histological features (Figure 2D).

A long-standing question that has been only partially answered is which cells contribute to the formation of the blastema, and on what proportion they do. On the latter issue, Muneoka, Fox, and Bryant (1986) reported that 43% of blastemal cells had a dermal origin, composing the majority of blastemal cells. Another important contributor to the blastema cell population are muscle-derived cells, and even though they compose the majority of cells of a normal limb, they seem to be outnumbered in the blastema by dermal-derived cells (Han et al., 2005). Other cells that contribute to the blastema but to a lesser extent are cartilage, periosteum and pericytes (Currie et al., 2016).

Although it is important to define which cells contribute to the blastema, Currie et al. (2016) discovered that the timing of migration is also important. In this instance, dermal fibroblasts are known to give rise to either cartilage or dermal connective tissue, through what could be considered as a type of transdifferentiation (Kragl et al., 2009). However, only fibroblasts that migrate during the onset of the regeneration process are able to transdifferentiate into cartilage, while late migrating fibroblast only give rise to connective tissue (Currie et al., 2016).

Morphogenesis

During this stage, the blastema still grows, however several cells start differentiating into their final cell lineage, for example, the development of precartilaginous

structures which translates into digital primordia, which start appearing in an orderly manner. As these primordia grow, they begin to get separated by grooves as the interdigital tissue regresses.

Other tissues start to experience changes towards differentiation as well. For example, regenerating muscle cells start to differentiate into myotubes in a similar manner as in embryonic limb formation, and cells from the lateral epidermis of the stump start to have a column shape morphology, as well as the epidermis now has a basement membrane that was absent during previous stages (Figure 2E).

Growth

After patterning is over, the limb has regenerated perfectly but it is shorter than the original limb. So, during the following weeks, the limb will continue to grow until it has reached the size of its predecessor.

2.2.2 Molecular aspects of limb regeneration

While understanding the histology and cellular dynamics of limb regeneration is important to achieve a full mechanistic description of the process, regeneration is governed at the molecular level, with tight regulation control. Several genes that act during limb regeneration or have been hypothesized to play an important role during this phenomenon have been described (reviewed in Haas & Whited, 2017). However, it is likely that there are many genes missing from the list presented in Haas & Whited (2017).

Homeobox (Hox) genes expression during regeneration

The Hox gene family is one of the most iconic when it comes to talking about developmental biology. Their main function lies in the patterning of the body plan, and are present in most of the bilaterian clade (Ryan et al., 2007). Another peculiarity of this gene family is its genomic arrangement. They are organized in a collinear manner, concurring with their spatial-temporal expression pattern, order in an anterior-posterior manner (from snout to trunk, Figure 3)(Graham, Papalopulu, & Krumlauf, 1989).

Gene clusters, however, are not numerous in ancestral animal lineages, for example, it has been shown that nematodes (H. Zhang et al., 2003) and insects (Mallo & Alonso, 2013) have only one Hox gene cluster encoded in their genomes. However, there was an increase in the number of clusters at some time during the evolution of organisms that gave rise to jawed vertebrates, since they all have at least four Hox gene clusters (Ruddle et al., 1994).

Hox genes have already been proven to play an important role on vertebrate limb development. For a normal limb development in vertebrates, clusters HoxB and HoxC seem dispensable, since there was no significant phenotypes on developing limbs exhibited upon deletion (Medina-Martínez, Bradley, & Ramírez-Solis, 2000; Suemori & Noguchi, 2000). In contrasts, HoxA and HoxD clusters seem to be necessary for normal limb development. While deleting only one of these clusters does not have a strong impact on limb development, deleting both of them stops limb development (Kmita et al., 2005).

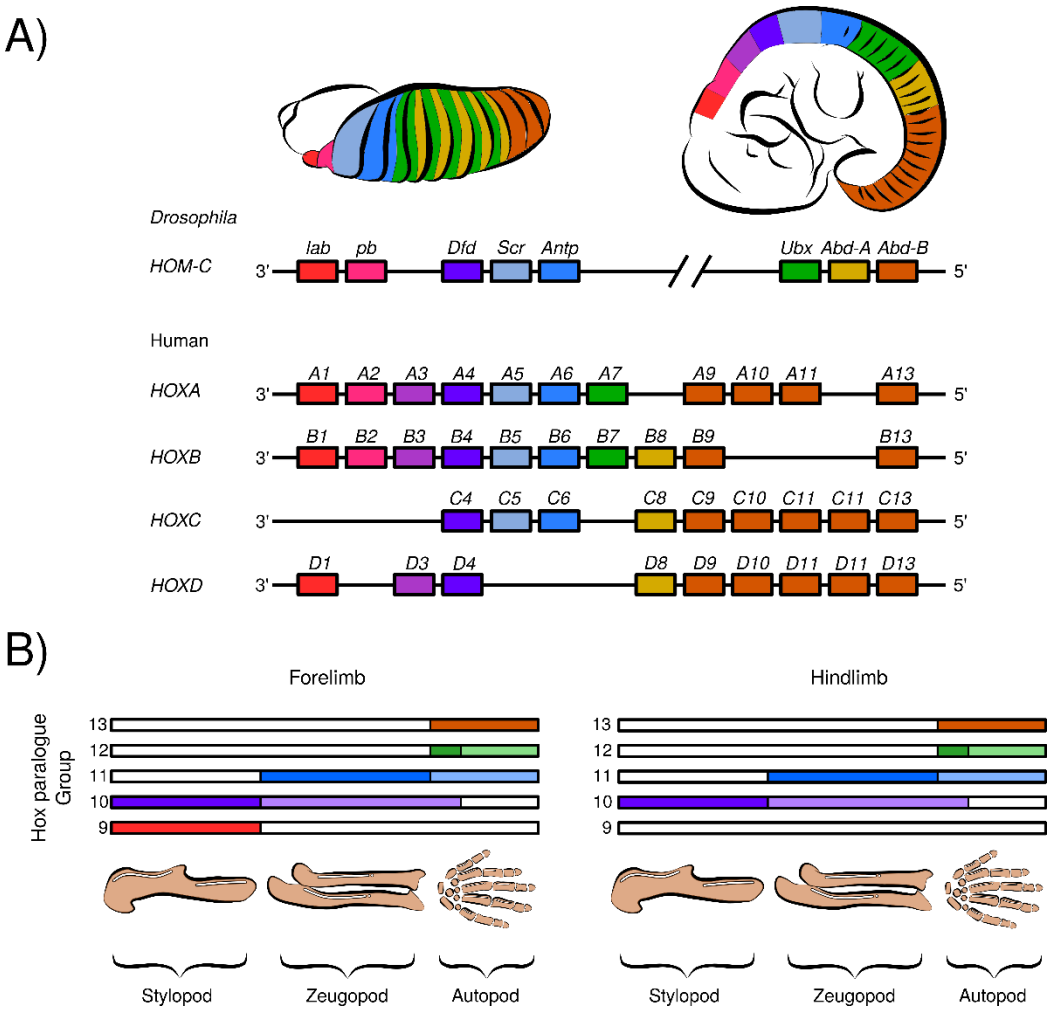

Figure 3 - Hox gene expression and genomic organization. A) On top the *Drosophila* and Mice Hox gene homologues expression pattern is shown during embryogenesis. On the bottom, the *Drosophila* Hox homologue cluster and the four Human Hox genes clusters are shown, colors depicting each paralogue group. B) Hox gene expression throughout vertebrate limb morphogenesis. Different genes are expressed across the limb, and subtle differences have been reported on the development of hindlimbs and forelimbs. Based on Gilbert (2010).

Knowing that Hox genes are actively involved during limb development, and limb regeneration being considered an homologous developmental process, several groups started describing the behavior of said genes during limb regeneration in salamanders (Gardiner & Bryant, 1996). Consistent with what was found during limb development, clusters HoxA and HoxD seem to be expressed in a collinear manner during limb regeneration (Gardiner, Blumberg, Komine, & Bryant, 1995; Torok, Gardiner, Shubin, & Bryant, 1998). However, some genes from other clusters seem to be expressed also during the regeneration process, but whether they are essential to the process remains to be tested. For example, *HoxC10* can be found in non-regenerating limbs, but after amputation it seems to be upregulated during the blastema formation stage (Simon & Tabin, 1993).

Establishment of the three axial regions during limb regeneration

Another key point that has been studied thoroughly during limb morphogenesis and in limb regeneration is the establishment of the different axis present in the regeneration/development plane: the distal-proximal axis, the dorsal-ventral axis and the posterior anterior axis (**Figure 4**A). While every axis has its own set of genes necessary for specification, it is important that specification of all the axes is coordinated during development through a genetic network (Figure 4C).

The most studied of all the genes presented in Figure 4C is Sonic Hedgehog (SHH). The protein encoded by the gene is a member of the Hedgehog protein family, comprised of three members: Indian Hedgehog (IHH), Desert Hedgehog (DHH) and SHH. They mainly possess three domains: signal peptide (SS), an amino-terminal signaling domain (HhN/Hedge) and a autocatalytic carboxyl-terminal domain (HhC/Hog), and they act through binding to a membrane receptor that activates a signaling cascade that ends with the activation of the Gli transcription factors, which are the final effectors of the signaling pathway (Bürglin, 2008).

SHH is essential for the establishment of the zone of polarizing activity (ZPA), since its presence alone is enough to induce it (Riddle, Johnson, Laufer, & Tabin, 1993). Through the ZPA, SHH establishes what will become the posterior-anterior axis, and when the number of ZPAs increased through the developmental plane, the number of digits also increases (Honig & Summerbell, 1985).

SHH promotes the expression of Grem1, which is an antagonistic protein to the TGF-β pathway, and inhibits the bone morphogenetic proteins (BMPs), mainly BMP2 and BPM4 (Church et al., 2015), by binding to them and inhibiting the so called BMP pathway. By doing so, Grem1 indirectly promotes the expression of FGF8, helping to establish the apical ectodermal ridge (AER). Simultaneously, when expression of

FGF8 passes a threshold, it inhibits the expression of Grem1, generating a negative feedback loop (Verheyden & Sun, 2008).

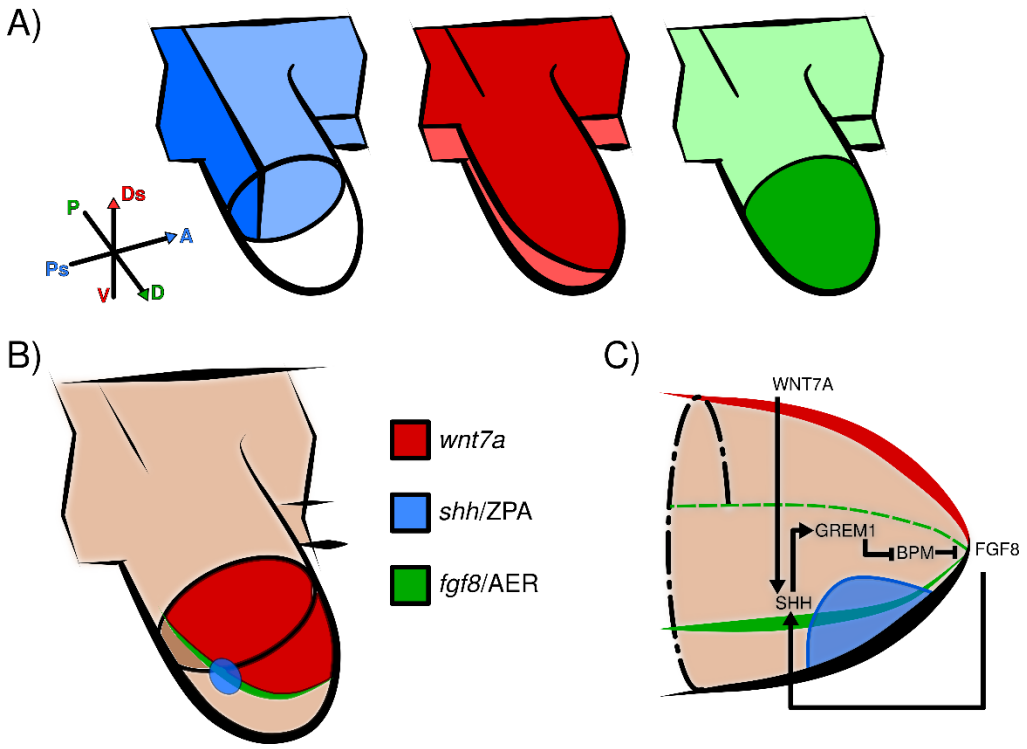

Figure 4 - Establishment of the three different axes in the developmental limb plane. A) The different axis that form during limb development, blue depicting the anterior-posterior axis, red the dorsal-ventral axis and green the proximal-distal axis. B) Diagram showing the main areas required for the establishment of the different axes, where the AER spans across the anterior-posterior axis in the most distal area of the limb (green), the ZPA on the posterior end of the limb (blue), and the zone where the genes necessary for dorsal axis to be established are expressed (red). C) Key factors involved in the establishment of the three different axes, and their interactions. Based on Mundlos & Horn (2014).

Through the expression of FGF8 across the AER, the proximal-distal axis is established. At the same time that SHH indirectly promotes the expression of FGF8 through Grem1, FGF8 promotes the expression of SHH by inhibiting its repressors (Z. Zhang, Verheyden, Hassell, & Sun, 2009), making FGF8 an important factor in the establishment of the posterior-anterior axis.

Last, but not least, Wnt7a is the main player element in the establishment of the dorsal-ventral axis, since its loss of function causes a phenotype where the whole limb exhibits ventral structure (Parr & Mc Mahon, 1995). Although it is not intermingled as strongly as SHH and FGF8, Wnt7a also plays a role in the

establishment of the posterior-anterior axis, since its removal also produces a significant decrease in the levels of SHH (Y. Yang & Niswander, 1995).

The establishment of these axis has been thoroughly studied during limb morphogenesis. However how these factors behave throughout limb regeneration has only recently started to be studied, finding that at least the interaction of SHH and FGF8, through Grem1, is important during axolotl limb regeneration (Nacu, Gromberg, Oliveira, Drechsel, & Tanaka, 2016). Yet, the behavior and relevance of factors like Wnt7a and BMP during limb regeneration remains to be described.

2.2.3 Transcriptomic efforts to study salamander limb regeneration

Wang, Gerstein, and Snyder (2009) have defined a transcriptome as "the complete set of transcripts in a cell, and their quantity, for a specific developmental stage or physiological condition". Through a transcriptome, scientists can begin to understand what elements of the genome are being transcribed and have an idea of what processes might be involved in a phenomenon of interest.

In this section, I present the transcriptomes that have been relevant to the subject of limb regeneration using axolotl as a model organism. Using different strategies, field experts have interpreted these transcriptomes to improve our understanding of the regeneration process.

Due to the high cost of the sequencing techniques in the decade of the 2000's, many opted to use microarrays to perform transcriptomic analyses. However, there is a shortcoming when using microarrays: since the probes that are on the array must be synthesized individually, there is a limited resolution to the diversity of transcripts that can be tested, so the information such as the expression levels of isoforms or transcripts that were not included in the microarray design are lost.

Axolotl microarrays were designed using expressed sequence tags (ESTs) (Habermann et al., 2004), and then used for several studies, including the analysis of the first regeneration transcriptomic analysis (Monaghan et al., 2009). In their work, genes involved with extracellular matrix remodeling (ECM) like metalloproteinases (MMPs), as well as genes involved in a variety of signaling pathways were found to be transcriptionally changing through regeneration.

Years later, the costs of sequencing began to drop making it possible to sequence transcriptomes and genomes with more ease (Wetterstrand, 2016). Therefore, it was possible to sequence the first axolotl regeneration transcriptome using RNA-seq, (Stewart et al., 2013). While this resource proved valuable, since it provided a full set of transcripts that could be used as a reference for molecule design such as probes, the transcriptome had several technical flaws: it had several missing transcripts

(Figure 5), and it had no biological replicates. In this work, they focused mainly on already reported transcripts like metalloproteinases, as well as developmental factors known to be present during limb development like SHH and the HOX genes. Also, they reported that pluripotency-related genes (also known as oncogenes), like MYC or KLF4, increase their expression a day after the amputation is performed. On a more general note, they report GO terms that were enriched during the regeneration process, some of the most significant being collagen catabolism processes during early and mid-regeneration, as well as bone development, which is enriched in the late stages of regeneration.

While the transcriptome provided by Stewart et al. (2013) was a valuable approach, it was a limited insight to the organism transcriptomic landscape, especially when many transcripts were known to have their expression restricted to a certain tissue or phenomenon (Sonawane et al., 2017). Keeping in mind these facts, there were three separate efforts to generate a transcriptome that was representative of most axolotl transcripts.

The first effort was carried out by Bryant et al. (2017), who made a transcriptome using 16 tissues including proximal and distal blastema, skeletal muscle, bone and cartilage, as well as testes and ovaries. The aim of their work was to generate a transcriptome that captured the most axolotl transcripts, but they were capable of identifying factors that are important for limb regeneration. Between those were *cirbp* and *kazald1*, which are two of the few factors that have been reported to be expressed during regeneration but not limb development, although their exact mechanism of action remains to be studied.

The second effort was made by Nowoshilow et al. (2018), who made a composite transcriptome using 22 different tissues, including tissues like liver and lungs. However, in comparison to the transcriptome presented by Bryant et al., (2017), this transcriptome presented different tissues undergoing the regeneration process like brain, tail and limb.

The third effort was made by Caballero-Pérez et al. (2018), who used the sequencing data published by Stewart et al. (2013) and new sequencing data that included several tissues such as gills, heart, liver and different limbs. A peculiarity of this transcriptome is that it contains sequencing data of wild-type organisms, which could provide resources for SNP profiling in axolotl wild populations (Smith et al., 2018).

Together, these transcriptomes are the most complete in terms of single copy orthologues, having approximately 90% of the BUSCOs using a tetrapod database (Figure 5). Hence, these transcriptomes are suitable for use as a scaffold for future transcriptomic projects.

One of the problems traditional RNA-seq experiments have is that normally tissues used for sequencing are heterogeneous, having an impact on the quantification of certain transcripts, especially in samples such as the ones obtained in limb regeneration whose cell proportion change throughout the process (Muneoka et al., 1986). To overcome this problem, scientist have developed a method to sequence cells individually commonly known as single cell RNA-Seq (scRNA-Seq). With this method, we can not only pinpointing the exact origin of a transcript, but also track lineages during development (Hwang, Lee, & Bang, 2018).

A single cell sequencing dataset during the process of regeneration has been generated recently, with the objective of examining the faith of cells throughout limb regeneration. Gerber et al. (2018) performed two major scRNA-seq experiments: the first one, the authors perform a time-course scRNA-seq using six different time points, and thus classifying different lineages and their marker genes, but also the development trajectories of cells derived from connective tissue. The second one compared limb buds from developing axolotl larvae with regenerating limbs, finding that the transcriptional programs were similar depending on the position of the cell in the developmental axes.

In this work, we performed a time course RNA-Seq of axolotl's limb regeneration, in which we have included a wide selection of stages that cover most of the process. This transcriptome addresses several technical issues present in previous works, such as the lack of biological replicates. It is also the first regeneration transcriptome using wild-type organisms instead of the D/D breed that has been used as the axolotl stock breed for research work, and thus eliminating problems that come with inbreeding.

In this work, I aimed to make a limb regeneration transcriptome that englobes eight different time points that we consider to be representative of the process, using wild type animals instead of the stock lab breed. I used a variety of computational tools to analyze thoroughly the transcriptomic data, not only limiting the analysis to a differential gene expression analysis of coding protein genes, but also identifying lncRNAs, enrichment of different functional annotations, as well as the creation of a gene co-expression network. Overall, we found genes that had already been reported to be involved in regeneration, as well as novel factors that have yet to be characterized.

3 Objectives

3.1 General objective

The main objective of this thesis was to characterize the changes in the transcriptional program during progressive stages of the regeneration process of *A. mexicanum*.

3.2 Specific objectives

To achieve the main objective, we undertook several specific objectives:

- To obtain the transcriptional profiles in eight different time points (from 0 to 40 days post-amputation (dpa)) during limb regeneration in *Ambystoma mexicanum*.
- To determine the differentially expressed genes along the limb regeneration process in *A. mexicanum*.
- To assess the transcriptional behavior of previously reported genes associated with limb regeneration in *A. mexicanum*.
- To define the function of the differentially expressed genes through categorical enrichment during limb regeneration of *A. mexicanum*.

4 Materials and Methods

4.1 Amputation, RNA extraction and sequencing

Sixty-six neotenic *Ambystoma mexicanum* adult animals with a length between 18-19 cm of total length were used for amputation. Prior to the amputations, animals were sedated using a solution with benzocaine at a concentration of 50 mg/L for 30 min.

Once the organism was anesthetized, it was placed on a sterile tray and under a stereoscope, and with a sterile scalpel either the limb at the level of the zeugopod or the blastema at different time points (1, 3, 9, 15, 25, 32 and 40 dpa) were collected. Collected tissue was placed on an Eppendorf tube and frozen in liquid nitrogen for its posterior storage at -80°C. After amputation, organisms were placed on a 20L fish tanks with 2 drops of methylene blue to prevent infections.

To perform the RNA extraction, collected tissue was dipped into liquid nitrogen, and using a homogenizer samples were grinded along with 1 mL of Trizol per 50-100 mg of tissue. The solution was then centrifuged at 1,300 rpm for 10 min at 4°C, and supernatant was recovered with a micropipette and incubated for 5 min at room temperature.

After incubation, 2 µL of chloroform per 1 mL of Trizol were added to the supernatant, and then the tube is agitated for 15 s vigorously. The tubes were

incubated for 5 min or until there was visually a separation of phases, and then it was centrifuged at 1,300 rpm for 15 min at 4°C. Then, after been cooled on ice the aqueous phase was transferred to a new tube. Finally, isopropyl alcohol was added in a proportion of 1:3 of Trizol, and was left to rest overnight at 4°C.

The samples were then centrifuged at 1300 rpm for 10 min at 4°C, and the supernatant was discarded. The resulting pellet was then washed twice by adding 1mL of ethanol, vortexing the sample and then centrifuging it at 7500 rpm for 7min at 4°C, discarding the aqueous phase and drying for 3 min. The pellet was then resuspended in DEPC water, 20 µL if tissue was less than, otherwise 50 µL of DEPC water were used, prior to their storage in at -80°C.

RNA samples from the same time-points were then pooled together making a biological replicate, which made for up to two biological replicates in most time-points (Table 1). Each biological replicate library was prepared independently.

Sequencing libraries were prepared using the TruSeq Library Preparation kit, and it was sequenced using a NextSeq 500, in a format of 150bp paired-end reads, generating approximately 10 million reads per sample (Table 1). Sequencing was done by the Laboratorio de Servicios Genómicos at the Unidad de Genómica Avanzada del Cinvestav Irapuato.

All animal experiments were performed according to the Mexican Official Norm (NOM-062-ZOO-1999) “Technical Specifications for the Care and Use of Laboratory Animals” based on the Guide for the Care and Use of Laboratory Animals “The Guide”, 2011, NRC, USA, with the Federal Register Number # BOO.02.08.01.01.0095/2014, awarded by the National Health Service, Food Safety and Quality (SENASICA-SAGARPA). The Institutional Animal Care and Use Committee (IACUC) from the CINVESTAV approved the project “Management and husbandry of *Ambystoma* spp. and experimental processing of tissue for functional analyses and genetic expression” ID animal use protocol number: 0209-16.

4.2 Filtering and cleaning sequencing data

Raw sequencing data were analyzed using FastQC v0.11.5 (Andrews, 2010) to perform a diagnosis on the sequencing quality, making special emphasis on detecting the presence of sequencing adapters and other factors that could influence downstream analyses, like GC content and per base quality. After the diagnosis was complete, reads were trimmed using Trimmomatic v0.36 (Bolger, Lohse, & Usadel, 2014) under the parameters --threads 8 LEADING:20 TRAILING:20 HEADCROP:2 SLIDINGWINDOW:4:15 MINLEN:60.

4.3 Transcriptome assembly and annotation

Paired-end reads were assembled using the software Trinity v2.5.1 (Haas et al., 2013) with the default parameters except for the following: --max_memory 250G --CPU 10 --no_normalize_reads. Transcripts resulting from the assembly were then filtered by length, keeping those that were at least 500 nucleotides in length.

Afterwards, the transcriptome was subjected to a quality assessment and completeness with BUSCO v3 (Waterhouse et al., 2017), using a tetrapod single copy orthologue database provided by the software developers as reference.

To comprehensively annotate the transcriptome, I followed the workflow established by the Trinotate tool: firstly, all open reading frames (ORFs) that were at least 100 amino acids in length were predicted by Transdecoder. Relevant protein homologues were identified using BLASTx and BLASTp (from the software ncbi-blast+ v2.6.0), with the Swiss-Prot database as reference, which is a non-redundant highly inclusive manually annotated protein database. Protein domains were annotated using HMMER v3.1b2 and the PFAM's protein domain database (version 31). Lastly, trans-membrane domains and signal peptides were annotated using tmHMM v2.0c and SignalP v4.1 respectively. All the outputs from the different steps were loaded into Trinotate and filtered using a threshold of $1x10^{-10}$ for the BLAST e-value to consider an annotation as existing (BLAST, 2013; Boutet, Lieberherr, Tognolli, Schneider, & Bairoch, 2007; Finn et al., 2015; Krogh, Larsson, von Heijne, & Sonnhammer, 2001; Mistry & Finn, 2007; Petersen, Brunak, Von Heijne, & Nielsen, 2011).

The transcriptome was checked for contamination using FASTQ-Screen v0.11.3 (Wingett, 2018), with the trimmed reads used for the transcriptome assembly as input, comparing them against the assembled transcriptome, two other published axolotl transcriptomes (Nowoshilow et al., 2018), and the maize transcriptome obtained from ENSEMBL-Plants database (version 42) as references. Contaminating transcripts were identified by comparing the assembled transcriptome against the maize transcriptome, removing those transcripts that had at least 400 bit-score and a percentage of identity above 90%.

4.3.1 Annotation of lncRNAs

Long non-coding RNAs (lncRNAs) were annotated using CPC v0.9r2 (Kong et al., 2007) with UniRef90 as a reference database, and CPC2 (no version information available) (Kang et al., 2017). To discard transcripts that may have been wrongly assembled, I mapped the transcripts to the axolotl genome (Nowoshilow et al., 2018) using BLAT v35 (Kent, 2002), and selected transcripts where at least half of their nucleotides mapped with at least 95% identity. It is important to note that if a transcript had multiple mapping sites across the genome, only the best hit was conserved for further

analysis. Long non-coding transcripts were later confirmed by comparing against already published transcriptomes (Bryant, Johnson, DiTommaso, et al., 2017; Nowoshilow et al., 2018) using BLASTn, discarding transcripts that were not covered at 80% length at 95% identity by one of the published transcripts.

4.3.2 Annotation of Transcription Factors

Transcription factors were annotated using the data presented by Lambert et al., (2018) as a reference. Firstly, domains that have been characterized to be DNA binding factors were obtained from the reference, finding 310 PFAM terms. Transcripts that possessed these domains were extracted from the annotation made using Trinotate. To finalize the search, and since not all proteins with these domains are considered transcription factors, axolotl proteins designated as TFs were aligned against the human transcriptome using BLAST, and vice versa, in order to extract just the best bi-directional hits (BBH). Only proteins whose BBH was a transcription factor were classified as such.

4.4 Gene quantification and differential gene expression analysis

Transcript abundances were estimated using paired-end reads and Kallisto v0.43.1 (Bray, Pimentel, Melsted, & Pachter, 2016) with the parameters --bias -b 100 --seed 1992 -t 8. Since most of the differential expression packages require raw counts to perform a differential expression analysis, the estimations were then converted using tximport v1.4.0 in R v3.3.0 (Soneson, Love, & Robinson, 2016), for both genes and transcripts, separately. To further reduce the number of genes, those that did not have at least 1 count per million (cpm), in at least 2 libraries, were discarded.

Differential expression analysis was tested under a quasi-likelihood F-test, which accounts for type-I errors more rigorously using the R-package edgeR (Bryant, Johnson, DiTommaso, et al., 2017). Also, to obtain the most complete panorama on gene expression, contrasts were made across all different samples. A cut-off value of 0.05 in false discovery rate (FDR) was used to determine if a gene is differentially expressed.

4.4.1 Identification of regeneration related genes

A list of 51 genes associated with regeneration was obtained from Haas & Whited (2017), and orthologs for those genes were obtained from the ENSEMBL database for human (GRCh38.p12) and *Xenopus tropicalis* (JGI 4.2). Axolotl orthologs for these genes were obtained taking the best bi-directional hits from the comparison between the assembly generated as a result of the process described in section 4.3, and the software NCBI-BLAST+'s (v2.6.0) tBLASTn and BLASTx tools (BLAST, 2013).

4.4.2 Identification of enriched genes per regeneration stage

To identify enriched genes per stage, the following equations were used:

$$= \frac{\sum_{=1} (1 - \hat{})}{- 1} \; ; \quad = \frac{}{1 \leq \leq ( )}$$

Where Tau (τ) represents specificity and varies from 0 to 1, 0 meaning a gene is broadly expressed across all tissues/samples, and 1 that it is highly specific to a certain sample; n represents the number of tissues/samples; and lastly, represents the expression value of a gene.

For this work, counts per million (cpm) normalized values that were averaged per type of sample were used as expression values ( ). To decide whether a gene was preferentially expressed in a sample, with threshold of 0.85 for τ, and also to be differentially expressed in at least 4 contrasts.

4.5 Gene Ontology (GO) term and KEGG pathway enrichment analysis of differentially expressed genes

4.5.1 Gene Ontology term enrichment

A GO term enrichment analysis was performed to give a functional interpretation to the results obtained by doing the differential gene expression analysis. Firstly, I took the GO terms already provided by the annotation made using Trinity as explained in section 4.3.

GO term enrichment was statistically tested using the R package topGO (v2.30.0) (Alexa & Rahnenführer, 2007), using a combination of two different algorithms: the elimination algorithm, or *elim*, which eliminates nodes and genes from the bottom up in terms of the GO term tree depending on their significance; and a weighting algorithm, or *weight*, that assigns significance to genes contained depending on the significance differences between parent and children nodes that contain them (Alexa, Rahnenführer, & Lengauer, 2006). The statistical test used to test whether a term is enriched or not was the Fisher exact test. Terms whose p-value was below 0.01 were considered as enriched.

4.5.2 KEGG pathway enrichment

KEGG term annotations were obtained from the Trinotate annotation made in section 4.3. Since the annotation made by Trinotate is very homogeneous in terms of which species the homologous genes come from, it was difficult to apply any of the enrichment tools currently available. Taking this into account, a Fisher test was performed test assuming a hypergeometric distribution, using KEGG pathways

(Ogata et al., 1999), which encompass several KEGG terms related to metabolism, genetic information processing, environmental information processing and cellular processes ; and used a p-value of 0.01 as a threshold.

4.6 Gene co-expression network construction

To construct a gene co-expression network, counts normalized using the variance-stabilizing transformation (vst) function from the DESeq2 R-package (v1.18.1) (Love, Huber, & Anders, 2014). To further filter the number of genes used for the construction of the network, we calculated the median absolute deviation (mad), and selected those genes whose mad was in the top 20,000. A signed network was constructed using these genes with a power of 32 and a tree cutoff distance of 0.20.

A Gene Ontology term enrichment analysis was performed as described in section 4.5.1 for each of the modules obtained.

5 Results and Discussion

5.1 Filtering and cleaning sequencing data

Sequencing was performed on RNA samples from 8 different timepoints throughout the regeneration process, each time point had at least two biological replicates, obtaining a total of 158,317,036 paired-end reads. After removing low quality reads, 141,588,326 reads remained, which is approximately 90% of the original reads (**Table 1**).

Table 1 - Number of reads before and after removing low quality sequences. Time points are days post-amputation (dpa). Technical replicates are represented with uppercase letters and biological replicates with numbers.

Time point	Replicate	Number of raw reads	Number of high-quality reads	Percentage of kept reads (%)
0 dpa	1	11,128,090	10,068,324	90.48
	2	10,029,377	9,129,224	91.02
1 dpa	1A	6,613,785	5,901,204	89.23
	1B	4,187,085	3,549,661	84.78
	2	9,927,518	8,926,537	89.92
3 dpa	1	13,526,455	12,313,912	91.04
	2	9,779,562	8,863,380	90.63
9 dpa	1	11,168,628	10,143,789	90.82
	2	13,348,038	12,305,123	92.19
15 dpa	1A	5,314,310	4,727,625	88.96
	1B	4,724,682	4,003,674	84.74
	2A	6,960,777	6,281,224	90.24
	2B	4,966,995	4,285,333	86.28
25 dpa	1A	3,271,888	2,238,313	68.41
	1B	3,014,922	2,561,857	84.97
32 dpa	1	9,949,789	8,951,578	89.97
	2	8,151,995	7,348,975	90.15
40 dpa	1	12,275,133	10,963,818	89.32
	2	9,978,007	9,024,775	90.45
Total		158,317,036	141,588,326	89.43

5.2 Transcriptome assembly and annotation

High quality reads were then assembled into a transcriptome, which yielded 681,125 transcripts representing 553,990 genes. From these, I removed those that did not have at least 500 nucleotides in length, keeping 115,243 transcripts, distributed in 69,466 genes.

To corroborate whether real transcripts were lost over the length filter, I assessed the completeness on both transcriptomes using BUSCO, which searches the single copy orthologs from a pre-compiled database of a certain genus of the tree of life, in this case, the tetrapod database. In the unfiltered transcriptome, I found 3,179 complete,

360 fragmented and 411 missing BUSCOs; while on the filtered transcriptome 3,174 complete, 338 fragmented and 438 missing were found (Figure 5).

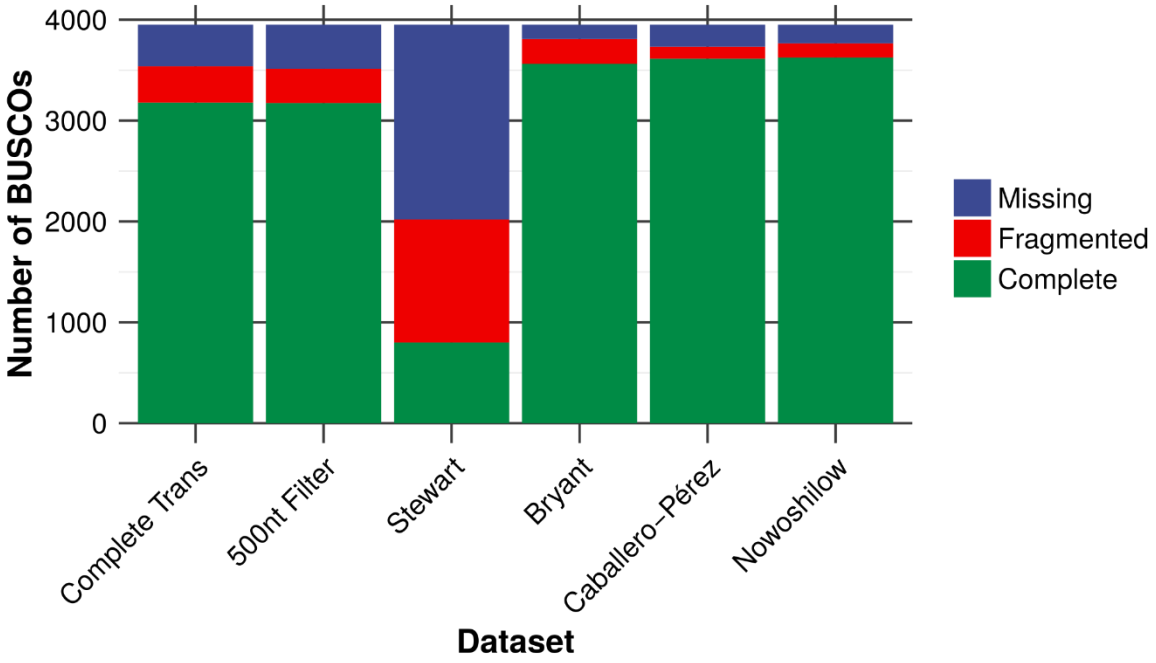

Figure 5 - **Completeness assessment between multiple axolotl transcriptomes using BUSCO**. Color denotes whether the BUSCOs are missing (blue), fragmented (red) or complete (green) in a given transcriptome.

Compared to more diverse axolotl transcriptomes (Bryant, Johnson, DiTommaso, et al., 2017; Caballero-Pérez et al., 2018; Nowoshilow et al., 2018), ours bares ~10% less BUSCOs. This can be easily explained due to the nature of the samples used in each transcriptome, since Bryant et al., (2017) and Nowoshilow et al., (2018) used a combination of 16 and 22 different tissues respectively, including samples of embryonic states and differentiated tissues, making the transcriptome more comprehensive in terms of transcript diversity in the axolotl. However, none of these transcriptomes included a wide limb regeneration time course, leaving the possibility of having missing regeneration-specific transcripts. Caballero-Pérez et al. (2018) transcriptome assembly used a combination of tissues such as gills and liver, as well as a limb regeneration time course providing enough transcript diversity to be at a similar level of completeness as Nowoshilow et al. (2018), Bryant et al. (2017) and Caballero-Pérez et al. (2018) transcriptomes.

In contrast, the transcriptome reported by Stewart et al., (2013), which represented thoroughly the regeneration process, has a rather poor number of complete BUSCOs in comparison to other transcriptomes (Figure 5). Thus, we can conclude that our

transcriptome is close in completeness to the other three transcriptomes and is more complete than Stewart et al. (2013).

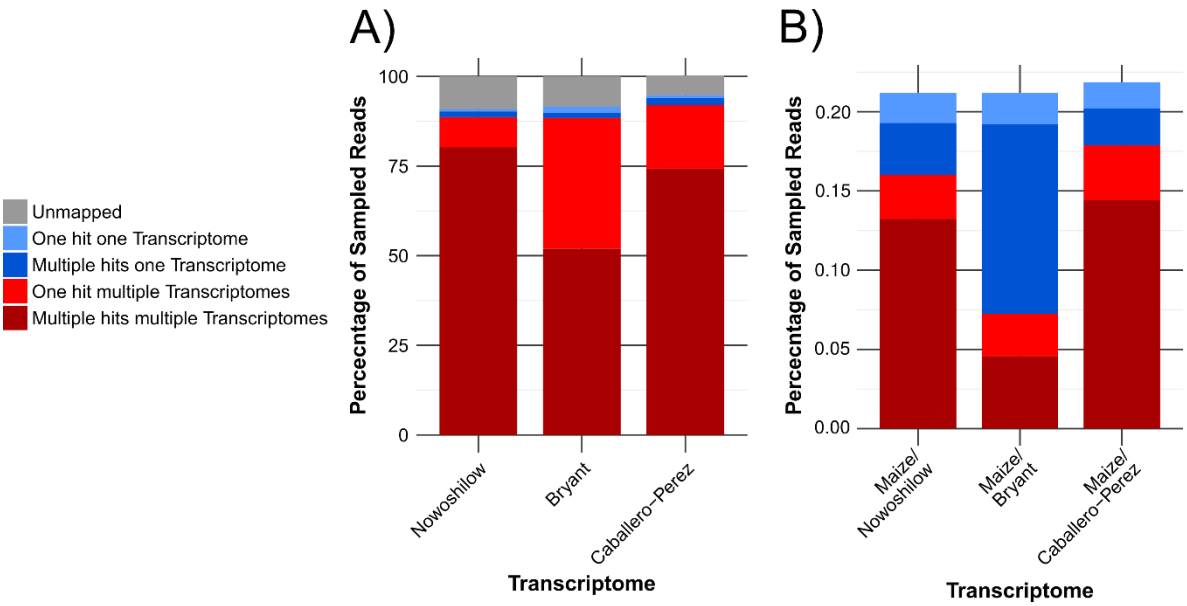

Figure 6 - Similarity between the axolotl regeneration transcriptome and reported axolotl transcriptomes of interest. A) Comparison against two reported axolotl transcriptomes. B) Comparison against a maize transcriptome, only portraying the fraction of the reads that were mapped.

Also, to verify that our reads are similar to the ones used to assemble other axolotl transcriptomes I used FASTQ-Screen, using the transcriptomes presented in Caballero-Pérez et al. (2018), Nowoshilow et al. (2018) and Bryant et al., (2017) and found that 94.58%, 91.53% and 90.81% of the reads align to each transcriptome, respectively (Figure 6A). These results further confirm that most of the reads used for the transcriptome assembly were indeed derived from axolotl transcripts.

To fully annotate the transcriptome, I used the pipeline known as Trinotate, which uses a combination of databases and tools that help annotate transcriptomes systematically (Haas, 2017). Using the pipeline, I annotated 25,966 genes, however, there was a substantial amount of plant genes within the annotation, suggesting potential contamination.

To quantify how much of the sequencing data can be attributed to contamination, I used FASTQ-Screen using a maize transcriptome and the transcriptomes reported by Caballero-Pérez et al. (2018), Nowoshilow et al. (2018) and Bryant et al. (2017) in order to have a comparison against a maize-free dataset. The result showed that a small portion of the reads (0.05% to 0.13%) mapped exclusively to the maize transcriptome (Figure 6B).

To remove the contaminating sequences, I compared the Maize transcriptome to the axolotl regeneration transcriptome using BLASTn, finding 2,064 maize transcripts within the axolotl transcriptome, which were excluded from subsequent analyses.

After the elimination of contaminating sequences, I annotated the lncRNAs present in the transcriptome using CPC and CPC2, obtaining 51,657 and 59,857 respectively, in which 47,202 lncRNAs are shared. To further confirm the existence of these lncRNAs, I searched the sequences of the lncRNAs in published transcriptomes using BLASTn and that had an 80% coverage and a minimum identity of 95% (Bryant, Johnson, DiTommaso, et al., 2017; Nowoshilow et al., 2018), finding 13,901 and 16,863 lncRNAs that were shared across both transcriptomes using CPC and CPC2 respectively, and having 12,897 genes shared between the two tools (**Figure 7**).

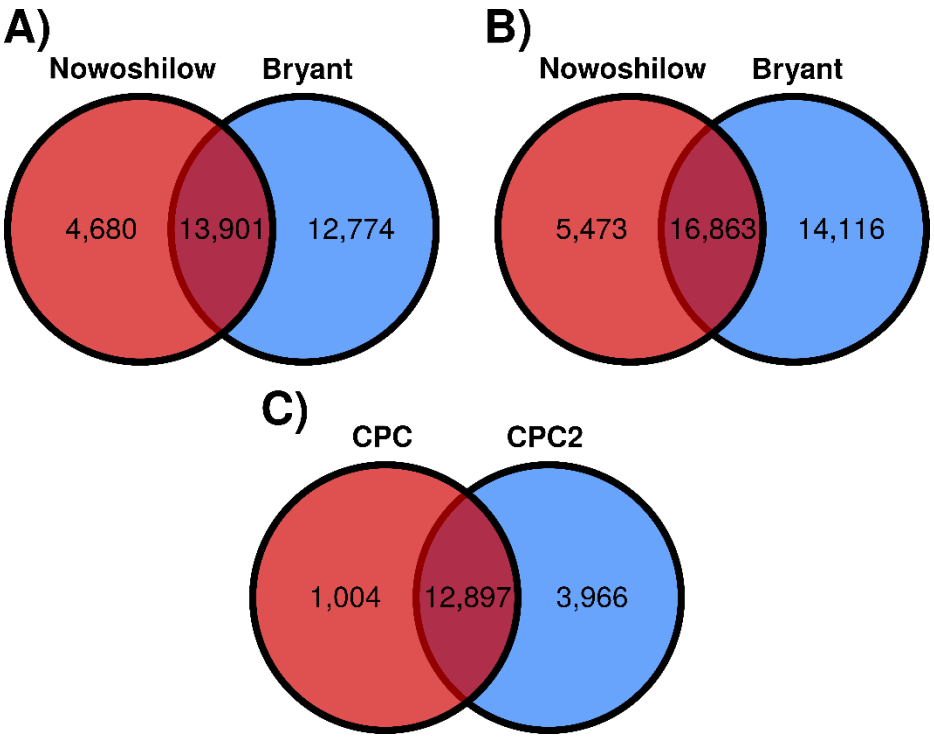

Figure 7 - lncRNAs found in axolotl using two different prediction tools. A) lncRNAs reported by CPC in the axolotl transcriptome assembled in this work that were also found in published transcriptomes. B) lncRNAs reported by CPC2 in the axolotl transcriptome assembled in this work that were also found in published transcriptomes. C) Shared lncRNAs reported by CPC and CPC2 and that are found in both reported transcriptomes, missing 34,305 lncRNAs.

Trinotate's transcription factor (TF) annotation is not very reliable because it is primarily based on sequence identity, rather than on the presence of protein motifs. Therefore, I followed a strategy similar to the one presented by Lambert et al. (2018) for the identification of all human TFs. Firstly, I searched thoroughly in the literature

for TFs that have been experimentally characterized and we were able to identify 463 putative axolotl TFs using the protein domain annotation already generated by Trinotate and a BBH strategy.

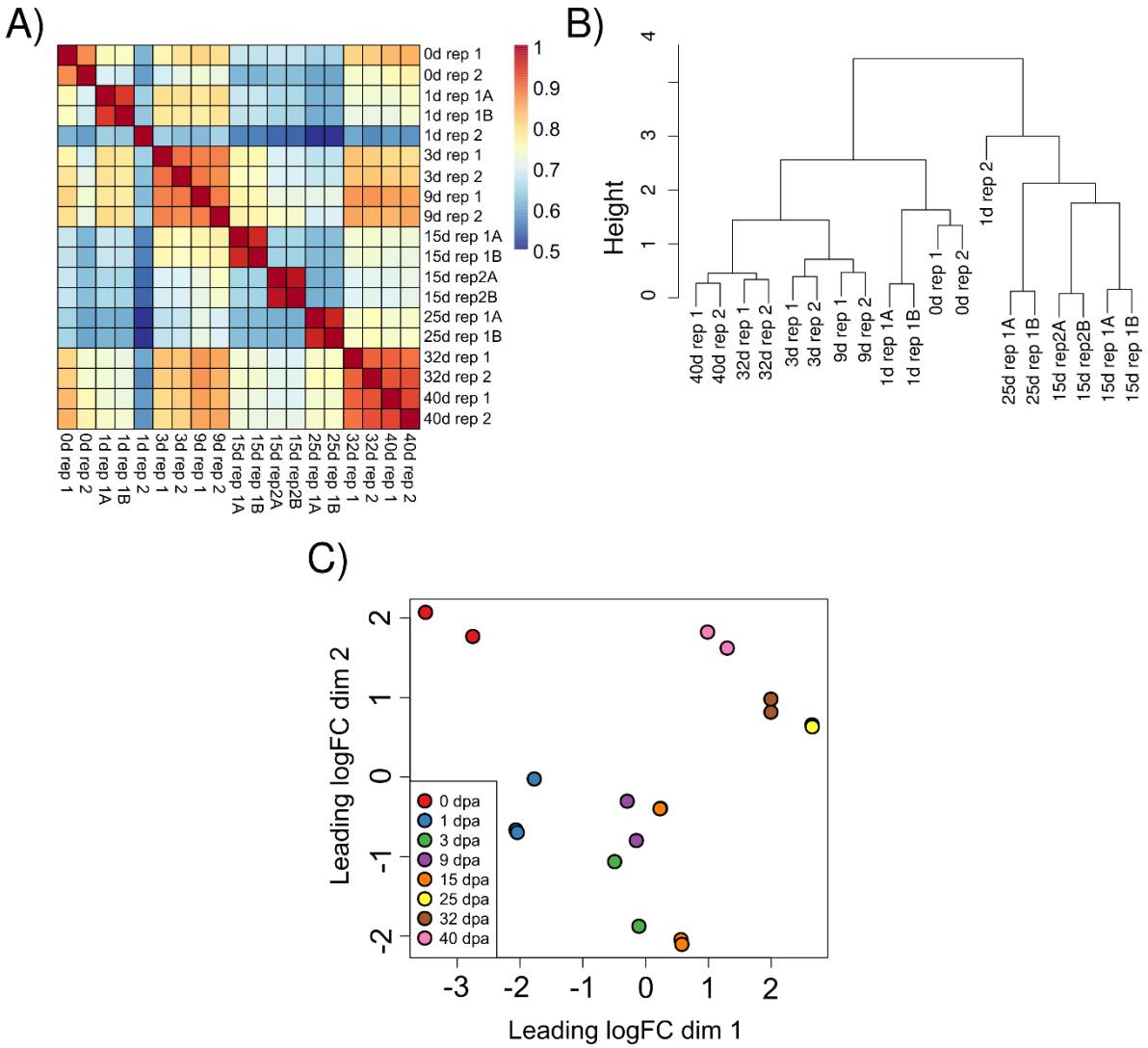

Figure 8 - Correlation between sequencing samples. A) Heatmap showing the Spearman correlation between samples B) Manhattan clustering between different samples. The term rep denotes different biological replicates, while the letter after the number of biological replicates denotes technical replicates. C) MDS plot of the fold change.

5.3 Gene quantification and differential gene expression analyses

After quantifying gene expression and applying a cutoff value of 1 cpm in at least two samples, we were left off with 36,573 genes. In order to verify the reproducibility of the experiments we calculated the Spearman correlation between the counts in all

samples (Figure 8A), and also performed a clustering of the samples using the Manhattan clustering method (Figure 8B).

From the correlations between samples, there are several features that stand out. Firstly, there are groups of samples that do not come from the same time point that are highly correlated, specifically between samples coming from 3 and 9 dpa, and 32 and 40 dpa, with correlations higher than 0.8. This suggests fewer transcriptional changes between these samples than with the rest of the samples.

In contrast, there are several samples where correlation is low even between biological replicates (less than 0.7), even though they are chronologically close. This phenomenon can be attributable to the nature of the samples, since 15 and 25 dpa is where the blastema displays the highest growth rate, and probably the most heterogeneous cell composition throughout the whole regeneration process.

Finally, to add supplementary confirmation that the experiment is reproducible, we performed a multidimensional scaling (MDS) plot (Figure 8C). As expected, most biological replicates from the same condition grouped together with the few exceptions being the biological replicates belonging to 15 dpa.

Following these preliminary analyses, we performed a differential gene expression analysis accounting for all possible comparisons, finding a variable number of differentially expressed genes for each comparison (Figure 9). We found that the most differentially expressed genes were concentrated in comparisons that involve 15 dpa and 25 dpa, which are time points corresponding to the stages of blastema formation and differentiation (Figure 2).

From these results, I looked at specific genes that had previously been reported or suggested to be involved in limb regeneration in previous works. I searched the axolotl transcriptome for 51 core genes involved in regeneration (Haas & Whited, 2017), being able to find 29. Not being able to find the rest of the core genes can be attributed to their low expression under these conditions, perhaps due to these genes are expressed in tissues that are not predominantly expressed in the most abundant cell types present in the tissue where the RNA was extracted from, resulting in the assembler not being able to assemble them due to the lack of sequencing reads (Grabherr et al., 2011).

As for the core genes that were present on the axolotl transcriptome, many of them display an expression pattern similar to the ones as reported in the literature. For example, *hox* genes in Figure 10 behave similarly, increasing their expression dramatically at 25 dpa.

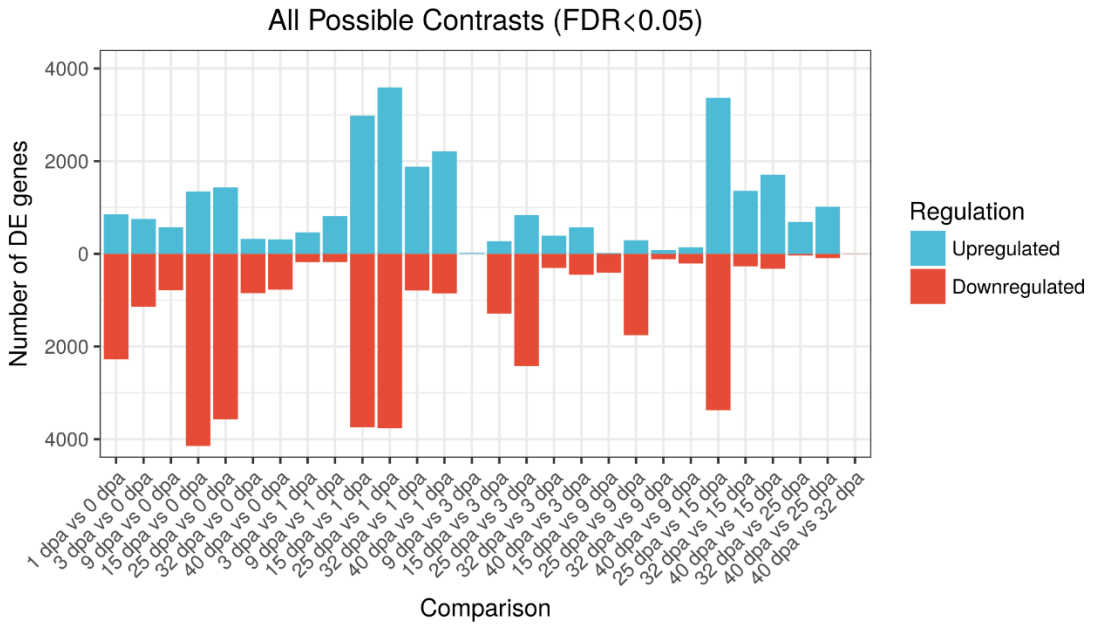

Figure 9 - Differentially expressed genes across all conditions. The number of downregulated (red) and upregulated (blue) genes (vertical axis) per comparison (horizontal axis).

Due to the nature of the transcriptome itself (whole limb and blastema), it is impossible for us to determine where each individual *hox* gene is expressed, however due to its collinear nature (Lemons & McGinnis, 2006) it is safe to assume that they are being expressed temporarily similar., but they might not be expressed in a similar spatial manner.

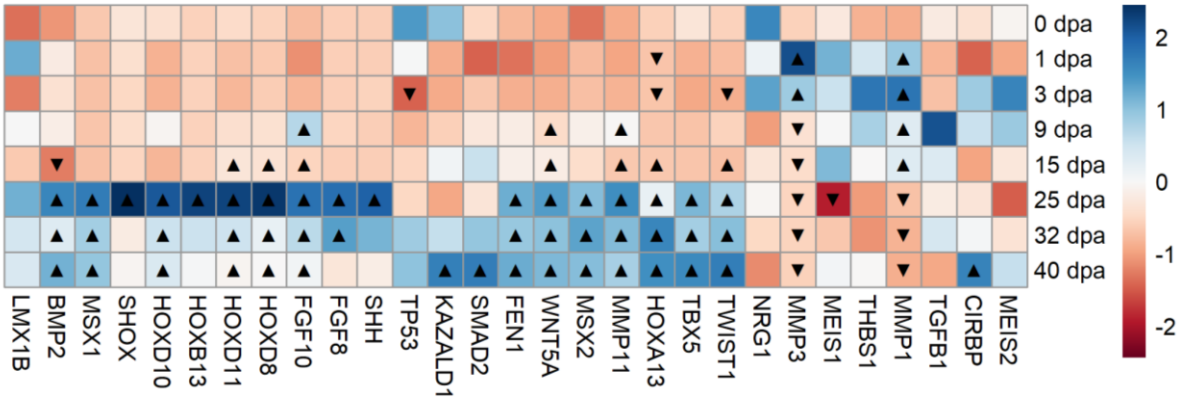

Figure 10 - Expression patterns of genes previously reported as involved in the regeneration process. Relative expression (z-score) of each gene, where triangles (triangles pointing upwards show upregulated genes, downwards downregulated genes) in each cell denote differential expression in a specific stage in reference to its predecessor stages.

In the specific case of the hoxD cluster, the latter members of the cluster (*hoxD-8* to *hoxD-13*) are usually expressed in early and late regenerating limb buds until the first digits start to form (Torok et al., 1998), which is consistent our findings (Figure 10).

Similarly, MMPs, which are essential in the initial stages of the regeneration process, change their expression in various occasions. Three out of five MMPs present in the set of core genes (*mmp*-1,3 and 11) showed diverse expression patterns through regeneration. It is known that *mmp-1* and *mmp-3* act during early stages of regeneration, remodeling the ECM and therefore promoting cell migration and proliferation (Kato et al., 2003; Mu, Bellayr, Pan, Choi, & Li, 2013; Seifert, Monaghan, Voss, & Maden, 2012). I indeed found their expression levels rise between 1 and 3 dpa. In contrast, *mmp-11* exhibits a different pattern of expression, reaching its maximum level of expression towards the end of regeneration (25 to 40 dpa). Although the role of *mmp-11* in regeneration has not been studied thoroughly, it is known that the protein encoded in this gene is required for the morphogenesis of the myotendinous junction (Jenkins, Alrowaished, Goody, Crawford, & Henry, 2016), which is an interface between the muscle and the tendon. Thus, it is likely that *mmp-11* is regulating the morphogenesis of this tissue towards the end of the regeneration.

Another group of interesting genes that are presented in Figure 10 is the one comprised by *fgf8* and *ssh*. As mentioned in section 2.2.2, these two genes play a key role in the establishment of the different axes during the regeneration process. Their expression pattern is similar, having a significant increase around 25 dpa and gradually decreasing towards the patterning stage at 40 dpa (Figure 10). Their expression pattern is analogous to what has been reported in the literature, where *ssh* and *fgf8* reach their maximum expression at the late blastema stage, fading away afterwards indicating the disappearance of the ZPA and the AER (Gilbert, 2010; Nacu et al., 2016).

While we found genes that behave as expected from what is reported in different studies, some did not agree with the previously reported transcriptional behavior. For example, *kazald1*, which is a gene whose function or mechanism of action has yet to be described, has been found to be expressed since early blastema and maintained through the regeneration process while the blastema is still sustained (Bryant, Johnson, Ditommaso, et al., 2017), however, I found it to be upregulated towards the differentiation and patterning stage (Figure 10).

5.4 Transcription factor and stage-enriched gene expression

5.4.1 Transcription factor expression

As mentioned in section 5.2, we identified 463 TFs within our axolotl transcriptome, and proceeded to analyze their expression through regeneration. To our surprise, we

found that most TFs exhibit a stage-enriched behavior, and most of them displayed low transcript abundance, having only 88 surpass 10 cpm (Figure 11).

It also came to my attention that replicates from the 15 dpa and 1 dpa stage exhibit antagonist behavior in most transcription factors that are specific for that stage. However, it is difficult to pinpoint the cause of this phenomenon, be it of technical or biological nature. To corroborate this finding, a proposed solution would be to either validate some of the genes that are preferentially expressed in one of the replicates via qRT-PCR, or by comparing the expression of a similar transcriptome.

Firstly, I checked the expression of several oncogenes that have been reported to induce stemness and whose expression has already been reported in previous works. As expected from what was reported in Stewart et al. (2013), *oct4* and *nanog* transcripts are absent on the set of TF's, probably because their expression is low and therefore they are being left out of the differential gene expression analyses; another transcript that is not highly expressed during regeneration is *sox2* whose expression is below 5 cpm.

Other stemness factors that had been reported as being expressed in regeneration like *c-myc* and *klf4* were not identified in the TF annotation perhaps because their transcripts were incomplete, and thus their protein domain annotation inadequate. However, upon closer inspection of the general annotation made in section 4.3, I found that the transcript for *klf4* is highly expressed between 3 and 9 dpa, which is consistent with the finding of Stewart et al. (2013).

The forkhead box transcription factor superfamily (FOX) has not been studied during limb regeneration. This TF superfamily is highly conserved in metazoans, and has important roles during development as it is involved in major signalling pathways such as the Hedgehog, TGF-β/SMAD and Wnt/β-Catenin pathways (Benayoun, Caburet, & Veitia, 2011). Transcripts that have been annotated as members of this superfamily are abundant in the limb regeneration transcriptomes, and several of these transcripts are differentially expressed during regeneration including *foxd1*, *foxf2*, *foxi1*, *foxj3*, *foxn1*, *foxo1* and *foxo4* among the most expressed TFs during the early and late blastema stages (15 and 25 dpa) (Figure 11). To the best of my knowledge, this family had not been previously identified as relevant to the regeneration process.

It has been reported that *foxf2*, through its interaction with the TGF-β/SMAD pathway, promotes the transition from epithellium to mesenchyma and thus the migration of cells, and also acts as an inducer of apoptosis, both in breast cancer (Meyer-Schaller, Heck, Tiede, Yilmaz, & Christofori, 2018). Its rapid upregulation directly after amputation (0 dpa) might be linked with its apoptosis inducing role, while later

upregulation (15 dpa) might be linked with the migration of cells to the blastema (Figure 11).

A subgroup of the FOX superfamily, FOXO transcription factors, have a very dynamic range of action, interacting with Insulin/IGF, MAPK, TFG-β/SMAD and Wnt/β-catenin pathways (Benayoun et al., 2011). Transcripts for *foxo1* and *foxo4* have similar expression patterns, having their maximum expression levels after amputation and early regeneration (0 and 1 dpa respectively, Figure 11), and they might have an important role in the regulation of the cell cycle, as the targets of *foxo4* are similar to *p53*, and are also regulated by *mdm2* (Brenkman, de Keizer, van den Broek, Jochemsen, & Burgering, 2008) (see section 5.5.1).

Members of the SMAD transcription factor family *smad1* and *smad4* are also present among the most expressed TFs, and they both display similar expression patterns. SMAD proteins are downstream in the TGF-β/SMAD pathway, as they form different protein complexes in order to control the expression of different genes, such as Myc, p15 and p21 (Feng, Liang, Liang, Zhai, & Lin, 2002; Massagué, Seoane, & Wotton, 2005). SMAD genes have begun to be studied during regeneration, where a study revealed that although SMAD3 has a more dominant role than SMAD2 (De Kroon et al., 2017), SMAD2 is required in order to activate *mmp-2* and *mmp-9*, which are responsible of ECM remodelling (Denis et al., 2016). The transcript for *smad2* is not among the most expressed TFs, however, its expression reached its maximum at 25 dpa (appendix 10.4), while the expression of *mmp-2* and *mmp-9* has been reported to reach its peak at very early stages of regeneration, meaning that perhaps the latter two are being transcriptionally activated by other elements (Seifert et al., 2012; E. V. Yang, Gardiner, Carlson, Nugas, & Bryant, 1999).

Some Hox genes are also crucial for regeneration, as they play an important role in the establishment of the anterior-posterior axis in limb development. A member of the HOXD cluster, *hoxd13*, is found between the most expressed TFs, having its peak of expression at early stages of regeneration during blastema formation (3 and 9 dpa), but also having a moderate expression at later stages (32 and 40 dpa) (Figure 11). Interestingly, in my analysis *hoxc11* is expressed after amputation (0 dpa) and in late stages (40 dpa). It has already been reported that members of the HOXC cluster are expressed in the axolotl limb (Nye, Cameron, Chernoff, & Stocum, 2003), however there is no described role for *hoxc11* in limb regeneration. Nevertheless, it is known that in mice, *hoxc11* is expressed in hindlimbs, restricted to the posterior part of the autopod (Hostikka & Capecchi, 1998). Its expression at the latter stages might be required for the establishment and maintainance of the anterior-posterior axis in the autopod, in correlation with its expression at early and late stages of regeneration.

Lastly, the T-box transcription factors *tbx4* and *tbx5* are indispensable for both limb development and regeneration. Contrary to other vertebrates, like human or mice, these proteins are expressed in both hindlimb and forelimb during embryogenesis. During limb regeneration, *tbx5* is expressed exclusively in forelimbs, while *tbx4* is expressed in hindlimbs (Khan, Linkhart, & Simon, 2002). While there is no characterization of the expression pattern of *tbx5*, based on the expression found on Figure 11, we can assume that its transcriptional expression is required mid/late blastema until redifferentiation (25 to 40 dpa). Although it is not among the most expressed TFs, *tbx4* seems to be present in the set of transcription factors that were identified, but its expression is low (< 3 cpm), implying that *tbx5* is the T-box transcription factor required out of the pair during regeneration.

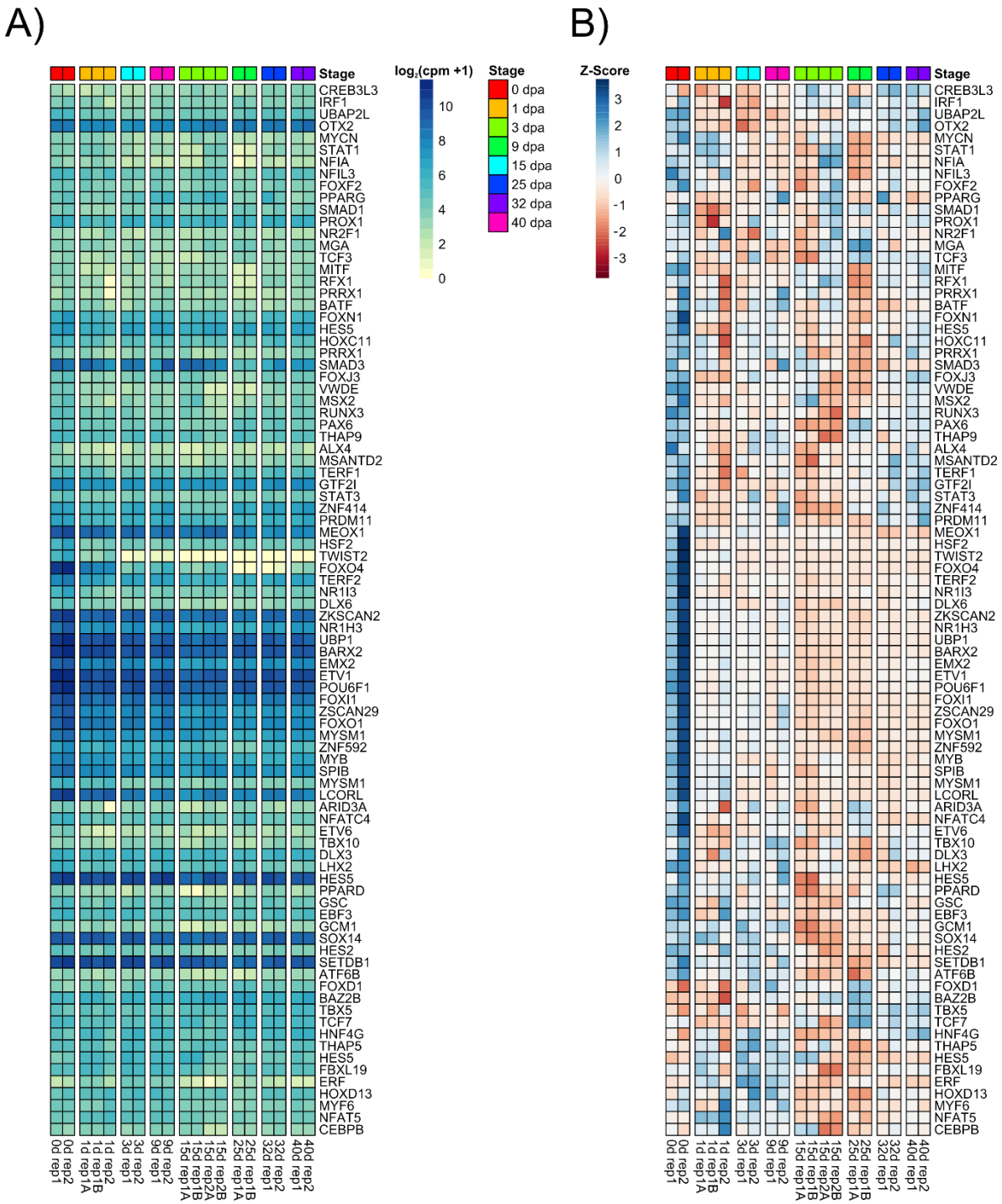

Figure 11 - Transcription Factor expression patterns during limb regeneration. A) Transcript levels in log2 of cpm of TFs that had at least 10 cpm in at least one sample B) Expression pattern of TFs that had at least 10 cpm in one sample as Z-Scores calculated by row.

5.4.2 Time point enriched gene expression

I was able to identify 520 genes that were preferentially expressed in one of the stages, and that were significantly differentially expressed in at least 4 of the time point comparisons. The first stage (0 dpa) had the most genes specifically enriched (320 genes). Out of the 520 enriched genes, 317 had an annotation.

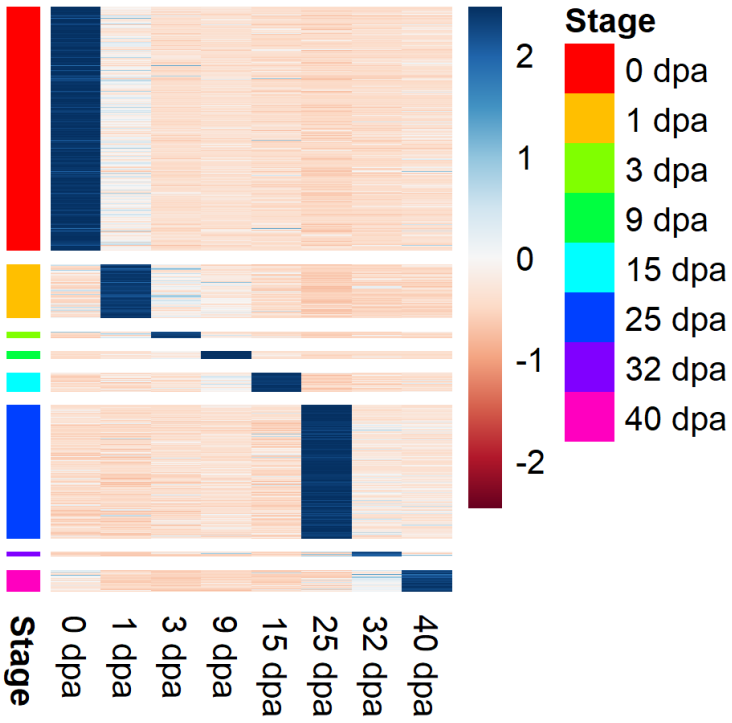

Figure 12 -Enriched genes per time point. Gene expression is represented using a Z-score, and enriched genes per stage are separated using horizontal blocks.

After the amputation (0 dpa), there is a high number of enriched genes being expressed. However, most of these genes are associated with muscle ECM structure such as Triadin, Myosin and Nebulin. Perhaps the abundance of these genes is due to the cellular composition of the stump, as before starting regeneration, muscle is the most abundant tissue in this structure (Han et al., 2005).

Early response (1 dpa) genes include genes such as hemoglobin, which has been reported to stimulate the expression of metalloproteases *mmp-2* and *mmp-9* through means that are yet to be elucidated (Tajima et al., 2005). Metalloproteases are, in turn, required for ECM remodeling during limb regeneration (E. V. Yang et al., 1999). Also, the LINE-1 retrotransposable elements are overexpressed at very early time points confirming the findings of Zhu et al. (2012), although the biological role of LINE-1 induction in regeneration remains unknown.

Of special interest to this project are the genes preferentially expressed during the mid and late blastema (15 and 25 dpa, respectively). Although our results did not delivered many annotated genes enriched in mid blastema, there are genes like *hpx*, which binds to heme groups with the highest affinity among all known proteins and induces a pro-inflammatory response (Tolosano & Altruda, 2002); and *tgs-6*, which is induced after injury promoting autophagy (S. Wang et al., 2017), that suggests that there are genes related with immune response and tissue repair at this stage.

The late blastema stage (25 dpa time point), which is the stage with the second most abundant set of enriched genes (Figure 9), involves diverse cellular processes necessary for the development of the limb, maintenance of stemness, but also differentiation. For example, *pdzrn3*, which is an ubiquitin-protein ligase, has been reported in previous studies to be correlated with the differentiation of myoblasts into myotubes by downregulating the differentiation inhibitor Id2 both transcriptionally and post-translationally (Honda & Inui, 2018). The transcript for this gene is upregulated during late blastema, suggesting the start of the differentiation of blastema cells into muscle tissues. Another gene involved in differentiation and upregulated at late blastema is *tenm4*, which is normally a regulator of axon guidance that has been reported to be expressed during myogenic differentiation (He et al., 2017), supporting the hypothesis that blastema cells start re-differentiating into muscle tissues at this stage.

As for genes involved in limb development, our results show that *hoxd-8* and *xhox-3* transcripts are enriched at 25 dpa. Even though their function has not been described during limb regeneration nor in development, *xhox-3* is required to establish the patterning axis during the gastrula and neurula stages during *Xenopus* embryogenesis (Altaba & Melton, 1989) and it is plausible that *xhox-3* may play a role in the establishment of the posterior-anterior axis during limb regeneration along with *ssh* in axolotl regeneration.

Another gene enriched during late blastema is *rif1*, which encodes a telomere-associated protein that regulates telomere length and the maintenance of H3K9me3 mark, maintaining the capabilities of self-renewal of embryonic stem cells (Dan et al., 2014). Cell replication tends to shorten telomeres, however, this is countered in stem and progenitor cells by activating telomerases keeping the telomeres from shortening, and thus delaying aging (Flores & Blasco, 2010). The increase of progenitor cell population in the limb may be responsible of the induction of telomerase associated genes, with the purpose of maintaining telomere length.

Approaching the end of regeneration (32 and 40 dpa), *hoxd-13* is enriched during this stage, which is normally expressed during zeugopod development (Figure 3B), as well

as elements of the ECM, keratin and *col1a2* (collagen alpha-2 chain) (Mouw, Ou, & Weaver, 2014), possibly due to the formation of the new ECM in the regenerated limb.

5.5 GO and KEGG pathway enrichment analyses

To analyze further than a set of known genes the regeneration process using these transcriptomes, I opted to use an enrichment analysis on two different functional annotations: the gene ontology (GO) and the KEGG pathway. By doing so, I expected to find known categories that have previously been described as involved in limb regeneration, as well as novel categories that might give us a deeper understanding of the limb regeneration process.

5.5.1 GO term enrichment analysis

Overall, I found 1,118 enriched GO terms in at least one of the time point comparisons described in section 5.3, using both up and downregulated gene sets identified in the differential expression analysis. In Figure 13, I show only the 3 most enriched GO terms per comparison delivered by up and downregulated genes.

One of the most dynamic GO terms is “collagen catabolic process” (GO:0030574), which is enriched in upregulated genes in early (3 to 15 dpa) and later stages (25 to 40 dpa) (Figure 13). Among the transcripts annotated with this GO term found several encoding proteins that form collagen chains, as well as metalloproteases, which are required for remodeling of the ECM (E. V. Yang et al., 1999).

In the first stages of regeneration (0-3 dpa), terms related to wound healing and immune response are found, confirming previous findings by (Stewart et al., 2013). Wound healing related terms including “positive regulation of response to wounding” (GO:1903036), positive regulation of epithelial cell proliferation involved in wound healing (GO:006005), “regulation of response to wounding” (GO:1903034) and “wound healing” (GO: 0042060), which are enriched in upregulated genes at 1 and 3 dpa, and in downregulated genes at 25 dpa (Appendix 0).

Amongst the genes that are changing through the first stages, and is related with wound healing is *sdc1*, which has been reported to act as a receptor for ligands and amplifies the spatial reach of the latter; *sdc1* also binds to factors regulating the pro-inflammatory response (Bartlett, Park, & Pyong, 2007). Another gene that changes its expression is the one encoding *eppk1*, a protein coding gene that relieves injury through the organization of keratin (Szabo et al., 2015). Other pro-inflammatory response genes, such as *il8*, interleukin receptors and *ptgs2*, are also upregulated during the early stages of regeneration.

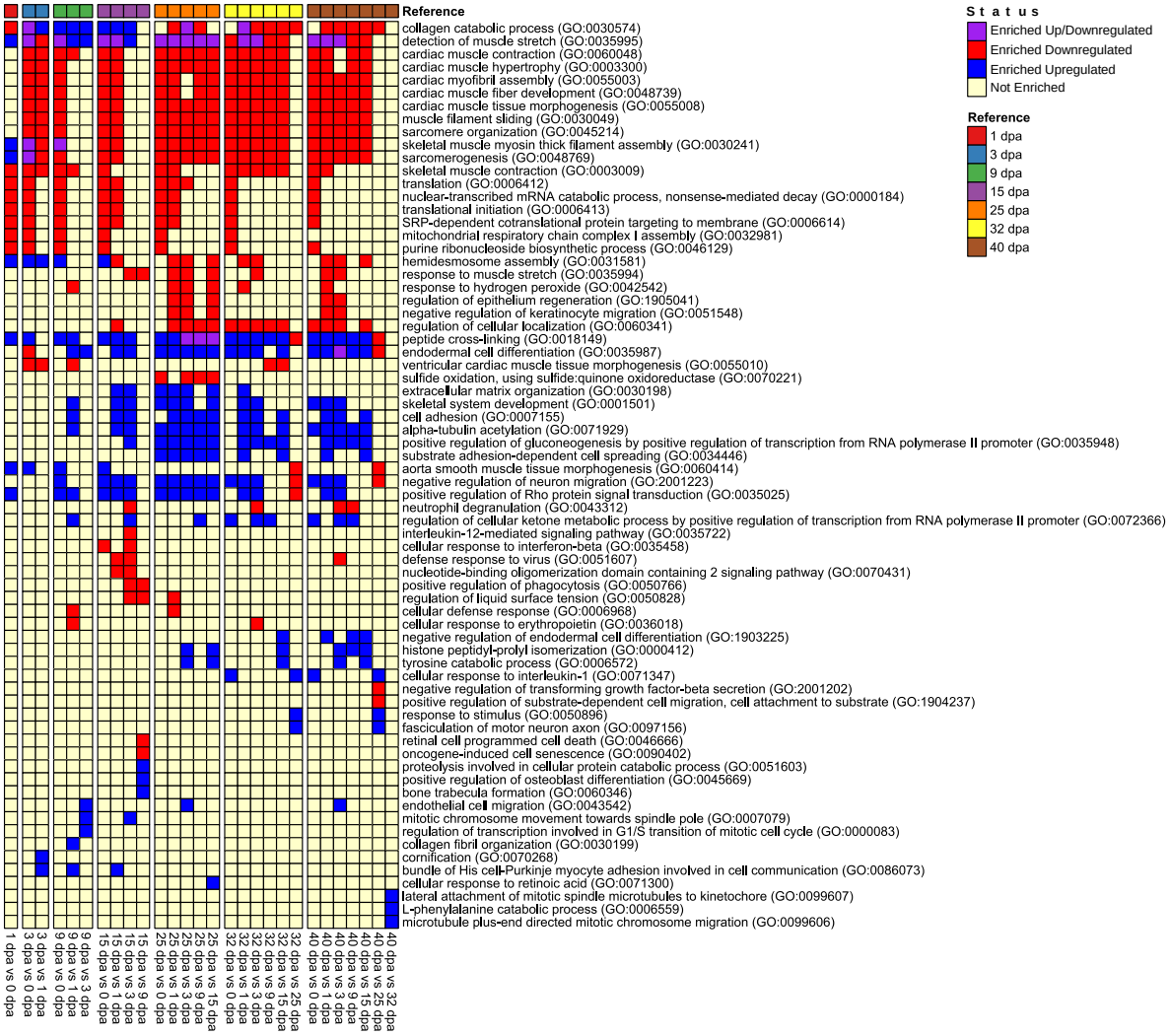

Figure 13 - Most enriched GO terms throughout the DGE analysis. Top three GO terms in terms of p-value for up and downregulated genes in each comparison are shown, showing in a trinary manner whether a category in enriched amongst up or downregulated genes, or both. Each vertical block represents the comparisons using a specific time as a reference used for the differential gene expression analyses, showing the status (up and down regulated) for that specific reference.

For immune response related terms, “leukocyte chemotaxis involved in inflammatory response” (GO:0002232) is found enriched in upregulated genes early during regeneration (3-9 dpa), and other terms like “positive regulation of monocyte chemotaxis” (GO:0090026) and “neutrophil chemotaxis” (GO:0030593) are enriched amongst downregulated genes at later stages (25 dpa) (Appendix 0). This is coherent with the process, since it indicates that the inflammatory response is triggered after the amputation, preventing wound infection and mediating the generation of new blood vessels (Godwin & Rosenthal, 2014; Stewart et al., 2013).

Interestingly, macrophage related terms are overrepresented at 15 dpa, having "regulation of macrophage migration inhibitory factor signaling pathway" (GO:2000446) overrepresented in genes that are upregulated and "negative regulation of macrophage derived foam cell differentiation" (GO:0010745) in downregulated genes. Macrophages are key for carrying a successful regeneration (Godwin, Pinto, & Rosenthal, 2013). Among the genes in these categories is *angpt1*, which has been proven to guide macrophage differentiation towards a pro-inflammatory response (Seok et al., 2013).

Also upregulated and present among the immune response GO terms during the first stages of regeneration, is the inhibitor of kappa B α (*iκbα*), which sequesters NF-κB blocking its nuclear localization signal and impeding its translocation into the nuclei. This inhibition is terminated by the protein IKK, which phosphorylates the inhibitors and thus releases NF-κB, promoting a pro-inflammatory response after an injury (Fan et al., 2004). Although it is counterintuitive to have a protein that inhibits the inflammatory response in an early stage of regeneration, perhaps the analysis of the expression dynamics of *iκbα* at earlier stages after amputation could provide an insight of the immune response, since it is known that drastic changes occur during the first 24 hours in humans (Rabani et al., 2011; Zhao, Fung-Leung, Bittner, Ngo, & Liu, 2014). Also, the interaction between IKK and IκBα occurs at a post-translational level (Fan et al., 2004), making impossible to measure if IκBα is inhibiting the immune response using RNA-seq during axolotl limb regeneration.

Another molecular factor that has been shown to be involved in the response upon damage or wounding are reactive oxygen species (ROS), which have been characterized as signal molecules produced after mechanical injuries in both animals (Mittal, Siddiqui, Tran, Reddy, & Malik, 2014) and plants (Baxter, Mittler, & Suzuki, 2014). The GO term "cellular response to reactive oxygen species" (GO:0034614) is overrepresented in upregulated genes at the start of regeneration (1 dpa) and in downregulated genes at 40 dpa (Appendix 0). From this category, a few genes that stand out due to their role in different developmental processes, like E3 ubiquitin-protein ligase *mdm2*, which is known for its role of inactivating tumor protein p53 by ubiquitin-mediated degradation (Brooks & Gu, 2006). Mdm2 is indirectly induced by ROS, when the latter one induces the activity of p53, which in turn transcriptionally activates Mdm2 in a negative feedback loop (Y. Chen, Liu, Shi, & Shao, 2018). By activating Mdm2, a series of different cellular processes are modulated, such as the activation of cell cycle arrest, allowing cells within the stump to proliferate.

Recently, Herrera-Rincon et al. (2018) reported that upon application of progesterone in amputated limbs of *Xenopus laevis*, they were able to achieve successful regeneration even at an adult stage, this by modifying the transcriptional networks

that included signaling pathways as the ones involving Ca^{2+} and K^{+}. In my transcriptomes, I observed that the term “response to progesterone” (GO:0032570) is enriched in upregulated genes during most of the stages (Appendix 0), and among the genes that are changing associated with progesterone are transcription factor *jun-b*, which have been proven to induce aberrant proliferation in fibroblasts (Bossy-Wetzel, Bravo, & Hanahan, 1992); also Fos-related antigen 2 (*fosl2*), whose function is to dimerize with JUN transcription factors and, as a complex, are involved in cell proliferation and cell cycle is upregulated during most stages (Cook, Aziz, & McMahon, 1999).

Since regeneration can be seen as the reactivation of developmental programs, it is important that certain morphogenetic programs are expressed after damage or amputation. Among some of the morphogenesis-related enriched GO terms in our transcriptome are “embryonic limb morphogenesis” (GO:0030326) in upregulated genes at 3 and 9 dpa; “bone morphogenesis” (GO:0060349) in upregulated genes at 32 dpa; and “aorta smooth muscle tissue morphogenesis” (GO:0060414) in upregulated genes from 1 to 15 dpa, as well as downregulated genes at 32 and 40 dpa (Figure 13, Appendix 0).

Among the genes which show differential expression along the process are several well-known limb developmental factors such as *rspo2*, which is required for the activation of Wnt proteins and thus involved in the dorsal-ventral axis specification (Jin, Turcotte, Crocker, Han, & Yoon, 2011). Another transcript that has been reported to be involved in the establishment of the aforementioned axis and upregulated in this same category is the one corresponding to β-Catenin (*ctnnb1*), which activates transcription factors in response to Wnt signaling (Jin et al., 2011). A classical gene associated with blastema formation is changing in our transcriptome is Paired mesoderm homeobox protein 1 (*prrx1*), which is enriched in connective tissue derived cells and has been shown that its expression increases as regeneration advances, bus associated with proliferative stages, just as reported in previous works (Gerber et al., 2018). These findings confirm that the limb regeneration process is fairly similar to that of limb morphogenesis during embryo development (M. R. J. Carlson, Bryant, & Gardiner, 1998; Gerber et al., 2018).

A cellular process that has been overlooked in previous regeneration studies is the transition between mesenchymal and epithelial cells. This transitions allow mesenchymal cells to migrate, proliferate, and differentiate (Yao, Dai, & Peng, 2011), which are processes required for a successful limb regeneration. A term that is present in groups of up-regulated genes across most regeneration stages is “mesenchyme migration” (GO:0090131), this is coherent with the developmental process since mesenchymal cells migrate to the region of the wound after injury (Yao

et al., 2011). Nearing the end of regeneration (32 dpa), the term “negative regulation of epithelial to mesenchymal transition” (GO:0010719) is enriched among upregulated genes, perhaps marking the end of the migration of these cells to the blastema and defining the start of the re-differentiation stage. Genes among this category are Disabled homolog 2-interacting protein (*dab2ip*), which inhibits the transition of epithelium to mesenchymal fate through interaction of Wnt signaling pathway (Nauseef & Henry, 2011), and Secreted frizzled-related protein 1 (*sfrp1*), which is induced in mesenchymal cells, which in turn halts Wnt in function of the transition of current epithelial cells to mesenchyme (Bovolenta, Esteve, Ruiz, Cisneros, & Lopez-Rios, 2008).

One of the most interesting and studied cell types in limb regeneration are fibroblasts, as they contribute the majority of the progenitor cells that generate the blastema population (Gerber et al., 2018). After 25 dpa, the term “positive regulation of fibroblast proliferation” (GO:0048146) was found enriched among upregulated genes. Between the genes that were found upregulated and within this category, is Fibroblast growth factor 10 (*fgf10*), which has been shown to play a role in the establishment of the AER (Sekine et al., 1999), and in the induction of proliferation of certain epithelial cells (Turner & Grose, 2010). Another gene present within this category is Discoidin domain-containing receptor 2 (*ddr2*), which is involved in multiple processes including cell proliferation and ECM remodeling (Kawai, Hisaki, Sugiura, Naito, & Kano, 2012).

5.5.2 KEGG pathway enrichment analysis

I decided to analyze my data using a KEGG term enrichment analysis, based on the following criteria: i) the linear structure of the hierarchy of KEGG terms, ii) their reduced number in comparison to GO terms, and iii) the content of several categories for important signaling pathways involved in animal developmental processes. Our analyses with KEGG retrieved 174 enriched terms in at least one of the comparisons made in section 5.3 using either up or downregulated gene groups (Figure 14 and Appendix 10.3).

A KEGG term that was expected and found to be enriched in upregulated genes during the first stages of regeneration and in downregulated later is the IL-17 signaling pathway. This cytokine is secreted by T-helper cells and is required for an inflammatory response. Interestingly, IL-17 is also expressed during the development of limbs, especially during bone development, and it has been suggested that it fulfills functions during general organogenesis (Bie, Jin, Zhang, & Dong, 2017). Among the genes associated with this category, the TNF receptor-associated factors appear to be a majority. These proteins have multiple functions including proinflammatory responses activation and response to different stress (Bradley & Pober, 2001)

Also, these factors appear to be involved in early injury responses and promoting oxidative stres$Ray, Huang, & Tsuji, 2012)

Another term I was interested in was “Cell cycle” (Appendix 10.3). From 15 dpa onwards, Cell cycle term appears to be enriched in upregulated genes. Most of the genes found within this category are related with the transition of phase G1 to S o f the cell cycle, like G1/S-specific cyclin-E1, DNA replication licensing factor mcm2, mcm3 and mcm7; as well as Serine/threonine-protein kinase Chk1. This strongly suggest that cell cycle is active and thus there is proliferation within these stages, where there is a blastema present.

One of the signaling pathways that changes the most is the PI3K-Akt signaling pathway. This pathway has several cellular functions, including, but not limited to, angiogenesis, metabolism, growth and proliferation. The activation of AKT lead to the interaction of other factors such as FOXO transcription factors and mTOR, who in turn regulate strongly cell proliferation (Hemmings & Restuccia, 2012). The PI3K-Akt pathway is also able to interact with development-related protein SHH (Riobo, Lu, Ai, Haines, & Emerson, 2006). During regeneration, PI3K-Akt signaling pathway KEGG term is enriched in upregulated genes at 15 dpa and seems to maintain the levels of expression for the remainder of the regeneration stages (Appendix 10.3).

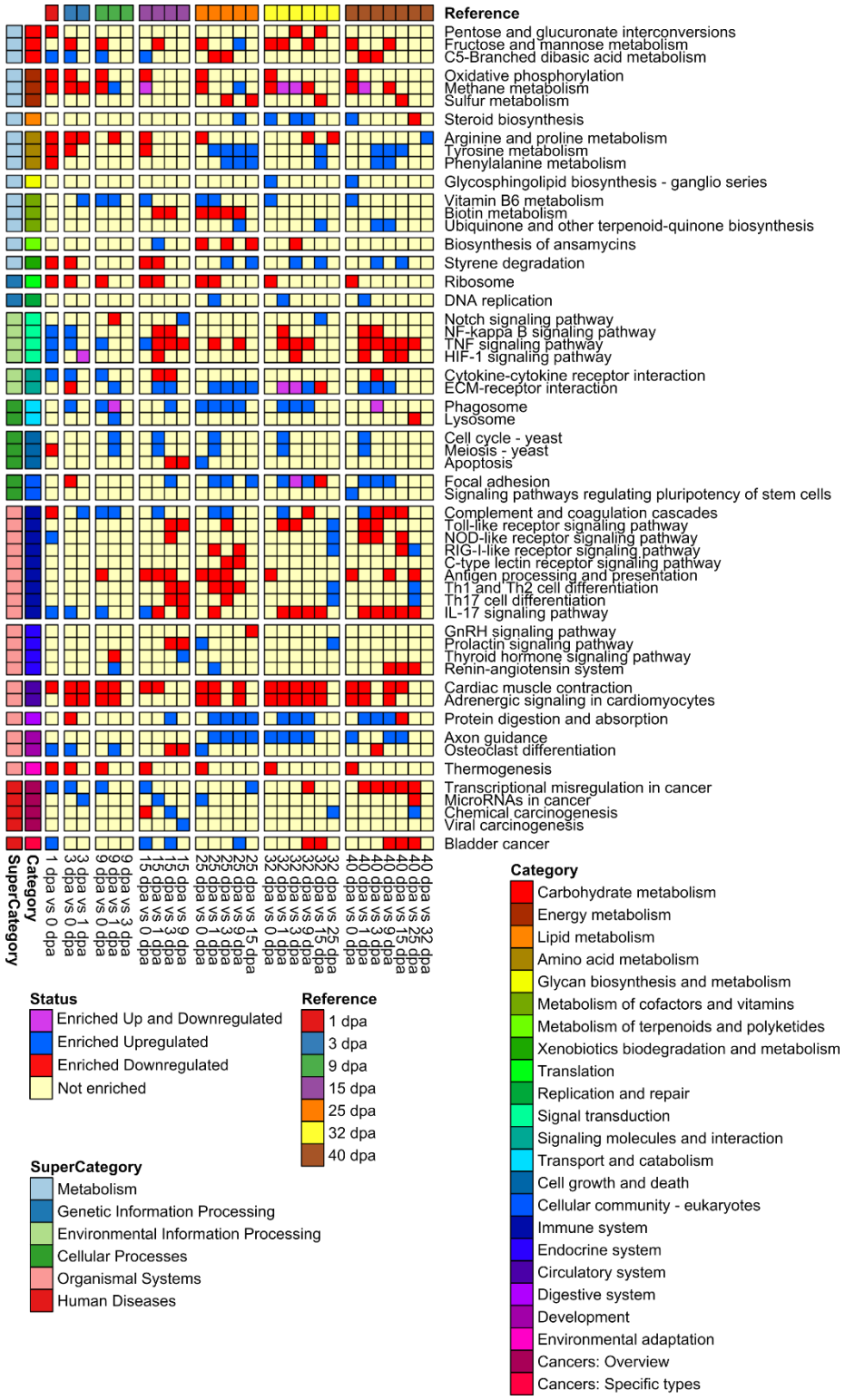

Figure 14 - Top KEGG enriched terms. Top three enriched categories in each contrast are shown in each spot for each of the comparison made, showing enriched categories in upregulated (blue), downregulated (red) or both (purple) gene sets.

5.6 Gene co-expression networks

To identify groups of genes that have a similar transcriptional behavior, I generated a gene co-expression network using WGCNA. I categorized the 20,000 most changing genes into 63 different modules, ranging from 38 to 990 genes per module. Gene modules were classified in a heuristic manner into 5 different categories (Figure 15).

Module MEsalmon seems to lower its expression at 15 and 25 dpa, while having high expression on early stages (0-9 dpa). This module has 325 genes, and most genes are enriched with the GO term “negative regulation of interleukin-1 beta secretion” (GO:0050713) and trans-differentiation (GO:0060290). Interleukin-1 beta is produced by macrophages as part of the inflammatory response, so its negative regulation is no longer required as regeneration progresses and macrophages begin to disappear from the amputation site (Tank et al., 1976). Regarding trans-differentiation, a gene associated with this term is MyoG, and although it might not be likely that it is inducing trans-differentiation during regeneration as it has been reported that muscle cells don’t form other tissues during regeneration (Kragl et al., 2009; Takimoto, Oro, Hiraki, & Shukunami, 2012), it is expressed during regeneration, although it is suspected that its role is not essential (Zammit, 2017).

Late blastema associated module MEblue, which has low expression from 0 dpa until 15 dpa, and then having a peak of transcriptional expression levels at 25 dpa. The module contains 856 genes that are associated with the GO terms “extracellular matrix disassembly” (GO:0022617), “positive regulation of histone H3-K9 methylation” (GO:0051574) and “signal transduction involved in mitotic G1 DNA damage checkpoint” (GO:0072431). In transcripts associated with the histone H3K9 methylation I found the previously discussed gene Telomere-associated protein RIF1 (see section 5.4.2). Among transcripts that are associated with the G1 phase DNA damage is E2F7, which is a transcriptional repressor of E2F1 and an indirect inhibitor of proliferation (Carvajal, Hamard, Tonnessen, & Manfredi, 2012), and since there is no evidence of tissue was damaged at this stage, it is hard to pinpoint a function for E2F7.

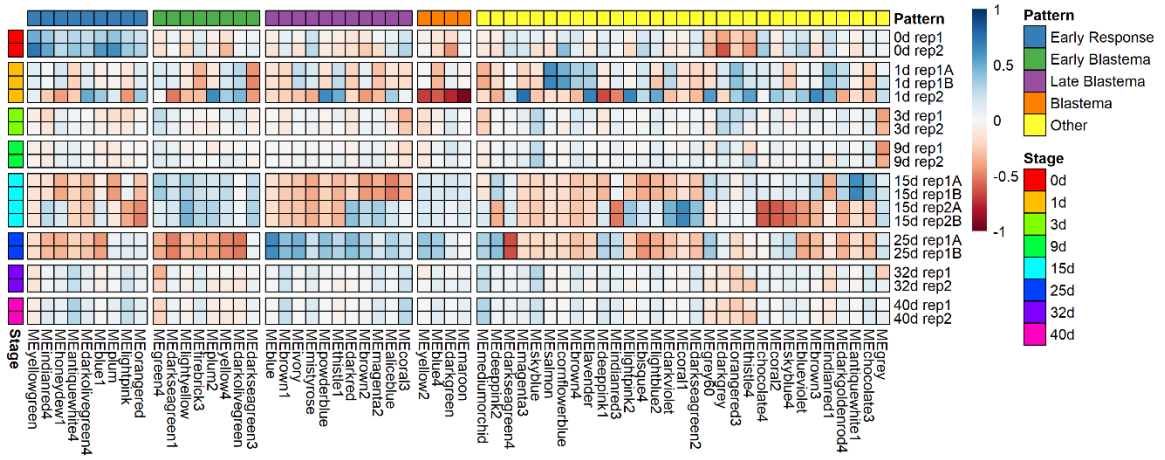

Figure 15 - Gene co-expression network eigengenes. The general behavior of the gene module is represented by an eigengene, with a color scale where blue shows a trend of genes having higher expression and red lower expression. Pattern clusters were identified manually.

The MEplum2 module, which is primarily expressed in early blastema (15 dpa) and a lower expression on late blastema (25 dpa), contains 208 genes. Terms that are enriched among this module's transcripts are associated with "DNA recombination" (GO:0006310) and "DNA replication" (GO:0006260). Almost all genes that are associated with DNA recombination and replication are transposons (LINE-1, PEG10, Tf2-11, etcetera), suggesting that germline specific elements act on this stage, as described by Zhu et al. (2012).

6 Conclusions

By looking for known regeneration factors, we found that genes such as FGF8, SHH, and members from the HoxD cluster, follow the already described behavior in our transcriptomes. However, KAZALD1, a gene that had previously been described as a blastema enriched gene, does not present the reported behavior in our transcriptomic data.

I identified 12,897 lncRNAs that are present in other published transcriptomes, suggesting a potential function in the regeneration process, however no biological function can be assigned to them through computational analyses.

Through our TF annotation and analysis of expression, it was clear that many TF factors have a peak in expression right after amputation (0 dpa), and many of them seem to be preferentially expressed in one of the time points, suggesting that their expression is bound to a specific molecular process. Some of them, like the forkhead

(FOX) TFs, which have not been characterized during limb regeneration, seem to be abundant among TFs that are being overexpressed right after amputation.

The search for enriched genes per time point revealed that LINE-1 transposable elements are preferentially expressed in an early time point (1 dpa), confirming what had already been described in the literature.

GO terms allowed us to identified genes involved with immune response, more specifically genes involved with inflammatory response being upregulated in the first time points (3 and 9 dpa), as well as the genes related with the differentiation and migration of macrophages being downregulated as early as the early blastema (15 dpa). Also, this analysis allowed us to identify MDM2, a gene that inactivates p53, which is known to be expressed during regeneration.

KEGG term enrichment analysis also permitted to further confirm the changes in the immune system during regeneration, but also allowing us to identify genes related to the transition of the cell cycle from phase G1 to S like cyclin E1, being upregulated at the early blastema stage.

Overall, we were able to characterize the transcriptional landscape changes during the limb regeneration process in the Mexican axolotl *Ambystoma mexicanum*.

7 Perspectives

7.1 Validate and characterize novel genes found

While we were able to pinpoint interesting genes that had already been characterized in limb regeneration as well as novel elements, we aren't able to pinpoint their exact function through RNA-seq data alone. Consequently, it is required that we further study the genes that we have found using other available data sets such as the single cell RNA-seq generated by Gerber et al. (2018), as well as other techniques such as immunoprecipitation in the case of TFs, immunolocalization and *in situ* hybridization experiments.

7.2 Study the role of transposable elements during regeneration

It has already been described that most of the axolotl's genome is composed of transposable elements (Nowoshilow et al., 2018), however their role in regeneration as well as their presence in the axolotl genome remains to be studied. In this work, I was able to identify transposable element LINE-1 to be enriched in certain time points of the regeneration, but in order to understand what its role is in regeneration one of the steps necessary would be to study further small RNA-seq data during this process, as well as the localization in the blastema of these elements through in-situ hybridization.

7.3 Assign function to lncRNAs

Since lncRNAs don't normally have conserved RNA motifs present in their primary structure, it is difficult to assign them a function. However, there are a variety of approaches we could follow to further characterize these elements. To start, we could use the GO term enrichment analysis and the gene co-expression network done in this work to identify the function of its co-expressed genes and following a "guilty by association" approach we could assign them a putative function. Nonetheless, a more if a stricter characterization is required, we could perform ChAR-seq experiments to pinpoint where the lncRNAs are interacting with the genome.

8 Acknowledgements

We thank Annie Espinal Centeno and Tania Janeth Quintana Gómez, members of the Molecular and Developmental Complexity Group (Cruz-Ramírez lab), and who were responsible for animal husbandry and all wet lab experiments described in section 4.1. We also Thank Dr. Alfredo Herrera Estrella for the support with a termination fellowship. We would also like to thank the Consejo Nacional de Ciencia y Tecnología (CONACYT) for the scholarship provided during this project.

9 References

Alexa, A., & Rahnenführer, J. (2007). Gene set enrichment analysis with topGO. *Bioconductor Improvments*, 27. Retrieved from http://scholar.google.com/scholar?hl=en&btnG=Search&q=intitle:Gene+set+enrichment+analysis+with+topGO#0%5Cnftp://mirrors.nic.funet.fi/bioconductor.org/2.7/bioc/vignettes/topGO/inst/doc/topGO.pdf

Alexa, A., Rahnenführer, J., & Lengauer, T. (2006). Improved scoring of functional groups from gene expression data by decorrelating GO graph structure. *Bioinformatics*, *22*(13), 1600–1607. https://doi.org/10.1093/bioinformatics/btl140

Altaba, A. R. i., & Melton, D. A. (1989). Involvement of the Xenopus homeobox gene Xhox3 in pattern formation along the anterior-posterior axis. *Cell*. https://doi.org/10.1016/0092-8674(89)90969-0

Andrews, S. (2010). FastQC: A quality control tool for high throughput sequence data. https://doi.org/citeulike-article-id:11583827

Bartlett, A. H., Park, K. H., & Pyong, W. (2007). Molecular and Cellular Mechanisms of Syndecans in Tissue Injury and Inflammation. *Mol. Cells*, *24*(2), 153–166.

Baxter, A., Mittler, R., & Suzuki, N. (2014). ROS as key players in plant stress signalling. *Journal of Experimental Botany*. https://doi.org/10.1093/jxb/ert375

Benayoun, B. A., Caburet, S., & Veitia, R. A. (2011). Forkhead transcription factors: Key players in health and disease. *Trends in Genetics*. https://doi.org/10.1016/j.tig.2011.03.003

Bie, Q., Jin, C., Zhang, B., & Dong, H. (2017). IL-17B: A new area of study in the IL-17 family. *Molecular Immunology*. https://doi.org/10.1016/j.molimm.2017.07.004

BLAST. (2013). BLAST Basic Local Alignment Search Tool. Retrieved from http://blast.ncbi.nlm.nih.gov/Blast.cgi?CMD=Web&PAGE_TYPE=BlastDocs&amp...

Bolger, A. M., Lohse, M., & Usadel, B. (2014). Trimmomatic: A flexible trimmer for Illumina sequence data. *Bioinformatics*, *30*(15), 2114–2120. https://doi.org/10.1093/bioinformatics/btu170

Bossy-Wetzel, E., Bravo, R., & Hanahan, D. (1992). Transcription factors JunB and c-Jun are selectively up-regulated and functionally implicated in fibrosarcoma development. *Genes and Development*. https://doi.org/10.1101/gad.6.12a.2340

Boutet, E., Lieberherr, D., Tognolli, M., Schneider, M., & Bairoch, A. (2007). UniProtKB/Swiss-Prot. *Methods in Molecular Biology (Clifton, N.J.)*, *406*, 89–112. https://doi.org/10.1007/978-1-4939-3167-5_2

Bovolenta, P., Esteve, P., Ruiz, J. M., Cisneros, E., & Lopez-Rios, J. (2008). Beyond Wnt inhibition: new functions of secreted Frizzled-related proteins in development and disease. *Journal of Cell Science*. https://doi.org/10.1242/jcs.026096

Bradley, J. R., & Pober, J. S. (2001). Tumor necrosis factor receptor-associated factors (TRAFs). *Oncogene*. https://doi.org/10.1038/sj.onc.1204788

Bray, N. L., Pimentel, H., Melsted, P., & Pachter, L. (2016). Near-optimal probabilistic RNA-seq quantification. *Nature Biotechnology*, *34*(5), 525–527. https://doi.org/10.1038/nbt.3519

Brenkman, A. B., de Keizer, P. L. J., van den Broek, N. J. F., Jochemsen, A. G., & Burgering, B. M. T. (2008). Mdm2 induces mono-ubiquitination of FOXO4. *PLoS ONE*. https://doi.org/10.1371/journal.pone.0002819

Brooks, C. L., & Gu, W. (2006). p53 ubiquitination: Mdm2 and beyond. *Molecular Cell*. https://doi.org/10.1016/j.molcel.2006.01.020

Bryant, D. M., Johnson, K., Ditommaso, T., Regev, A., Haas, B. J., Whited, J. L., … Peshkin, L. (2017). A Tissue-Mapped Axolotl De Novo Transcriptome. *CellReports*, *18*(3), 762–776. https://doi.org/10.1016/j.celrep.2016.12.063

Bryant, D. M., Johnson, K., DiTommaso, T., Tickle, T., Couger, M. B., Payzin-Dogru, D., … Whited, J. L. (2017). A Tissue-Mapped Axolotl De Novo Transcriptome Enables Identification of Limb Regeneration Factors. *Cell Reports*, *18*(3), 762–776. https://doi.org/10.1016/j.celrep.2016.12.063

Bürglin, T. R. (2008). The Hedgehog protein family. *Genome Biology*. https://doi.org/10.1186/gb-2008-9-11-241

Caballero-Pérez, J., Espinal-Centeno, A., Falcon, F., García-Ortega, L. F., Curiel-Quesada, E., Cruz-Hernández, A., … Cruz-Ramírez, A. (2018). Transcriptional landscapes of Axolotl (Ambystoma mexicanum). *Developmental Biology*. https://doi.org/10.1016/j.ydbio.2017.08.022

Carlson, B. M. (2007). *Principles of Regenerative Biology*. *Principles of Regenerative Biology*. https://doi.org/10.1016/B978-0-12-369439-3.X5000-4

Carlson, M. R. J., Bryant, S. V., & Gardiner, D. M. (1998). Expression of Msx-2 during development, regeneration, and wound healing in axolotl limbs. *Journal of Experimental Zoology*. https://doi.org/10.1002/(SICI)1097-010X(19981215)282:6<715::AID-JEZ7>3.0.CO;2-F

Carvajal, L. A., Hamard, P. J., Tonnessen, C., & Manfredi, J. J. (2012). E2F7, a novel target, is up-regulated by p53 and mediates DNA damage-dependent transcriptional repression. *Genes and Development*. https://doi.org/10.1101/gad.184911.111

Chen, T. S., & Chen, P. S. (1994). The myth of Prometheus and the liver. *Journal of the*

Royal Society of Medicine, *87*(12), 754–755. Retrieved from https://www.ncbi.nlm.nih.gov/pubmed/7853302

Chen, Y., Liu, K., Shi, Y., & Shao, C. (2018). The tango of ROS and p53 in tissue stem cells. *Cell Death & Differentiation*, *25*(4), 637–639. https://doi.org/10.1038/s41418-018-0062-2

Church, R. H., Krishnakumar, A., Urbanek, A., Geschwindner, S., Meneely, J., Bianchi, A., … Brazil, D. P. (2015). Gremlin1 preferentially binds to bone morphogenetic protein-2 (BMP-2) and BMP-4 over BMP-7. *Biochemical Journal*. https://doi.org/10.1042/BJ20140771

Cook, S. J., Aziz, N., & McMahon, M. (1999). The repertoire of fos and jun proteins expressed during the G1 phase of the cell cycle is determined by the duration of mitogen-activated protein kinase activation. *Mol Cell Biol*. https://doi.org/10.1128/MCB.19.1.330

Currie, J. D., Kawaguchi, A., Traspas, R. M., Schuez, M., Chara, O., & Tanaka, E. M. (2016). Live Imaging of Axolotl Digit Regeneration Reveals Spatiotemporal Choreography of Diverse Connective Tissue Progenitor Pools. *Developmental Cell*. https://doi.org/10.1016/j.devcel.2016.10.013

Dan, J., Liu, Y., Liu, N., Chiourea, M., Okuka, M., Wu, T., … Liu, L. (2014). Rif1 Maintains Telomere Length Homeostasis of ESCs by Mediating Heterochromatin Silencing. *Developmental Cell*. https://doi.org/10.1016/j.devcel.2014.03.004

De Kroon, L. M. G., Narcisi, R., Van Den Akker, G. G. H., Vitters, E. L., Blaney Davidson, E. N., Van Osch, G. J. V. M., & Van Der Kraan, P. M. (2017). SMAD3 and SMAD4 have a more dominant role than SMAD2 in TGFβ-induced chondrogenic differentiation of bone marrow-derived mesenchymal stem cells. *Scientific Reports*. https://doi.org/10.1038/srep43164

Denis, J.-F., Sader, F., Gatien, S., Villiard, É., Philip, A., & Roy, S. (2016). Activation of Smad2 but not Smad3 is required to mediate TGF-β signaling during axolotl limb regeneration. *Development*. https://doi.org/10.1242/dev.131466

Fan, C., Li, Q., Zhang, Y., Liu, X., Luo, M., Abbott, D., … Engelhardt, J. F. (2004). IκBα and IκBβ possess injury context-specific functions that uniquely influence hepatic NF-κB induction and inflammation. *Journal of Clinical Investigation*. https://doi.org/10.1172/JCI17337

Fei, J.-F., Schuez, M., Knapp, D., Taniguchi, Y., Drechsel, D. N., & Tanaka, E. M. (2017). Efficient gene knockin in axolotl and its use to test the role of satellite cells in limb regeneration. *Proceedings of the National Academy of Sciences*, 201706855. https://doi.org/10.1073/pnas.1706855114

Feng, X. H., Liang, Y. Y., Liang, M., Zhai, W., & Lin, X. (2002). Direct interaction of c-Myc with Smad2 and Smad3 to inhibit TGF-β-mediated induction of the CDK

inhibitor p15Ink4B. *Molecular Cell*. https://doi.org/10.1016/S1097-2765(01)00430-0

Finn, R. D., Clements, J., Arndt, W., Miller, B. L., Wheeler, T. J., Schreiber, F., … Eddy, S. R. (2015). HMMER web server: 2015 Update. *Nucleic Acids Research*, *43*(W1), W30–W38. https://doi.org/10.1093/nar/gkv397

Flores, I., & Blasco, M. A. (2010). The role of telomeres and telomerase in stem cell aging. *FEBS Letters*. https://doi.org/10.1016/j.febslet.2010.07.042

Gardiner, D. M., Blumberg, B., Komine, Y., & Bryant, S. V. (1995). Regulation of HoxA expression in developing and regenerating axolotl limbs. *Development*, *121*.

Gardiner, D. M., & Bryant, S. V. (1996). Molecular mechanisms in the control of limb regeneration: the role of homeobox genes. *The International Journal of Developmental Biology*. https://doi.org/10.1387/IJDB.8877453

Gerber, T., Murawala, P., Knapp, D., Masselink, W., Schuez, M., Hermann, S., … Treutlein, B. (2018). Single-cell analysis uncovers convergence of cell identities during axolotl limb regeneration. *Science*. https://doi.org/10.1126/science.aaq0681

Gilbert, S. F. (2010). *Developmental Biology*. *Developmental Biology*. https://doi.org/10.1016/j.ydbio.2010.03.016

Godwin, J. W., Pinto, A. R., & Rosenthal, N. A. (2013). Macrophages are required for adult salamander limb regeneration. *Proceedings of the National Academy of Sciences*. https://doi.org/10.1073/pnas.1300290110

Godwin, J. W., & Rosenthal, N. (2014). Scar-free wound healing and regeneration in amphibians: immunological influences on regenerative success. *Differentiation; Research in Biological Diversity*. https://doi.org/10.1016/j.diff.2014.02.002

Grabherr, M. G., Haas, B. J., Yassour, M., Levin, J. Z., Thompson, D. A., Amit, I., … Regev, A. (2011). Full-length transcriptome assembly from RNA-Seq data without a reference genome. *Nature Biotechnology*, *29*(7), 644–652. https://doi.org/10.1038/nbt.1883

Graham, A., Papalopulu, N., & Krumlauf, R. (1989). The murine and Drosophila homeobox gene complexes have common features of organization and expression. *Cell*. https://doi.org/10.1016/0092-8674(89)90912-4

Haas, B. J. (2017). Trinotate: Transcriptome Functional Annotation and Analysis. Retrieved from https://trinotate.github.io/

Haas, B. J., Papanicolaou, A., Yassour, M., Grabherr, M., Philip, D., Bowden, J., … Regev, A. (2013). De novo transcript sequence recostruction from RNA-Seq: reference generation and analysis with Trinity. *Nature Protocols*, *8*(8), 1–43. https://doi.org/10.1038/nprot.2013.084.De

Haas, B. J., & Whited, J. L. (2017). Advances in Decoding Axolotl Limb Regeneration. *Trends in Genetics*. https://doi.org/10.1016/j.tig.2017.05.006

Habermann, B., Bebin, A.-G., Herklotz, S., Volkmer, M., Eckelt, K., Pehlke, K., … Tanaka, E. M. (2004). An Ambystoma mexicanum EST sequencing project: analysis of 17,352 expressed sequence tags from embryonic and regenerating blastema cDNA libraries. *Genome Biology*, *5*(9), R67. https://doi.org/10.1186/gb-2004-5-9-r67

Han, M., Yang, X., Taylor, G., Burdsal, C. A., Anderson, R. A., & Muneoka, K. (2005). Limb regeneration in higher vertebrates: Developing a roadmap. *Anatomical Record - Part B New Anatomist*. https://doi.org/10.1002/ar.b.20082

He, K., Wu, G., Li, W. X., Guan, D., Lv, W., Gong, M., … Lu, A. (2017). A transcriptomic study of myogenic differentiation under the overexpression of PPARγ by RNA-Seq. *Scientific Reports*. https://doi.org/10.1038/s41598-017-14275-2

Hemmings, B. A., & Restuccia, D. F. (2012). PI3K-PKB / Akt Pathway. *Cold Spring Harbor Perspectives in Biology*. https://doi.org/10.1101/cshperspect.a011189

Hernández-Oñate, M. A., & Herrera-Estrella, A. (2015). Damage response involves mechanisms conserved across plants, animals and fungi. *Current Genetics*. https://doi.org/10.1007/s00294-014-0467-5

Herrera-Rincon, C., Golding, A. S., Moran, K. M., Harrison, C., Martyniuk, C. J., Guay, J. A., … Levin, M. (2018). Brief Local Application of Progesterone via a Wearable Bioreactor Induces Long-Term Regenerative Response in Adult Xenopus Hindlimb. *Cell Reports*, *25*(6), 1593–1609.e7. https://doi.org/https://doi.org/10.1016/j.celrep.2018.10.010

Honda, T., & Inui, M. (2018). PDZRN3 regulates differentiation of myoblasts into myotubes through transcriptional and posttranslational control of Id2. *Journal of Cellular Physiology*. https://doi.org/10.1002/jcp.27113

Honig, L. S., & Summerbell, D. (1985). Maps of strength of positional signalling activity in the developing chick wing bud. *Journal of Embryology and Experimental Morphology*.

Hostikka, S. L., & Capecchi, M. R. (1998). The mouse Hoxc11 gene: Genomic structure and expression pattern. *Mechanisms of Development*. https://doi.org/10.1016/S0925-4773(97)00182-2

Hwang, B., Lee, J. H., & Bang, D. (2018). Single-cell RNA sequencing technologies and bioinformatics pipelines. *Experimental & Molecular Medicine*. https://doi.org/10.1038/s12276-018-0071-8

Iten, L. E., & Bryant, S. V. (1973). Forelimb regeneration from different levels of amputation in the newt, Notophthalmus viridescens: Length, rate, and stages. *Wilhelm Roux' Archiv Für Entwicklungsmechanik*, *173*(4), 263–282.

282. https://doi.org/10.1007/BF00575834

Jenkins, M. H., Alrowaished, S. S., Goody, M. F., Crawford, B. D., & Henry, C. A. (2016). Laminin and Matrix metalloproteinase 11 regulate Fibronectin levels in the zebrafish myotendinous junction. *Skeletal Muscle*. https://doi.org/10.1186/S13395-016-0089-3

Jin, Y. R., Turcotte, T. J., Crocker, A. L., Han, X. H., & Yoon, J. K. (2011). The canonical Wnt signaling activator, R-spondin2, regulates craniofacial patterning and morphogenesis within the branchial arch through ectodermal-mesenchymal interaction. *Developmental Biology*. https://doi.org/10.1016/j.ydbio.2011.01.004

Kang, Y. J., Yang, D. C., Kong, L., Hou, M., Meng, Y. Q., Wei, L., & Gao, G. (2017). CPC2: A fast and accurate coding potential calculator based on sequence intrinsic features. *Nucleic Acids Research*, *45*(W1), W12–W16. https://doi.org/10.1093/nar/gkx428

Kato, T., Miyazaki, K., Shimizu-Nishikawa, K., Koshiba, K., Obara, M., Mishima, H. K., & Yoshizato, K. (2003). Unique expression patterns of matrix metalloproteinases in regenerating newt limbs. *Developmental Dynamics*, *226*(2), 366–376. https://doi.org/10.1002/dvdy.10247

Kawai, I., Hisaki, T., Sugiura, K., Naito, K., & Kano, K. (2012). Discoidin domain receptor 2 (DDR2) regulates proliferation of endochondral cells in mice. *Biochemical and Biophysical Research Communications*, *427*(3), 611–617. https://doi.org/https://doi.org/10.1016/j.bbrc.2012.09.106

Kent, W. J. (2002). BLAT - The BLAST-like alignment tool. *Genome Research*, *12*(4), 656–664. https://doi.org/10.1101/gr.229202. Article published online before March 2002

Khan, P., Linkhart, B., & Simon, H. G. (2002). Different regulation of T-box genes Tbx4 and Tbx5 during limb development and limb regeneration. *Developmental Biology*. https://doi.org/10.1006/dbio.2002.0801

Kmita, M., Tarchini, B., Zàkàny, J., Logan, M., Tabin, C. J., & Duboule, D. (2005). Early developmental arrest of mammalian limbs lacking HoxA/HoxD gene function. *Nature*. https://doi.org/10.1038/nature03648

Kong, L., Zhang, Y., Ye, Z. Q., Liu, X. Q., Zhao, S. Q., Wei, L., & Gao, G. (2007). CPC: Assess the protein-coding potential of transcripts using sequence features and support vector machine. *Nucleic Acids Research*, *35*(SUPPL.2). https://doi.org/10.1093/nar/gkm391

Kragl, M., Knapp, D., Nacu, E., Khattak, S., Maden, M., Epperlein, H. H., & Tanaka, E. M. (2009). Cells keep a memory of their tissue origin during axolotl limb regeneration. *Nature*. https://doi.org/10.1038/nature08152

Krogh, A., Larsson, B., von Heijne, G., & Sonnhammer, E. L. (2001). Predicting transmembrane protein topology with a hidden Markov model: application to complete genomes. *Journal of Molecular Biology*, *305*(3), 567–580. https://doi.org/10.1006/jmbi.2000.4315

Lambert, S. A., Jolma, A., Campitelli, L. F., Das, P. K., Yin, Y., Albu, M., … Weirauch, M. T. (2018). The Human Transcription Factors. *Cell*, *172*(4), 650–665. https://doi.org/10.1016/j.cell.2018.01.029

Lemons, D., & McGinnis, W. (2006). Genomic evolution of hox gene clusters. *Science*. https://doi.org/10.1126/science.1132040

Lenhoff, H. M., & Lenhoff, S. O. (1984). Tissue grafting in animals: Its discovery in 1742 by Abraham Trembley as he experimented with Hydra. *Biol. Bull.*, *166*(November 1983), 1–10. https://doi.org/10.2307/1541425

Love, M. I., Huber, W., & Anders, S. (2014). Moderated estimation of fold change and dispersion for RNA-seq data with DESeq2. *Genome Biology*. https://doi.org/10.1186/s13059-014-0550-8

Mallo, M., & Alonso, C. R. (2013). The regulation of Hox gene expression during animal development. *Development (Cambridge, England)*. https://doi.org/10.1242/dev.068346

Massagué, J., Seoane, J., & Wotton, D. (2005). Smad transcription factors. *Genes and Development*. https://doi.org/10.1101/gad.1350705

Medina-Martínez, O., Bradley, A., & Ramírez-Solis, R. (2000). A large targeted deletion of Hoxb1-Hoxb9 produces a series of single- segment anterior homeotic transformations. *Developmental Biology*. https://doi.org/10.1006/dbio.2000.9683

Meyer-Schaller, N., Heck, C., Tiede, S., Yilmaz, M., & Christofori, G. (2018). Foxf2 plays a dual role during transforming growth factor beta-induced epithelial to mesenchymal transition by promoting apoptosis yet enabling cell junction dissolution and migration. *Breast Cancer Research*, *20*(1), 118. https://doi.org/10.1186/s13058-018-1043-6

Mistry, J., & Finn, R. (2007). Pfam. In *Comparative Genomics* (pp. 43–58). https://doi.org/10.1007/978-1-59745-515-2_4

Mittal, M., Siddiqui, M. R., Tran, K., Reddy, S. P., & Malik, A. B. (2014). Reactive Oxygen Species in Inflammation and Tissue Injury. *Antioxidants & Redox Signaling*. https://doi.org/10.1089/ars.2012.5149

Monaghan, J. R., Epp, L. G., Putta, S., Page, R. B., Walker, J. A., Beachy, C. K., … Voss, S. R. (2009). Microarray and cDNA sequence analysis of transcription during nerve-dependent limb regeneration. *BMC Biology*, *7*, 1. https://doi.org/10.1186/1741-7007-7-1

Morgan, T. H. (1901). Regeneration. *Columbia University Biological Series VII.*, 342.

Mouw, J. K., Ou, G., & Weaver, V. M. (2014). Extracellular matrix assembly: A multiscale deconstruction. *Nature Reviews Molecular Cell Biology*. https://doi.org/10.1038/nrm3902

Mu, X., Bellayr, I., Pan, H., Choi, Y., & Li, Y. (2013). Regeneration of Soft Tissues Is Promoted by MMP1 Treatment after Digit Amputation in Mice. *PLoS ONE*, *8*(3). https://doi.org/10.1371/journal.pone.0059105

Mundlos, S., & Horn, D. (2014). Development of the Limbs. In *Limb Malformations: An Atlas of Genetic Disorders of Limb Development* (pp. 2–9). Berlin, Heidelberg: Springer Berlin Heidelberg. https://doi.org/10.1007/978-3-540-95928-1_1

Muneoka, K., Fox, W. F., & Bryant, S. V. (1986). Cellular contribution from dermis and cartilage to the regenerating limb blastema in axolotls. *Developmental Biology*. https://doi.org/10.1016/0012-1606(86)90062-X

Nacu, E., Gromberg, E., Oliveira, C. R., Drechsel, D., & Tanaka, E. M. (2016). FGF8 and SHH substitute for anterior-posterior tissue interactions to induce limb regeneration. *Nature*. https://doi.org/10.1038/nature17972

Nauseef, J. T., & Henry, M. D. (2011). Epithelial-to-mesenchymal transition in prostate cancer: Paradigm or puzzle? *Nature Reviews Urology*. https://doi.org/10.1038/nrurol.2011.85

Nowoshilow, S., Schloissnig, S., Fei, J. F., Dahl, A., Pang, A. W. C., Pippel, M., … Myers, E. W. (2018). The axolotl genome and the evolution of key tissue formation regulators. *Nature*, *554*(7690), 50–55. https://doi.org/10.1038/nature25458

Nye, H. L. D., Cameron, J. A., Chernoff, E. A. G., & Stocum, D. L. (2003). Regeneration of the urodele limb: A review. *Developmental Dynamics*, *226*(2), 280–294. https://doi.org/10.1002/dvdy.10236

Ogata, H., Goto, S., Sato, K., Fujibuchi, W., Bono, H., & Kanehisa, M. (1999). KEGG: Kyoto encyclopedia of genes and genomes. *Nucleic Acids Research*. https://doi.org/10.1093/nar/27.1.29

Parr, B. A., & Mc Mahon, A. P. (1995). Dorsalizing signal Wnt-7a required for normal polarity of D–V and A–P axes of mouse limb. *Nature*. https://doi.org/10.1038/374350a0

Petersen, T. N., Brunak, S., Von Heijne, G., & Nielsen, H. (2011). SignalP 4.0: Discriminating signal peptides from transmembrane regions. *Nature Methods*. https://doi.org/10.1038/nmeth.1701

Rabani, M., Levin, J. Z., Fan, L., Adiconis, X., Raychowdhury, R., Garber, M., … Regev, A. (2011). Metabolic labeling of RNA uncovers principles of RNA production and degradation dynamics in mammalian cells. *Nature Biotechnology*.

https://doi.org/10.1038/nbt.1861

Ratcliff, M. J. (2005). Experimentation, communication and patronage: a perspective on René-Antoine Ferchault de Réaumur (1683-1757). *Biology of the Cell / under the Auspices of the European Cell Biology Organization*, *97*(4), 231–3. https://doi.org/10.1042/BC20040079

Ray, P. D., Huang, B. W., & Tsuji, Y. (2012). Reactive oxygen species (ROS) homeostasis and redox regulation in cellular signaling. *Cellular Signalling*. https://doi.org/10.1016/j.cellsig.2012.01.008

Reiß, C., Olsson, L., & Hoßfeld, U. (2015). The history of the oldest self-sustaining laboratory animal: 150 years of axolotl research. *Journal of Experimental Zoology Part B: Molecular and Developmental Evolution*, *324*(5), 393–404. https://doi.org/10.1002/jez.b.22617

Riddle, R. D., Johnson, R. L., Laufer, E., & Tabin, C. (1993). Sonic hedgehog mediates the polarizing activity of the ZPA. *Cell*. https://doi.org/10.1016/0092-8674(93)90626-2

Riobo, N. A., Lu, K., Ai, X., Haines, G. M., & Emerson, C. P. (2006). Phosphoinositide 3-kinase and Akt are essential for Sonic Hedgehog signaling. *Proceedings of the National Academy of Sciences*. https://doi.org/10.1073/pnas.0504337103

Ruddle, F. H., Bartels, J. L., Bentley, K. L., Kappen, C., Murtha, M. T., & Pendleton, J. W. (1994). Evolution of Hox genes. *Annual Review of Genetics*, *28*(1), 423–442.

Ryan, J. F., Mazza, M. E., Pang, K., Matus, D. Q., Baxevanis, A. D., Martindale, M. Q., & Finnerty, J. R. (2007). Pre-bilaterian origins of the hox cluster and the hox code: Evidence from the sea anemone, Nematostella vectensis. *PLoS ONE*. https://doi.org/10.1371/journal.pone.0000153

Schmidt, A. J. (1968). *Cellular Biology of Vertebrate Regeneration and Repair*. University of Chicago Press.

Seifert, A., Monaghan, J., Voss, R., & Maden, M. (2012). Skin regeneration in adult axolotls: A blueprint for scar-free healing in vertebrates. *PLoS ONE*, *7*(4). https://doi.org/10.1371/journal.pone.0032875

Sekine, K., Ohuchi, H., Fujiwara, M., Yamasaki, M., Yoshizawa, T., Sato, T., … Kato, S. (1999). Fgf10 is essential for limb and lung formation. *Nature Genetics*. https://doi.org/10.1038/5096

Seok, S. H., Heo, J. I., Hwang, J. H., Na, Y. R., Yun, J. H., Lee, E. H., … Cho, C. H. (2013). Angiopoietin-1 elicits pro-inflammatory responses in monocytes and differentiating macrophages. *Molecules and Cells*. https://doi.org/10.1007/s10059-013-0088-8

Simon, H. G., & Tabin, C. J. (1993). Analysis of Hox-4.5 and Hox-3.6 expression during

newt limb regeneration: differential regulation of paralogous Hox genes suggest different roles for members of different Hox clusters. *Development (Cambridge, England)*.

Smith, J. J., Timoshevskaya, N., Timoshevskiy, V. A., Keinath, M. C., Hardy, D., & Voss, S. R. (2018). A Chromosome-Scale Assembly of the Enormous (32 Gb) Axolotl Genome. *BioRxiv*. Retrieved from http://biorxiv.org/content/early/2018/07/20/373548.abstract

Sobkow, L., Epperlein, H. H., Herklotz, S., Straube, W. L., & Tanaka, E. M. (2006). A germline GFP transgenic axolotl and its use to track cell fate: Dual origin of the fin mesenchyme during development and the fate of blood cells during regeneration. *Developmental Biology*, *290*(2), 386–397. https://doi.org/10.1016/j.ydbio.2005.11.037

Sonawane, A. R., Platig, J., Fagny, M., Chen, C. Y., Paulson, J. N., Lopes-Ramos, C. M., … Kuijjer, M. L. (2017). Understanding Tissue-Specific Gene Regulation. *Cell Reports*. https://doi.org/10.1016/j.celrep.2017.10.001

Soneson, C., Love, M. I., & Robinson, M. D. (2016). Differential analyses for RNA-seq: transcript-level estimates improve gene-level inferences. *F1000Research*, *4*, 1521. https://doi.org/10.12688/f1000research.7563.2

Stewart, R., Rascón, C. A., Tian, S., Nie, J., Barry, C., Chu, L. F., … Dewey, C. N. (2013). Comparative RNA-seq Analysis in the Unsequenced Axolotl: The Oncogene Burst Highlights Early Gene Expression in the Blastema. *PLoS Computational Biology*, *9*(3). https://doi.org/10.1371/journal.pcbi.1002936

Suemori, H., & Noguchi, S. (2000). Hox C cluster genes are dispensable for overall body plan of mouse embryonic development. *Developmental Biology*. https://doi.org/10.1006/dbio.2000.9651

Szabo, S., Wögenstein, K. L., Österreicher, C. H., Guldiken, N., Chen, Y., Doler, C., … Fuchs, P. (2015). Epiplakin attenuates experimental mouse liver injury by chaperoning keratin reorganization. *Journal of Hepatology*. https://doi.org/10.1016/j.jhep.2015.01.007

Tajima, T., Yoshida, E., Yamashita, A., Ohmura, S., Tomitaka, Y., Sugiki, M., … Maruyama, M. (2005). Hemoglobin stimulates the expression of matrix metalloproteinases, MMP-2 and MMP-9 by synovial cells: a possible cause of joint damage after intra-articular hemorrhage. *Journal of Orthopaedic Research*, *23*(4), 891–898. https://doi.org/https://doi.org/10.1016/j.orthres.2005.01.003

Takimoto, A., Oro, M., Hiraki, Y., & Shukunami, C. (2012). Direct conversion of tenocytes into chondrocytes by Sox9. *Experimental Cell Research*. https://doi.org/10.1016/j.yexcr.2012.04.002

Tank, P. W., Carlson, B. M., & Connelly, T. G. (1976). A staging system for forelimb

regeneration in the axolotl, Ambystoma mexicanum. *Journal of Morphology*, *150*(1), 117–128. https://doi.org/10.1002/jmor.1051500106

Tolosano, E., & Altruda, F. (2002). Hemopexin: structure, function, and regulation. *DNA Cell Biol.* https://doi.org/10.1089/104454902753759717

Torok, M. A., Gardiner, D. M., Shubin, N. H., & Bryant, S. V. (1998). Expression of HoxD genes in developing and regenerating axolotl limbs. *Developmental Biology*, *200*(2), 225–233. https://doi.org/10.1006/dbio.1998.8956

Tsonis, P. A., & Fox, T. P. (2009). Regeneration according to Spallanzani. *Developmental Dynamics*. https://doi.org/10.1002/dvdy.22057

Turner, N., & Grose, R. (2010). Fibroblast growth factor signalling: From development to cancer. *Nature Reviews Cancer*. https://doi.org/10.1038/nrc2780

Verheyden, J. M., & Sun, X. (2008). An Fgf/Gremlin inhibitory feedback loop triggers termination of limb bud outgrowth. *Nature*. https://doi.org/10.1038/nature07085

Wang, S., Lee, C., Kim, J., Hyun, J., Lim, M., Cha, H. J., … Jung, Y. (2017). Tumor necrosis factor-inducible gene 6 protein ameliorates chronic liver damage by promoting autophagy formation in mice. *Experimental & Molecular Medicine*. https://doi.org/10.1038/emm.2017.140

Wang, Z., Gerstein, M., & Snyder, M. (2009). RNA-Seq: A revolutionary tool for transcriptomics. *Nature Reviews Genetics*. https://doi.org/10.1038/nrg2484

Waterhouse, R. M., Seppey, M., Simão, F. A., Manni, M., Ioannidis, P., Klioutchnikov, G., … Zdobnov, E. M. (2017). BUSCO Applications from Quality Assessments to Gene Prediction and Phylogenomics. *Molecular Biology and Evolution*. https://doi.org/10.1093/molbev/msx319

Wetterstrand, K. A. (2016). DNA Sequencing Costs: Data from the NHGRI Large-Scale Genome Sequencing Program. *Dostępny w Internec Www.Genome.Gov/Sequencingcostsdata*. https://doi.org/10.1016/S0965-2299(00)90833-1

Wingett, S. (2018). FastQ Screen. Retrieved August 20, 2005, from https://www.bioinformatics.babraham.ac.uk/projects/fastq_screen/

Yang, E. V., Gardiner, D. M., Carlson, M. R. J., Nugas, C. A., & Bryant, S. V. (1999). Expression of Mmp-9 and related matrix metalloproteinase genes during axolotl limb regeneration. *Developmental Dynamics*. https://doi.org/10.1002/(SICI)1097-0177(199909)216:1<2::AID-DVDY2>3.0.CO;2-P

Yang, Y., & Niswander, L. (1995). Interaction between the signaling molecules WNT7a and SHH during vertebrate limb development: Dorsal signals regulate anteroposterior patterning. *Cell*. https://doi.org/10.1016/0092-8674(95)90297-X

Yao, D., Dai, C., & Peng, S. (2011). Mechanism of the Mesenchymal-Epithelial Transition and Its Relationship with Metastatic Tumor Formation. *Molecular Cancer Research*. https://doi.org/10.1158/1541-7786.MCR-10-0568

Zammit, P. S. (2017). Function of the myogenic regulatory factors Myf5, MyoD, Myogenin and MRF4 in skeletal muscle, satellite cells and regenerative myogenesis. *Seminars in Cell & Developmental Biology*, *72*, 19–32. https://doi.org/https://doi.org/10.1016/j.semcdb.2017.11.011

Zhang, H., Azevedo, R. B. R., Lints, R., Doyle, C., Teng, Y., Haber, D., & Emmons, S. W. (2003). Global regulation of Hox gene expression in C. elegans by a SAM domain protein. *Developmental Cell*. https://doi.org/10.1016/S1534-5807(03)00136-9

Zhang, Z., Verheyden, J. M., Hassell, J. A., & Sun, X. (2009). FGF-Regulated Etv Genes Are Essential for Repressing Shh Expression in Mouse Limb Buds. *Developmental Cell*. https://doi.org/10.1016/j.devcel.2009.02.008

Zhao, S., Fung-Leung, W. P., Bittner, A., Ngo, K., & Liu, X. (2014). Comparison of RNA-Seq and microarray in transcriptome profiling of activated T cells. *PLoS ONE*. https://doi.org/10.1371/journal.pone.0078644

Zhu, W., Kuo, D., Nathanson, J., Satoh, A., Pao, G. M., Yeo, G. W., … Hunter, T. (2012). Retrotransposon long interspersed nucleotide element-1 (LINE-1) is activated during salamander limb regeneration. *Development Growth and Differentiation*. https://doi.org/10.1111/j.1440-169X.2012.01368.x

10 Appendix

10.1 Software versions

Software	Version
BLAT	v35
BUSCO	v3.0
CPC	v0.9.r2
CPC2	v0.1
edgeR	v3.20.7
Fastq Screen	v0.11.3
HMMER	v3.1b2
Kallisto	v0.43.1
ncbi-blast+	v2.6.0
R	v3.4.3
SignalP	v4.1
tmhmm	v2.0c
topGO	v2.30.0
Trimmomatic	v0.36
Trinotate	v3.0.1
WGCNA	v1.63

10.2 GO enriched terms

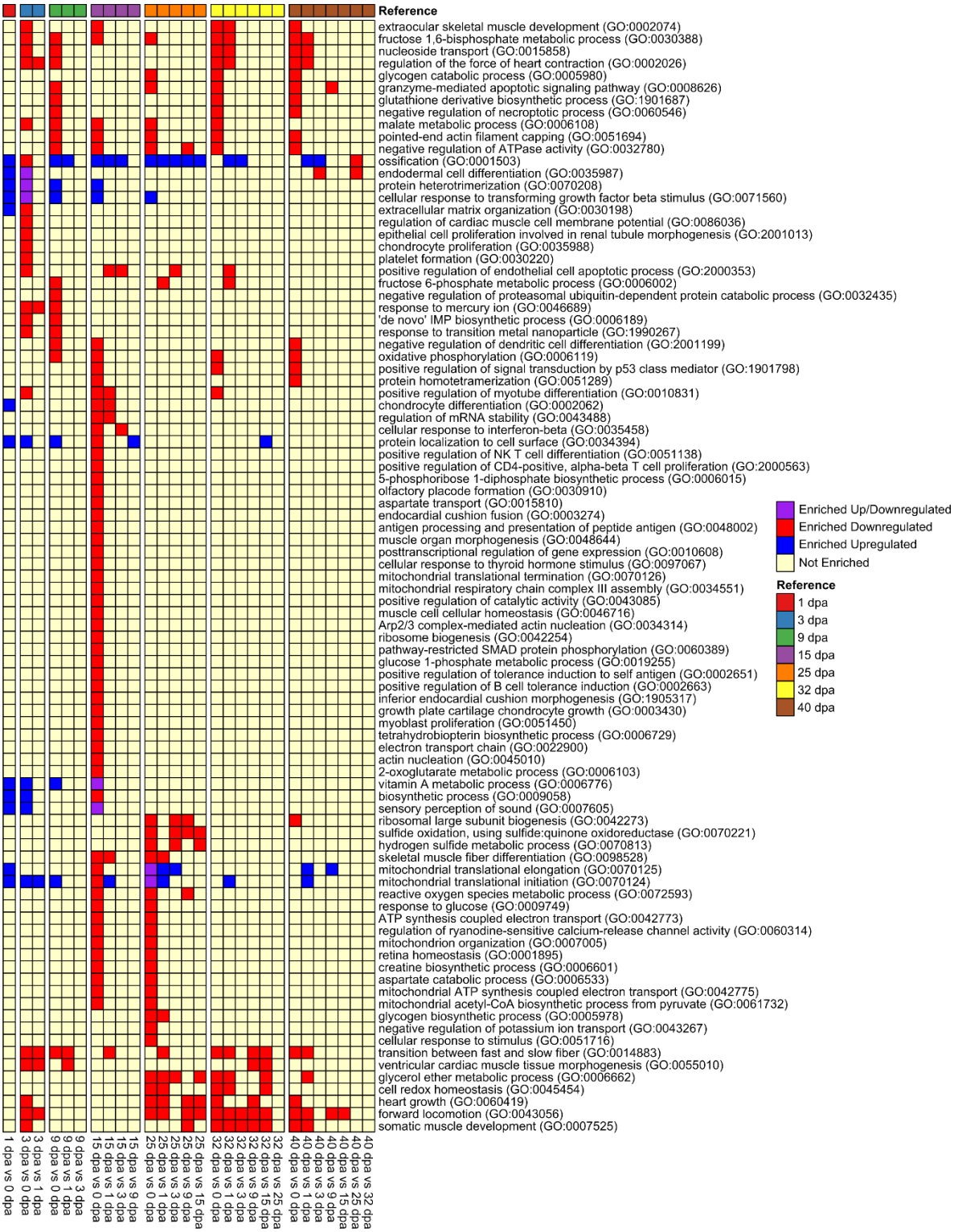
Reference
extraocular skeletal muscle development (GO:0002074)
fructose 1,6-bisphosphate metabolic process (GO:0030388)
nucleoside transport (GO:0015858)
regulation of the force of heart contraction (GO:0002026)
glycogen catabolic process (GO:0005980)
granzyme-mediated apoptotic signaling pathway (GO:0008626)
glutathione derivative biosynthetic process (GO:1901687)
negative regulation of necroptotic process (GO:0060546)
malate metabolic process (GO:0006108)
pointed-end actin filament capping (GO:0051694)
negative regulation of ATPase activity (GO:0032780)
ossification (GO:0001503)
endodermal cell differentiation (GO:0035987)
protein heterotrimerization (GO:0070208)
cellular response to transforming growth factor beta stimulus (GO:0071560)
extracellular matrix organization (GO:0030198)
regulation of cardiac muscle cell membrane potential (GO:0086036)
epithelial cell proliferation involved in renal tubule morphogenesis (GO:2001013)
chondrocyte proliferation (GO:0035988)
platelet formation (GO:0030220)
positive regulation of endothelial cell apoptotic process (GO:2000353)
fructose 6-phosphate metabolic process (GO:0006002)
negative regulation of proteasomal ubiquitin-dependent protein catabolic process (GO:0032435)
response to mercury ion (GO:0046689)
'de novo' IMP biosynthetic process (GO:0006189)
response to transition metal nanoparticle (GO:1990267)
negative regulation of dendritic cell differentiation (GO:2001199)
oxidative phosphorylation (GO:0006119)
positive regulation of signal transduction by p53 class mediator (GO:1901798)
protein homotetramerization (GO:0051289)
positive regulation of myotube differentiation (GO:0010831)
chondrocyte differentiation (GO:0002062)
regulation of mRNA stability (GO:0043488)
cellular response to interferon-beta (GO:0035458)
protein localization to cell surface (GO:0034394)
positive regulation of NK T cell differentiation (GO:0051138)
positive regulation of CD4-positive, alpha-beta T cell proliferation (GO:2000563)
5-phosphoribose 1-diphosphate biosynthetic process (GO:0006015)
olfactory placode formation (GO:0030910)
aspartate transport (GO:0015810)
endocardial cushion fusion (GO:0003274)
antigen processing and presentation of peptide antigen (GO:0048002)
muscle organ morphogenesis (GO:0048644)
posttranscriptional regulation of gene expression (GO:0010608)
cellular response to thyroid hormone stimulus (GO:0097067)
mitochondrial translational termination (GO:0070126)
mitochondrial respiratory chain complex III assembly (GO:0034551)
positive regulation of catalytic activity (GO:0043085)
muscle cell cellular homeostasis (GO:0046716)
Arp2/3 complex-mediated actin nucleation (GO:0034314)
ribosome biogenesis (GO:0042254)
pathway-restricted SMAD protein phosphorylation (GO:0060389)
glucose 1-phosphate metabolic process (GO:0019255)
positive regulation of tolerance induction to self antigen (GO:0002651)
positive regulation of B cell tolerance induction (GO:0002663)
inferior endocardial cushion morphogenesis (GO:1905317)
growth plate cartilage chondrocyte growth (GO:0003430)
myoblast proliferation (GO:0051450)
tetrahydrobiopterin biosynthetic process (GO:0006729)
electron transport chain (GO:0022900)
actin nucleation (GO:0045010)
2-oxoglutarate metabolic process (GO:0006103)
vitamin A metabolic process (GO:0006776)
biosynthetic process (GO:0009058)
sensory perception of sound (GO:0007605)
ribosomal large subunit biogenesis (GO:0042273)
sulfide oxidation, using sulfide:quinone oxidoreductase (GO:0070221)
hydrogen sulfide metabolic process (GO:0070813)
skeletal muscle fiber differentiation (GO:0098528)
mitochondrial translational elongation (GO:0070125)
mitochondrial translational initiation (GO:0070124)
reactive oxygen species metabolic process (GO:0072593)
response to glucose (GO:0009749)
ATP synthesis coupled electron transport (GO:0042773)
regulation of ryanodine-sensitive calcium-release channel activity (GO:0060314)
mitochondrion organization (GO:0007005)
retina homeostasis (GO:0001895)
creatine biosynthetic process (GO:0006601)
aspartate catabolic process (GO:0006533)
mitochondrial ATP synthesis coupled electron transport (GO:0042775)
mitochondrial acetyl-CoA biosynthetic process from pyruvate (GO:0061732)
glycogen biosynthetic process (GO:0005978)
negative regulation of potassium ion transport (GO:0043267)
cellular response to stimulus (GO:0051716)
transition between fast and slow fiber (GO:0014883)
ventricular cardiac muscle tissue morphogenesis (GO:0055010)
glycerol ether metabolic process (GO:0006662)
cell redox homeostasis (GO:0045454)
heart growth (GO:0060419)
forward locomotion (GO:0043056)
somatic muscle development (GO:0007525)
Enriched Up/Downregulated
Enriched Downregulated
Enriched Upregulated
Not Enriched
Reference
1 dpa
3 dpa
9 dpa
15 dpa
25 dpa
32 dpa
40 dpa
1 dpa vs 0 dpa
3 dpa vs 0 dpa
3 dpa vs 1 dpa
9 dpa vs 0 dpa
9 dpa vs 1 dpa
9 dpa vs 3 dpa
15 dpa vs 0 dpa
15 dpa vs 1 dpa
15 dpa vs 3 dpa
15 dpa vs 9 dpa
25 dpa vs 0 dpa
25 dpa vs 1 dpa
25 dpa vs 3 dpa
25 dpa vs 9 dpa
25 dpa vs 15 dpa
32 dpa vs 0 dpa
32 dpa vs 1 dpa
32 dpa vs 3 dpa
32 dpa vs 9 dpa
32 dpa vs 15 dpa
32 dpa vs 25 dpa
40 dpa vs 0 dpa
40 dpa vs 1 dpa
40 dpa vs 3 dpa
40 dpa vs 9 dpa
40 dpa vs 15 dpa
40 dpa vs 25 dpa
40 dpa vs 32 dpa

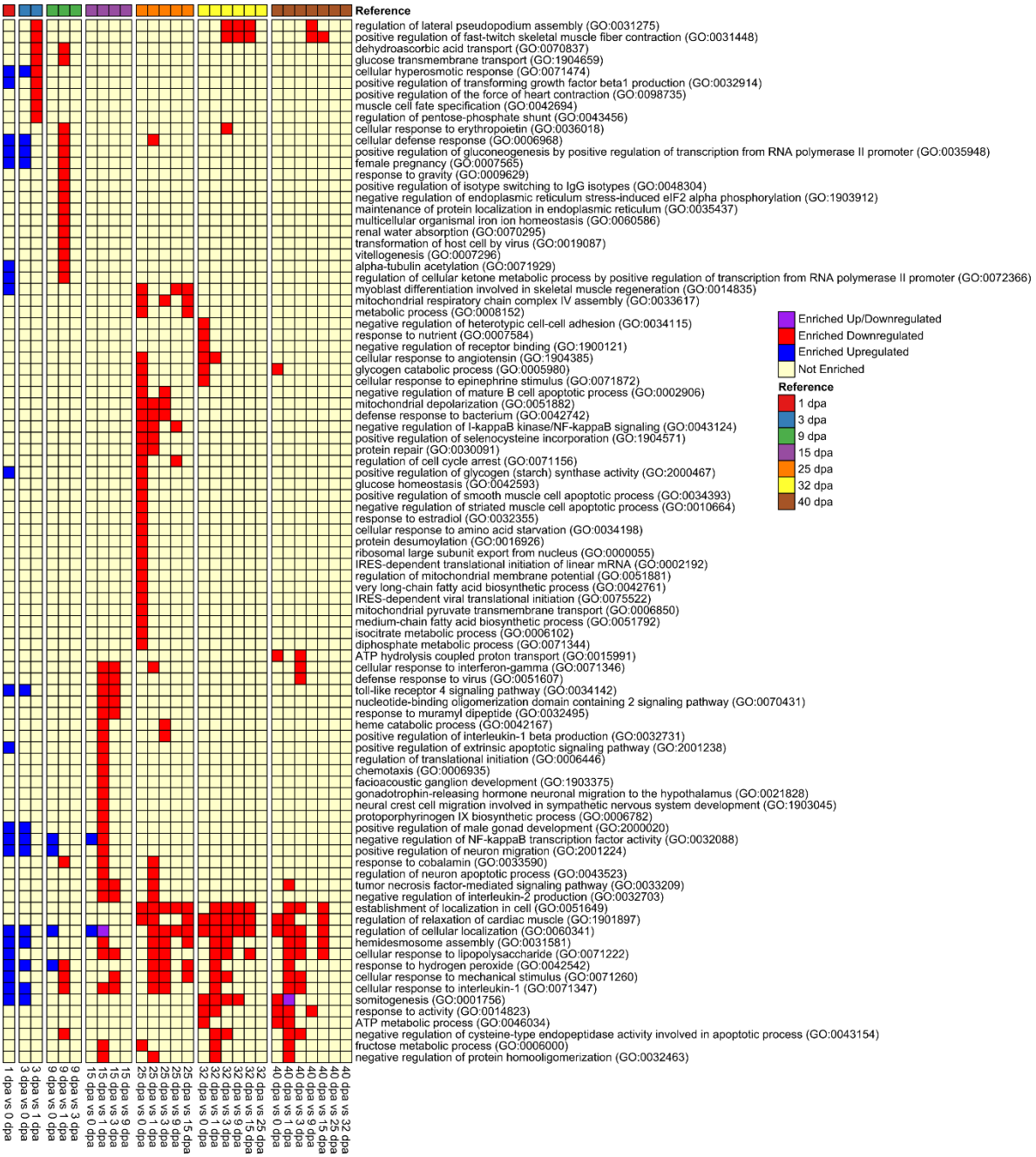
Reference
regulation of lateral pseudopodium assembly (GO:0031275)
positive regulation of fast-twitch skeletal muscle fiber contraction (GO:0031448)
dehydroascorbic acid transport (GO:0070837)
glucose transmembrane transport (GO:1904659)
cellular hyperosmotic response (GO:0071474)
positive regulation of transforming growth factor beta1 production (GO:0032914)
positive regulation of the force of heart contraction (GO:0098735)
muscle cell fate specification (GO:0042694)
regulation of pentose-phosphate shunt (GO:0043456)
cellular response to erythropoietin (GO:0036018)
cellular defense response (GO:0006968)
positive regulation of gluconeogenesis by positive regulation of transcription from RNA polymerase II promoter (GO:0035948)
female pregnancy (GO:0007565)
response to gravity (GO:0009629)
positive regulation of isotype switching to IgG isotypes (GO:0048304)
negative regulation of endoplasmic reticulum stress-induced eIF2 alpha phosphorylation (GO:1903912)
maintenance of protein localization in endoplasmic reticulum (GO:0035437)
multicellular organismal iron ion homeostasis (GO:0060586)
renal water absorption (GO:0070295)
transformation of host cell by virus (GO:0019087)
vitellogenesis (GO:0007296)
alpha-tubulin acetylation (GO:0071929)
regulation of cellular ketone metabolic process by positive regulation of transcription from RNA polymerase II promoter (GO:0072366)
myoblast differentiation involved in skeletal muscle regeneration (GO:0014835)
mitochondrial respiratory chain complex IV assembly (GO:0033617)
metabolic process (GO:0008152)
negative regulation of heterotypic cell-cell adhesion (GO:0034115)
response to nutrient (GO:0007584)
negative regulation of receptor binding (GO:1900121)
cellular response to angiotensin (GO:1904385)
glycogen catabolic process (GO:0005980)
cellular response to epinephrine stimulus (GO:0071872)
negative regulation of mature B cell apoptotic process (GO:0002906)
mitochondrial depolarization (GO:0051882)
defense response to bacterium (GO:0042742)
negative regulation of I-kappaB kinase/NF-kappaB signaling (GO:0043124)
positive regulation of selenocysteine incorporation (GO:1904571)
protein repair (GO:0030091)
regulation of cell cycle arrest (GO:0071156)
positive regulation of glycogen (starch) synthase activity (GO:2000467)
glucose homeostasis (GO:0042593)
positive regulation of smooth muscle cell apoptotic process (GO:0034393)
negative regulation of striated muscle cell apoptotic process (GO:0010664)
response to estradiol (GO:0032355)
cellular response to amino acid starvation (GO:0034198)
protein desumoylation (GO:0016926)
ribosomal large subunit export from nucleus (GO:0000055)
IRES-dependent translational initiation of linear mRNA (GO:0002192)
regulation of mitochondrial membrane potential (GO:0051881)
very long-chain fatty acid biosynthetic process (GO:0042761)
IRES-dependent viral translational initiation (GO:0075522)
mitochondrial pyruvate transmembrane transport (GO:0006850)
medium-chain fatty acid biosynthetic process (GO:0051792)
isocitrate metabolic process (GO:0006102)
diphosphate metabolic process (GO:0071344)
ATP hydrolysis coupled proton transport (GO:0015991)
cellular response to interferon-gamma (GO:0071346)
defense response to virus (GO:0051607)
toll-like receptor 4 signaling pathway (GO:0034142)
nucleotide-binding oligomerization domain containing 2 signaling pathway (GO:0070431)
response to muramyl dipeptide (GO:0032495)
heme catabolic process (GO:0042167)
positive regulation of interleukin-1 beta production (GO:0032731)
positive regulation of extrinsic apoptotic signaling pathway (GO:2001238)
regulation of translational initiation (GO:0006446)
chemotaxis (GO:0006935)
facioacoustic ganglion development (GO:1903375)
gonadotrophin-releasing hormone neuronal migration to the hypothalamus (GO:0021828)
neural crest cell migration involved in sympathetic nervous system development (GO:1903045)
protoporphyrinogen IX biosynthetic process (GO:0006782)
positive regulation of male gonad development (GO:2000020)
negative regulation of NF-kappaB transcription factor activity (GO:0032088)
positive regulation of neuron migration (GO:2001224)
response to cobalamin (GO:0033590)
regulation of neuron apoptotic process (GO:0043523)
tumor necrosis factor-mediated signaling pathway (GO:0033209)
negative regulation of interleukin-2 production (GO:0032703)
establishment of localization in cell (GO:0051649)
regulation of relaxation of cardiac muscle (GO:1901897)
regulation of cellular localization (GO:0060341)
hemidesmosome assembly (GO:0031581)
cellular response to lipopolysaccharide (GO:0071222)
response to hydrogen peroxide (GO:0042542)
cellular response to mechanical stimulus (GO:0071260)
cellular response to interleukin-1 (GO:0071347)
somitogenesis (GO:0001756)
response to activity (GO:0014823)
ATP metabolic process (GO:0046034)
negative regulation of cysteine-type endopeptidase activity involved in apoptotic process (GO:0043154)
fructose metabolic process (GO:0006000)
negative regulation of protein homooligomerization (GO:0032463)
Enriched Up/Downregulated
Enriched Downregulated
Enriched Upregulated
Not Enriched
Reference
1 dpa
3 dpa
9 dpa
15 dpa
25 dpa
32 dpa
40 dpa
1 dpa vs 0 dpa
3 dpa vs 0 dpa
3 dpa vs 1 dpa
9 dpa vs 0 dpa
9 dpa vs 1 dpa
9 dpa vs 3 dpa
15 dpa vs 0 dpa
15 dpa vs 1 dpa
15 dpa vs 3 dpa
15 dpa vs 9 dpa
25 dpa vs 0 dpa
25 dpa vs 1 dpa
25 dpa vs 3 dpa
25 dpa vs 9 dpa
25 dpa vs 15 dpa
32 dpa vs 0 dpa
32 dpa vs 1 dpa
32 dpa vs 3 dpa
32 dpa vs 9 dpa
32 dpa vs 15 dpa
32 dpa vs 25 dpa
40 dpa vs 0 dpa
40 dpa vs 1 dpa
40 dpa vs 3 dpa
40 dpa vs 9 dpa
40 dpa vs 15 dpa
40 dpa vs 25 dpa
40 dpa vs 32 dpa

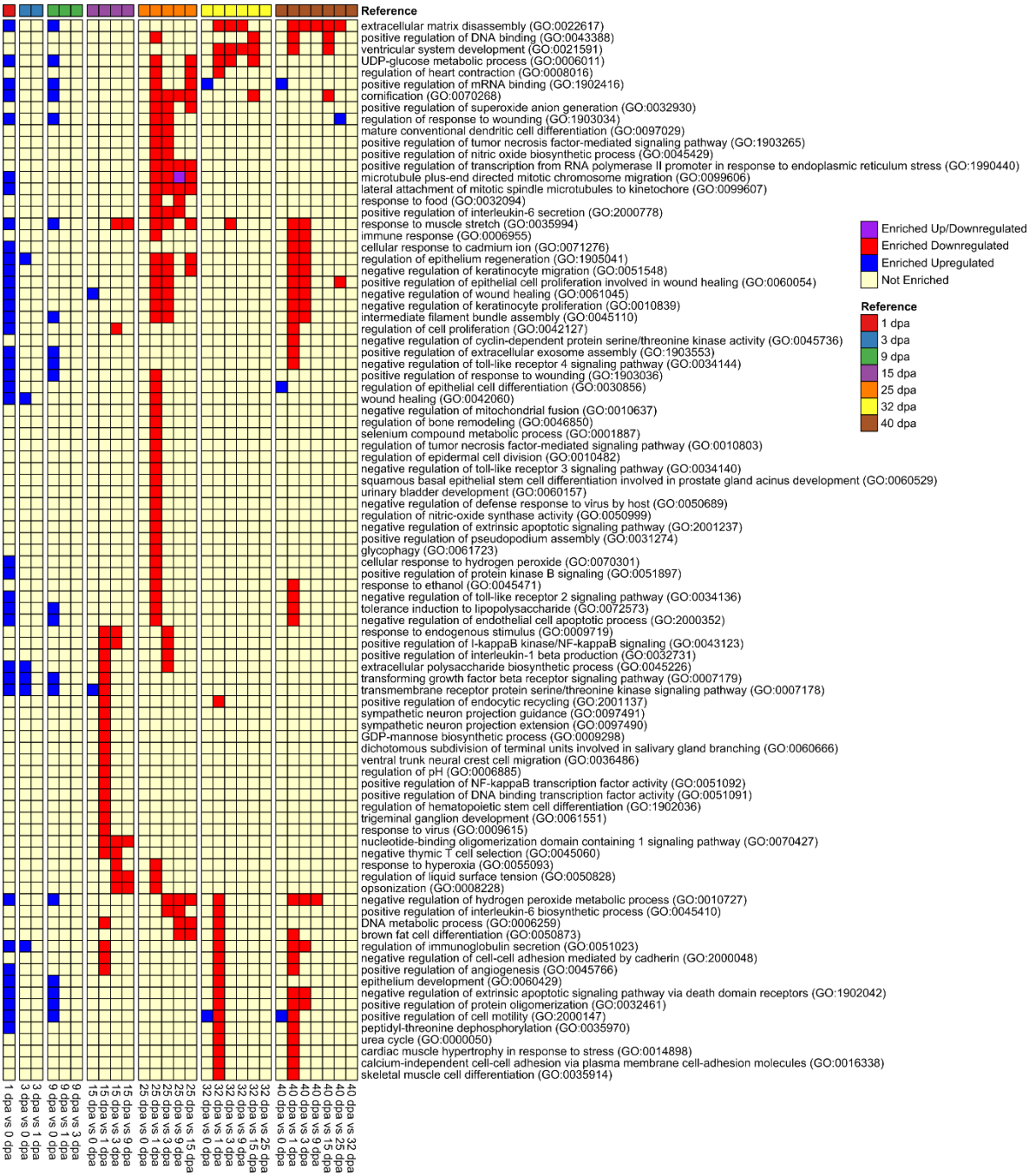
Reference
extracellular matrix disassembly (GO:0022617)
positive regulation of DNA binding (GO:0043388)
ventricular system development (GO:0021591)
UDP-glucose metabolic process (GO:0006011)
regulation of heart contraction (GO:0008016)
positive regulation of mRNA binding (GO:1902416)
cornification (GO:0070268)
positive regulation of superoxide anion generation (GO:0032930)
regulation of response to wounding (GO:1903034)
mature conventional dendritic cell differentiation (GO:0097029)
positive regulation of tumor necrosis factor-mediated signaling pathway (GO:1903265)
positive regulation of nitric oxide biosynthetic process (GO:0045429)
positive regulation of transcription from RNA polymerase II promoter in response to endoplasmic reticulum stress (GO:1990440)
microtubule plus-end directed mitotic chromosome migration (GO:0099606)
lateral attachment of mitotic spindle microtubules to kinetochore (GO:0099607)
response to food (GO:0032094)
positive regulation of interleukin-6 secretion (GO:2000778)
response to muscle stretch (GO:0035994)
immune response (GO:0006955)
cellular response to cadmium ion (GO:0071276)
regulation of epithelium regeneration (GO:1905041)
negative regulation of keratinocyte migration (GO:0051548)
positive regulation of epithelial cell proliferation involved in wound healing (GO:0060054)
negative regulation of wound healing (GO:0061045)
negative regulation of keratinocyte proliferation (GO:0010839)
intermediate filament bundle assembly (GO:0045110)
regulation of cell proliferation (GO:0042127)
negative regulation of cyclin-dependent protein serine/threonine kinase activity (GO:0045736)
positive regulation of extracellular exosome assembly (GO:1903553)
negative regulation of toll-like receptor 4 signaling pathway (GO:0034144)
positive regulation of response to wounding (GO:1903036)
regulation of epithelial cell differentiation (GO:0030856)
wound healing (GO:0042060)
negative regulation of mitochondrial fusion (GO:0010637)
regulation of bone remodeling (GO:0046850)
selenium compound metabolic process (GO:0001887)
regulation of tumor necrosis factor-mediated signaling pathway (GO:0010803)
regulation of epidermal cell division (GO:0010482)
negative regulation of toll-like receptor 3 signaling pathway (GO:0034140)
squamous basal epithelial stem cell differentiation involved in prostate gland acinus development (GO:0060529)
urinary bladder development (GO:0060157)
negative regulation of defense response to virus by host (GO:0050689)
regulation of nitric-oxide synthase activity (GO:0050999)
negative regulation of extrinsic apoptotic signaling pathway (GO:2001237)
positive regulation of pseudopodium assembly (GO:0031274)
glycophagy (GO:0061723)
cellular response to hydrogen peroxide (GO:0070301)
positive regulation of protein kinase B signaling (GO:0051897)
response to ethanol (GO:0045471)
negative regulation of toll-like receptor 2 signaling pathway (GO:0034136)
tolerance induction to lipopolysaccharide (GO:0072573)
negative regulation of endothelial cell apoptotic process (GO:2000352)
response to endogenous stimulus (GO:0009719)
positive regulation of I-kappaB kinase/NF-kappaB signaling (GO:0043123)
positive regulation of interleukin-1 beta production (GO:0032731)
extracellular polysaccharide biosynthetic process (GO:0045226)
transforming growth factor beta receptor signaling pathway (GO:0007179)
transmembrane receptor protein serine/threonine kinase signaling pathway (GO:0007178)
positive regulation of endocytic recycling (GO:2001137)
sympathetic neuron projection guidance (GO:0097491)
sympathetic neuron projection extension (GO:0097490)
GDP-mannose biosynthetic process (GO:0009298)
dichotomous subdivision of terminal units involved in salivary gland branching (GO:0060666)
ventral trunk neural crest cell migration (GO:0036486)
regulation of pH (GO:0006885)
positive regulation of NF-kappaB transcription factor activity (GO:0051092)
positive regulation of DNA binding transcription factor activity (GO:0051091)
regulation of hematopoietic stem cell differentiation (GO:1902036)
trigeminal ganglion development (GO:0061551)
response to virus (GO:0009615)
nucleotide-binding oligomerization domain containing 1 signaling pathway (GO:0070427)
negative thymic T cell selection (GO:0045060)
response to hyperoxia (GO:0055093)
regulation of liquid surface tension (GO:0050828)
opsonization (GO:0008228)
negative regulation of hydrogen peroxide metabolic process (GO:0010727)
positive regulation of interleukin-6 biosynthetic process (GO:0045410)
DNA metabolic process (GO:0006259)
brown fat cell differentiation (GO:0050873)
regulation of immunoglobulin secretion (GO:0051023)
negative regulation of cell-cell adhesion mediated by cadherin (GO:2000048)
positive regulation of angiogenesis (GO:0045766)
epithelium development (GO:0060429)
negative regulation of extrinsic apoptotic signaling pathway via death domain receptors (GO:1902042)
positive regulation of protein oligomerization (GO:0032461)
positive regulation of cell motility (GO:2000147)
peptidyl-threonine dephosphorylation (GO:0035970)
urea cycle (GO:0000050)
cardiac muscle hypertrophy in response to stress (GO:0014898)
calcium-independent cell-cell adhesion via plasma membrane cell-adhesion molecules (GO:0016338)
skeletal muscle cell differentiation (GO:0035914)
Enriched Up/Downregulated
Enriched Downregulated
Enriched Upregulated
Not Enriched
Reference
1 dpa
3 dpa
9 dpa
15 dpa
25 dpa
32 dpa
40 dpa
1 dpa vs 0 dpa
3 dpa vs 0 dpa
3 dpa vs 1 dpa
9 dpa vs 0 dpa
9 dpa vs 1 dpa
9 dpa vs 3 dpa
15 dpa vs 0 dpa
15 dpa vs 1 dpa
15 dpa vs 3 dpa
15 dpa vs 9 dpa
25 dpa vs 0 dpa
25 dpa vs 1 dpa
25 dpa vs 3 dpa
25 dpa vs 9 dpa
25 dpa vs 15 dpa
32 dpa vs 0 dpa
32 dpa vs 1 dpa
32 dpa vs 3 dpa
32 dpa vs 9 dpa
32 dpa vs 15 dpa
32 dpa vs 25 dpa
40 dpa vs 0 dpa
40 dpa vs 1 dpa
40 dpa vs 3 dpa
40 dpa vs 9 dpa
40 dpa vs 15 dpa
40 dpa vs 25 dpa
40 dpa vs 32 dpa


Reference
suckling behavior (GO:0001967)
peptide cross-linking (GO:0018149)
mitotic chromosome movement towards spindle pole (GO:0007079)
positive regulation of ruffle assembly (GO:1900029)
positive regulation of toll-like receptor 2 signaling pathway (GO:0034137)
ion transmembrane transport (GO:0034220)
neutrophil degranulation (GO:0043312)
cellular response to tumor necrosis factor (GO:0071356)
positive regulation of hematopoietic stem cell migration (GO:2000473)
positive regulation of B cell proliferation (GO:0030890)
neutrophil chemotaxis (GO:0030593)
chemokine-mediated signaling pathway (GO:0070098)
activation of MAPK activity (GO:0000187)
negative regulation of polynucleotide adenylyltransferase activity (GO:1904246)
positive regulation of deadenylation-independent decapping of nuclear-transcribed mRNA (GO:1901835)
positive regulation of phagocytosis (GO:0050766)
negative regulation of metanephric nephron tubule epithelial cell differentiation (GO:0072308)
negative regulation of homotypic cell-cell adhesion (GO:0034111)
negative regulation by virus of viral protein levels in host cell (GO:0046725)
lipopolysaccharide-mediated signaling pathway (GO:0031663)
metanephric mesenchymal cell differentiation (GO:0072162)
type I interferon signaling pathway (GO:0060337)
JAK-STAT cascade (GO:0007259)
positive regulation of interleukin-12 production (GO:0032735)
bicarbonate transport (GO:0015701)
positive thymic T cell selection (GO:0045059)
positive regulation of cholesterol efflux (GO:0010875)
immunological synapse formation (GO:0001771)
antigen processing and presentation of exogenous protein antigen via MHC class Ib, TAP-dependent (GO:0002481)
protein N-linked glycosylation via arginine (GO:0042543)
cellular response to iron(III) ion (GO:0071283)
epithelial to mesenchymal transition involved in coronary vasculature morphogenesis (GO:0003201)
histone biotinylation (GO:0071110)
snoRNA catabolic process (GO:0016077)
dITP catabolic process (GO:0035863)
negative regulation of regulatory T cell differentiation (GO:0045590)
positive regulation of transferrin receptor binding (GO:1904437)
positive regulation of ferrous iron binding (GO:1904434)
positive regulation of ferrous iron import across plasma membrane (GO:1904440)
optic cup structural organization (GO:0003409)
optic vesicle morphogenesis (GO:0003404)
'de novo' actin filament nucleation (GO:0070060)
oculomotor nerve formation (GO:0021623)
XDP catabolic process (GO:1901639)
cell wall mannoprotein biosynthetic process (GO:0000032)
regulation of isotype switching to IgG isotypes (GO:0048302)
regulation of T cell chemotaxis (GO:0010819)
immune response-regulating cell surface receptor signaling pathway (GO:0002768)
negative regulation of lipid storage (GO:0010888)
positive regulation of T cell migration (GO:2000406)
negative regulation of macrophage derived foam cell differentiation (GO:0010745)
response to growth factor (GO:0070848)
positive regulation of GTPase activity (GO:0043547)
surfactant homeostasis (GO:0043129)
positive regulation of interferon-gamma biosynthetic process (GO:0045078)
positive regulation of tyrosine phosphorylation of STAT protein (GO:0042531)
negative regulation of T cell apoptotic process (GO:0070233)
response to insulin (GO:0032868)
positive regulation of cellular protein metabolic process (GO:0032270)
stimulatory C-type lectin receptor signaling pathway (GO:0002223)
endoderm formation (GO:0001706)
T cell aggregation (GO:0070489)
interleukin-12-mediated signaling pathway (GO:0035722)
defense response to protozoan (GO:0042832)
nitrobenzene metabolic process (GO:0018916)
cellular detoxification of nitrogen compound (GO:0070458)
positive regulation of JNK cascade (GO:0046330)
positive regulation of behavior (GO:0048520)
positive regulation of cell migration (GO:0030335)
positive regulation of neutrophil chemotaxis (GO:0090023)
cell morphogenesis (GO:0000902)
interferon-gamma-mediated signaling pathway (GO:0060333)
positive regulation of interleukin-12 secretion (GO:2001184)
L-threonine catabolic process to glycine (GO:0019518)
glutathione metabolic process (GO:0006749)
positive regulation of interleukin-10 secretion (GO:2001181)
regulation of cytokine biosynthetic process (GO:0042035)
positive regulation of peptidyl-tyrosine autophosphorylation (GO:1900086)
positive regulation of skeletal muscle satellite cell proliferation (GO:1902724)
positive regulation of cell-matrix adhesion (GO:0001954)
response to progesterone (GO:0032570)
cellular response to extracellular stimulus (GO:0031668)
response to corticosterone (GO:0051412)
inflammatory response (GO:0006954)
negative regulation of T cell proliferation (GO:0042130)
negative regulation of G-protein coupled receptor protein signaling pathway (GO:0045744)
otic vesicle formation (GO:0030916)
negative regulation of toll-like receptor 4 signaling pathway (GO:0034144)
positive regulation of exosomal secretion (GO:1903543)
cellular response to reactive oxygen species (GO:0034614)
response to cytokine (GO:0034097)
Enriched Up/Downregulated
Enriched Downregulated
Enriched Upregulated
Not Enriched
Reference
1 dpa
3 dpa
9 dpa
15 dpa
25 dpa
32 dpa
40 dpa
1 dpa vs 0 dpa
3 dpa vs 0 dpa
3 dpa vs 1 dpa
9 dpa vs 0 dpa
9 dpa vs 1 dpa
9 dpa vs 3 dpa
15 dpa vs 0 dpa
15 dpa vs 1 dpa
15 dpa vs 3 dpa
15 dpa vs 9 dpa
25 dpa vs 0 dpa
25 dpa vs 1 dpa
25 dpa vs 3 dpa
25 dpa vs 9 dpa
25 dpa vs 15 dpa
32 dpa vs 0 dpa
32 dpa vs 1 dpa
32 dpa vs 3 dpa
32 dpa vs 9 dpa
32 dpa vs 15 dpa
32 dpa vs 25 dpa
40 dpa vs 0 dpa
40 dpa vs 1 dpa
40 dpa vs 3 dpa
40 dpa vs 9 dpa
40 dpa vs 15 dpa
40 dpa vs 25 dpa
40 dpa vs 32 dpa


Reference
positive regulation of leukotriene production involved in inflammatory response (GO:0035491)
negative regulation of vascular wound healing (GO:0061044)
positive regulation of cellular response to oxidative stress (GO:1900409)
sulfate assimilation, phosphoadenylyl sulfate reduction by phosphoadenylyl-sulfate reductase (thioredoxin) (GO:0019379)
L-methionine salvage from methionine sulphoxide (GO:1990355)
regulation of muscle filament sliding (GO:0032971)
skeletal muscle tissue development (GO:0007519)
negative regulation of cysteine-type endopeptidase activity involved in apoptotic signaling pathway (GO:2001268)
negative regulation of plasminogen activation (GO:0010757)
negative regulation of smooth muscle cell-matrix adhesion (GO:2000098)
chronological cell aging (GO:0001300)
toll-like receptor 7 signaling pathway (GO:0034154)
positive regulation of interleukin-8 production (GO:0032757)
CDP-diacylglycerol biosynthetic process (GO:0016024)
negative regulation of adiponectin secretion (GO:0070164)
negative regulation of translational initiation in response to stress (GO:0032057)
response to cAMP (GO:0051591)
cellular response to insulin stimulus (GO:0032869)
ERAD pathway (GO:0036503)
protein localization to nucleolus (GO:1902570)
positive regulation of monocyte chemotaxis (GO:0090026)
small GTPase mediated signal transduction (GO:0007264)
negative regulation of growth of symbiont in host (GO:0044130)
cell cycle (GO:0007049)
limb bud formation (GO:0060174)
myeloid dendritic cell activation involved in immune response (GO:0002277)
activation of cysteine-type endopeptidase activity (GO:0097202)
peptidyl-proline hydroxylation to 4-hydroxy-L-proline (GO:0018401)
activation of cysteine-type endopeptidase activity involved in apoptotic process (GO:0006919)
necroptotic signaling pathway (GO:0097527)
senescence-associated heterochromatin focus assembly (GO:0035986)
retinal cell programmed cell death (GO:0046666)
oncogene-induced cell senescence (GO:0090402)
response to alcohol (GO:0097305)
hyaluronan biosynthetic process (GO:0030213)
regulation of autophagy (GO:0010506)
positive regulation of interleukin-8 secretion (GO:2000484)
positive regulation of interleukin-10 secretion (GO:2001181)
positive regulation of actin filament depolymerization (GO:0030836)
multivesicular body assembly (GO:0036258)
positive regulation of interleukin-5 secretion (GO:2000664)
UDP-glucuronate biosynthetic process (GO:0006065)
negative regulation of high voltage-gated calcium channel activity (GO:1901842)
hydrogen peroxide catabolic process (GO:0042744)
positive regulation of myosin light chain kinase activity (GO:0035505)
negative regulation of interleukin-2 biosynthetic process (GO:0045085)
positive regulation of calcidiol 1-monooxygenase activity (GO:0060559)
heme oxidation (GO:0006788)
cobalt ion transport (GO:0006824)
epidermis development (GO:0008544)
uridine catabolic process (GO:0006218)
vacuolar protein processing (GO:0006624)
negative regulation of trophoblast cell migration (GO:1901164)
cell wall macromolecule catabolic process (GO:0016998)
activation of phospholipase A2 activity (GO:0032431)
diacylglycerol biosynthetic process (GO:0006651)
proteolysis (GO:0006508)
positive regulation of membrane protein ectodomain proteolysis (GO:0051044)
extrinsic apoptotic signaling pathway (GO:0097191)
defense response to Gram-negative bacterium (GO:0050829)
maintenance of granzyme B location in T cell secretory granule (GO:0033382)
maintenance of protease location in mast cell secretory granule (GO:0033373)
amelogenesis (GO:0097186)
platelet activation (GO:0030168)
negative regulation of extrinsic apoptotic signaling pathway in absence of ligand (GO:2001240)
positive regulation of protein targeting to membrane (GO:0090314)
embryo implantation (GO:0007566)
response to nematode (GO:0009624)
cellular response to tumor cell (GO:0071228)
protein heterooligomerization (GO:0051291)
protein homotrimerization (GO:0070207)
insulin receptor signaling pathway (GO:0008286)
positive regulation of homotypic cell-cell adhesion (GO:0034112)
calcium ion transport into cytosol (GO:0060402)
sensory perception of bitter taste (GO:0050913)
ectodermal cell differentiation (GO:0010668)
sensory perception of sweet taste (GO:0050916)
sensory perception of umami taste (GO:0050917)
phagosome acidification (GO:0090383)
leukocyte migration (GO:0050900)
negative regulation of interleukin-1-mediated signaling pathway (GO:2000660)
positive regulation of antimicrobial humoral response (GO:0002760)
negative regulation of complement activation, classical pathway (GO:0045959)
cellular response to nitric oxide (GO:0071732)
transferrin transport (GO:0033572)
activation of NF-kappaB-inducing kinase activity (GO:0007250)
propionate metabolic process, methylcitrate cycle (GO:0019679)
negative regulation of complement activation, alternative pathway (GO:0045957)
positive regulation of p38MAPK cascade (GO:1900745)
positive regulation of cell proliferation (GO:0008284)
negative regulation of interleukin-1 alpha secretion (GO:0050712)
Enriched Up/Downregulated
Enriched Downregulated
Enriched Upregulated
Not Enriched
Reference
1 dpa
3 dpa
9 dpa
15 dpa
25 dpa
32 dpa
40 dpa
1 dpa vs 0 dpa
3 dpa vs 0 dpa
3 dpa vs 1 dpa
9 dpa vs 0 dpa
9 dpa vs 1 dpa
9 dpa vs 3 dpa
15 dpa vs 0 dpa
15 dpa vs 1 dpa
15 dpa vs 3 dpa
15 dpa vs 9 dpa
25 dpa vs 0 dpa
25 dpa vs 1 dpa
25 dpa vs 3 dpa
25 dpa vs 9 dpa
25 dpa vs 15 dpa
32 dpa vs 0 dpa
32 dpa vs 1 dpa
32 dpa vs 3 dpa
32 dpa vs 9 dpa
32 dpa vs 15 dpa
32 dpa vs 25 dpa
40 dpa vs 0 dpa
40 dpa vs 1 dpa
40 dpa vs 3 dpa
40 dpa vs 9 dpa
40 dpa vs 15 dpa
40 dpa vs 25 dpa
40 dpa vs 32 dpa

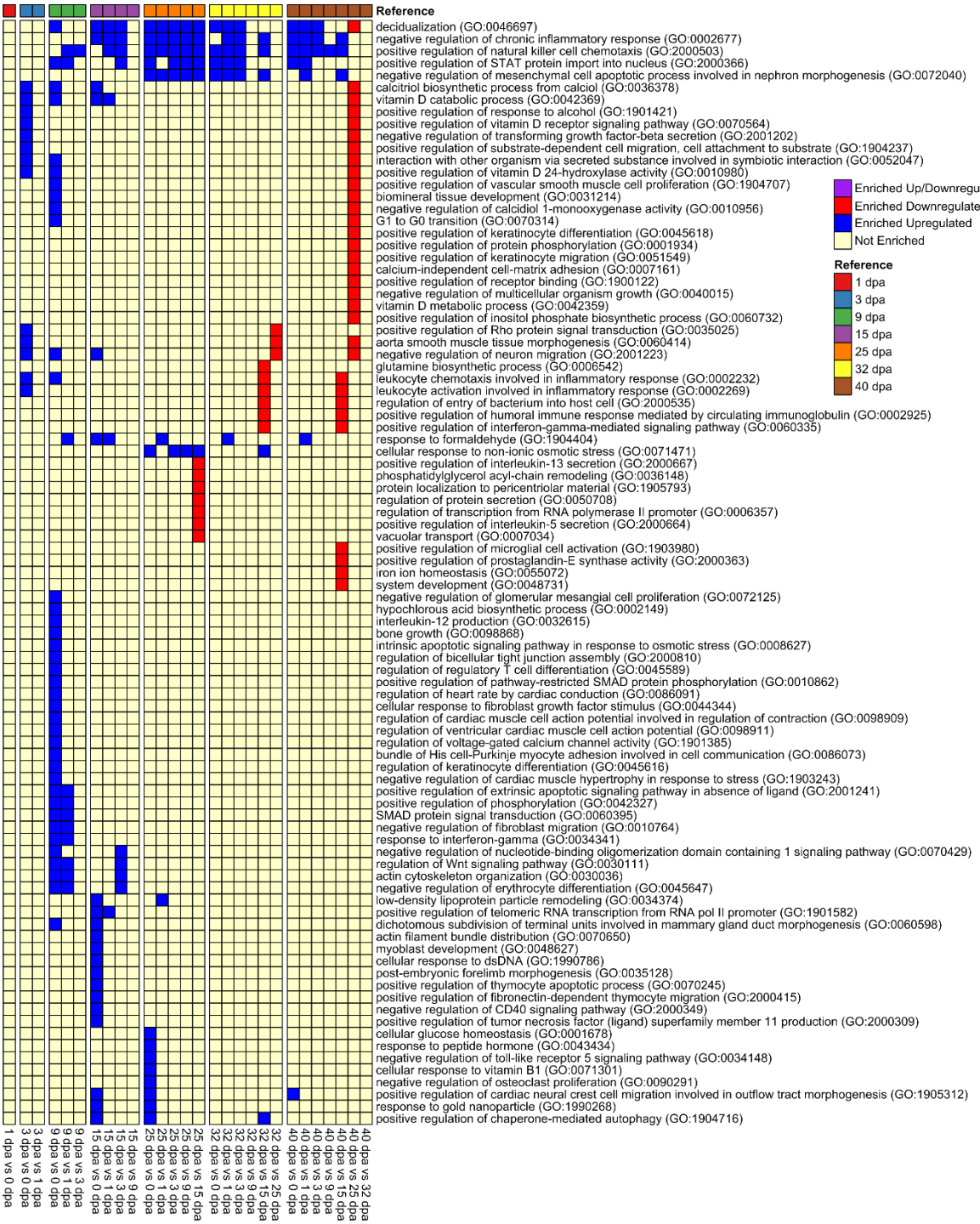
Reference
decidualization (GO:0046697)
negative regulation of chronic inflammatory response (GO:0002677)
positive regulation of natural killer cell chemotaxis (GO:2000503)
positive regulation of STAT protein import into nucleus (GO:2000366)
negative regulation of mesenchymal cell apoptotic process involved in nephron morphogenesis (GO:0072040)
calcitriol biosynthetic process from calciol (GO:0036378)
vitamin D catabolic process (GO:0042369)
positive regulation of response to alcohol (GO:1901421)
positive regulation of vitamin D receptor signaling pathway (GO:0070564)
negative regulation of transforming growth factor-beta secretion (GO:2001202)
positive regulation of substrate-dependent cell migration, cell attachment to substrate (GO:1904237)
interaction with other organism via secreted substance involved in symbiotic interaction (GO:0052047)
positive regulation of vitamin D 24-hydroxylase activity (GO:0010980)
positive regulation of vascular smooth muscle cell proliferation (GO:1904707)
biomineral tissue development (GO:0031214)
negative regulation of calcidiol 1-monooxygenase activity (GO:0010956)
G1 to G0 transition (GO:0070314)
positive regulation of keratinocyte differentiation (GO:0045618)
positive regulation of protein phosphorylation (GO:0001934)
positive regulation of keratinocyte migration (GO:0051549)
calcium-independent cell-matrix adhesion (GO:0007161)
positive regulation of receptor binding (GO:1900122)
negative regulation of multicellular organism growth (GO:0040015)
vitamin D metabolic process (GO:0042359)
positive regulation of inositol phosphate biosynthetic process (GO:0060732)
positive regulation of Rho protein signal transduction (GO:0035025)
aorta smooth muscle tissue morphogenesis (GO:0060414)
negative regulation of neuron migration (GO:2001223)
glutamine biosynthetic process (GO:0006542)
leukocyte chemotaxis involved in inflammatory response (GO:0002232)
leukocyte activation involved in inflammatory response (GO:0002269)
regulation of entry of bacterium into host cell (GO:2000535)
positive regulation of humoral immune response mediated by circulating immunoglobulin (GO:0002925)
positive regulation of interferon-gamma-mediated signaling pathway (GO:0060335)
response to formaldehyde (GO:1904404)
cellular response to non-ionic osmotic stress (GO:0071471)
positive regulation of interleukin-13 secretion (GO:2000667)
phosphatidylglycerol acyl-chain remodeling (GO:0036148)
protein localization to pericentriolar material (GO:1905793)
regulation of protein secretion (GO:0050708)
regulation of transcription from RNA polymerase II promoter (GO:0006357)
positive regulation of interleukin-5 secretion (GO:2000664)
vacuolar transport (GO:0007034)
positive regulation of microglial cell activation (GO:1903980)
positive regulation of prostaglandin-E synthase activity (GO:2000363)
iron ion homeostasis (GO:0055072)
system development (GO:0048731)
negative regulation of glomerular mesangial cell proliferation (GO:0072125)
hypochlorous acid biosynthetic process (GO:0002149)
interleukin-12 production (GO:0032615)
bone growth (GO:0098868)
intrinsic apoptotic signaling pathway in response to osmotic stress (GO:0008627)
regulation of bicellular tight junction assembly (GO:2000810)
regulation of regulatory T cell differentiation (GO:0045589)
positive regulation of pathway-restricted SMAD protein phosphorylation (GO:0010862)
regulation of heart rate by cardiac conduction (GO:0086091)
cellular response to fibroblast growth factor stimulus (GO:0044344)
regulation of cardiac muscle cell action potential involved in regulation of contraction (GO:0098909)
regulation of ventricular cardiac muscle cell action potential (GO:0098911)
regulation of voltage-gated calcium channel activity (GO:1901385)
bundle of His cell-Purkinje myocyte adhesion involved in cell communication (GO:0086073)
regulation of keratinocyte differentiation (GO:0045616)
negative regulation of cardiac muscle hypertrophy in response to stress (GO:1903243)
positive regulation of extrinsic apoptotic signaling pathway in absence of ligand (GO:2001241)
positive regulation of phosphorylation (GO:0042327)
SMAD protein signal transduction (GO:0060395)
negative regulation of fibroblast migration (GO:0010764)
response to interferon-gamma (GO:0034341)
negative regulation of nucleotide-binding oligomerization domain containing 1 signaling pathway (GO:0070429)
regulation of Wnt signaling pathway (GO:0030111)
actin cytoskeleton organization (GO:0030036)
negative regulation of erythrocyte differentiation (GO:0045647)
low-density lipoprotein particle remodeling (GO:0034374)
positive regulation of telomeric RNA transcription from RNA pol II promoter (GO:1901582)
dichotomous subdivision of terminal units involved in mammary gland duct morphogenesis (GO:0060598)
actin filament bundle distribution (GO:0070650)
myoblast development (GO:0048627)
cellular response to dsDNA (GO:1990786)
post-embryonic forelimb morphogenesis (GO:0035128)
positive regulation of thymocyte apoptotic process (GO:0070245)
positive regulation of fibronectin-dependent thymocyte migration (GO:2000415)
negative regulation of CD40 signaling pathway (GO:2000349)
positive regulation of tumor necrosis factor (ligand) superfamily member 11 production (GO:2000309)
cellular glucose homeostasis (GO:0001678)
response to peptide hormone (GO:0043434)
negative regulation of toll-like receptor 5 signaling pathway (GO:0034148)
cellular response to vitamin B1 (GO:0071301)
negative regulation of osteoclast proliferation (GO:0090291)
positive regulation of cardiac neural crest cell migration involved in outflow tract morphogenesis (GO:1905312)
response to gold nanoparticle (GO:1990268)
positive regulation of chaperone-mediated autophagy (GO:1904716)
Enriched Up/Downregulated
Enriched Downregulated
Enriched Upregulated
Not Enriched
Reference
1 dpa
3 dpa
9 dpa
15 dpa
25 dpa
32 dpa
40 dpa
1 dpa vs 0 dpa
3 dpa vs 0 dpa
3 dpa vs 1 dpa
9 dpa vs 0 dpa
9 dpa vs 1 dpa
9 dpa vs 3 dpa
15 dpa vs 0 dpa
15 dpa vs 1 dpa
15 dpa vs 3 dpa
15 dpa vs 9 dpa
25 dpa vs 0 dpa
25 dpa vs 1 dpa
25 dpa vs 3 dpa
25 dpa vs 9 dpa
25 dpa vs 15 dpa
32 dpa vs 0 dpa
32 dpa vs 1 dpa
32 dpa vs 3 dpa
32 dpa vs 9 dpa
32 dpa vs 15 dpa
32 dpa vs 25 dpa
40 dpa vs 0 dpa
40 dpa vs 1 dpa
40 dpa vs 3 dpa
40 dpa vs 9 dpa
40 dpa vs 15 dpa
40 dpa vs 25 dpa
40 dpa vs 32 dpa

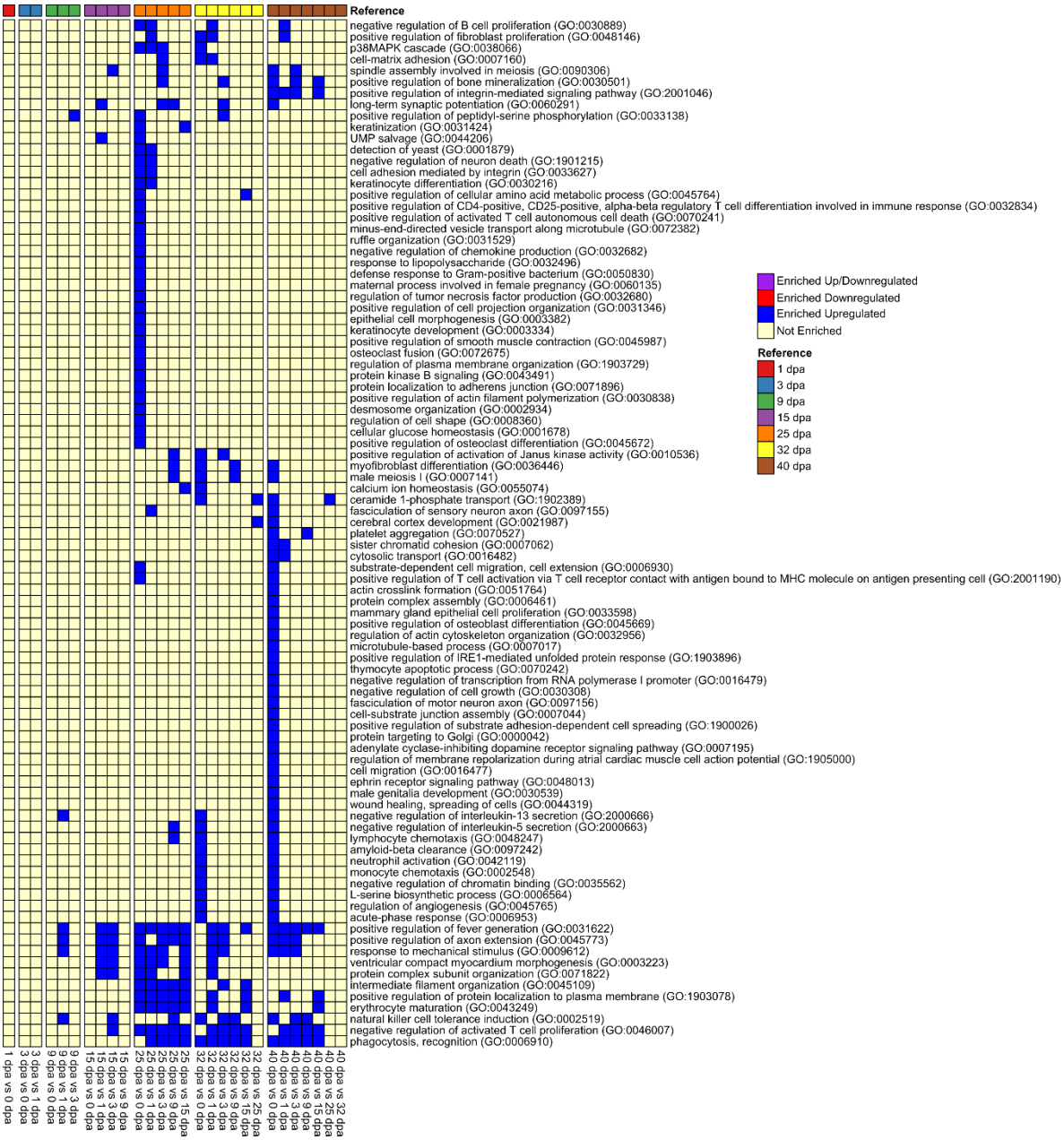
Reference
negative regulation of B cell proliferation (GO:0030889)
positive regulation of fibroblast proliferation (GO:0048146)
p38MAPK cascade (GO:0038066)
cell-matrix adhesion (GO:0007160)
spindle assembly involved in meiosis (GO:0090306)
positive regulation of bone mineralization (GO:0030501)
positive regulation of integrin-mediated signaling pathway (GO:2001046)
long-term synaptic potentiation (GO:0060291)
positive regulation of peptidyl-serine phosphorylation (GO:0033138)
keratinization (GO:0031424)
UMP salvage (GO:0044206)
detection of yeast (GO:0001879)
negative regulation of neuron death (GO:1901215)
cell adhesion mediated by integrin (GO:0033627)
keratinocyte differentiation (GO:0030216)
positive regulation of cellular amino acid metabolic process (GO:0045764)
positive regulation of CD4-positive, CD25-positive, alpha-beta regulatory T cell differentiation involved in immune response (GO:0032834)
positive regulation of activated T cell autonomous cell death (GO:0070241)
minus-end-directed vesicle transport along microtubule (GO:0072382)
ruffle organization (GO:0031529)
negative regulation of chemokine production (GO:0032682)
response to lipopolysaccharide (GO:0032496)
defense response to Gram-positive bacterium (GO:0050830)
maternal process involved in female pregnancy (GO:0060135)
regulation of tumor necrosis factor production (GO:0032680)
positive regulation of cell projection organization (GO:0031346)
epithelial cell morphogenesis (GO:0003382)
keratinocyte development (GO:0003334)
positive regulation of smooth muscle contraction (GO:0045987)
osteoclast fusion (GO:0072675)
regulation of plasma membrane organization (GO:1903729)
protein kinase B signaling (GO:0043491)
protein localization to adherens junction (GO:0071896)
positive regulation of actin filament polymerization (GO:0030838)
desmosome organization (GO:0002934)
regulation of cell shape (GO:0008360)
cellular glucose homeostasis (GO:0001678)
positive regulation of osteoclast differentiation (GO:0045672)
positive regulation of activation of Janus kinase activity (GO:0010536)
myofibroblast differentiation (GO:0036446)
male meiosis I (GO:0007141)
calcium ion homeostasis (GO:0055074)
ceramide 1-phosphate transport (GO:1902389)
fasciculation of sensory neuron axon (GO:0097155)
cerebral cortex development (GO:0021987)
platelet aggregation (GO:0070527)
sister chromatid cohesion (GO:0007062)
cytosolic transport (GO:0016482)
substrate-dependent cell migration, cell extension (GO:0006930)
positive regulation of T cell activation via T cell receptor contact with antigen bound to MHC molecule on antigen presenting cell (GO:2001190)
actin crosslink formation (GO:0051764)
protein complex assembly (GO:0006461)
mammary gland epithelial cell proliferation (GO:0033598)
positive regulation of osteoblast differentiation (GO:0045669)
regulation of actin cytoskeleton organization (GO:0032956)
microtubule-based process (GO:0007017)
positive regulation of IRE1-mediated unfolded protein response (GO:1903896)
thymocyte apoptotic process (GO:0070242)
negative regulation of transcription from RNA polymerase I promoter (GO:0016479)
negative regulation of cell growth (GO:0030308)
fasciculation of motor neuron axon (GO:0097156)
cell-substrate junction assembly (GO:0007044)
positive regulation of substrate adhesion-dependent cell spreading (GO:1900026)
protein targeting to Golgi (GO:0000042)
adenylate cyclase-inhibiting dopamine receptor signaling pathway (GO:0007195)
regulation of membrane repolarization during atrial cardiac muscle cell action potential (GO:1905000)
cell migration (GO:0016477)
ephrin receptor signaling pathway (GO:0048013)
male genitalia development (GO:0030539)
wound healing, spreading of cells (GO:0044319)
negative regulation of interleukin-13 secretion (GO:2000666)
negative regulation of interleukin-5 secretion (GO:2000663)
lymphocyte chemotaxis (GO:0048247)
amyloid-beta clearance (GO:0097242)
neutrophil activation (GO:0042119)
monocyte chemotaxis (GO:0002548)
negative regulation of chromatin binding (GO:0035562)
L-serine biosynthetic process (GO:0006564)
regulation of angiogenesis (GO:0045765)
acute-phase response (GO:0006953)
positive regulation of fever generation (GO:0031622)
positive regulation of axon extension (GO:0045773)
response to mechanical stimulus (GO:0009612)
ventricular compact myocardium morphogenesis (GO:0003223)
protein complex subunit organization (GO:0071822)
intermediate filament organization (GO:0045109)
positive regulation of protein localization to plasma membrane (GO:1903078)
erythrocyte maturation (GO:0043249)
natural killer cell tolerance induction (GO:0002519)
negative regulation of activated T cell proliferation (GO:0046007)
phagocytosis, recognition (GO:0006910)
Enriched Up/Downregulated
Enriched Downregulated
Enriched Upregulated
Not Enriched
Reference
1 dpa
3 dpa
9 dpa
15 dpa
25 dpa
32 dpa
40 dpa
1 dpa vs 0 dpa
3 dpa vs 0 dpa
3 dpa vs 1 dpa
9 dpa vs 0 dpa
9 dpa vs 1 dpa
9 dpa vs 3 dpa
15 dpa vs 0 dpa
15 dpa vs 1 dpa
15 dpa vs 3 dpa
15 dpa vs 9 dpa
25 dpa vs 0 dpa
25 dpa vs 1 dpa
25 dpa vs 3 dpa
25 dpa vs 9 dpa
25 dpa vs 15 dpa
32 dpa vs 0 dpa
32 dpa vs 1 dpa
32 dpa vs 3 dpa
32 dpa vs 9 dpa
32 dpa vs 15 dpa
32 dpa vs 25 dpa
40 dpa vs 0 dpa
40 dpa vs 1 dpa
40 dpa vs 3 dpa
40 dpa vs 9 dpa
40 dpa vs 15 dpa
40 dpa vs 25 dpa
40 dpa vs 32 dpa

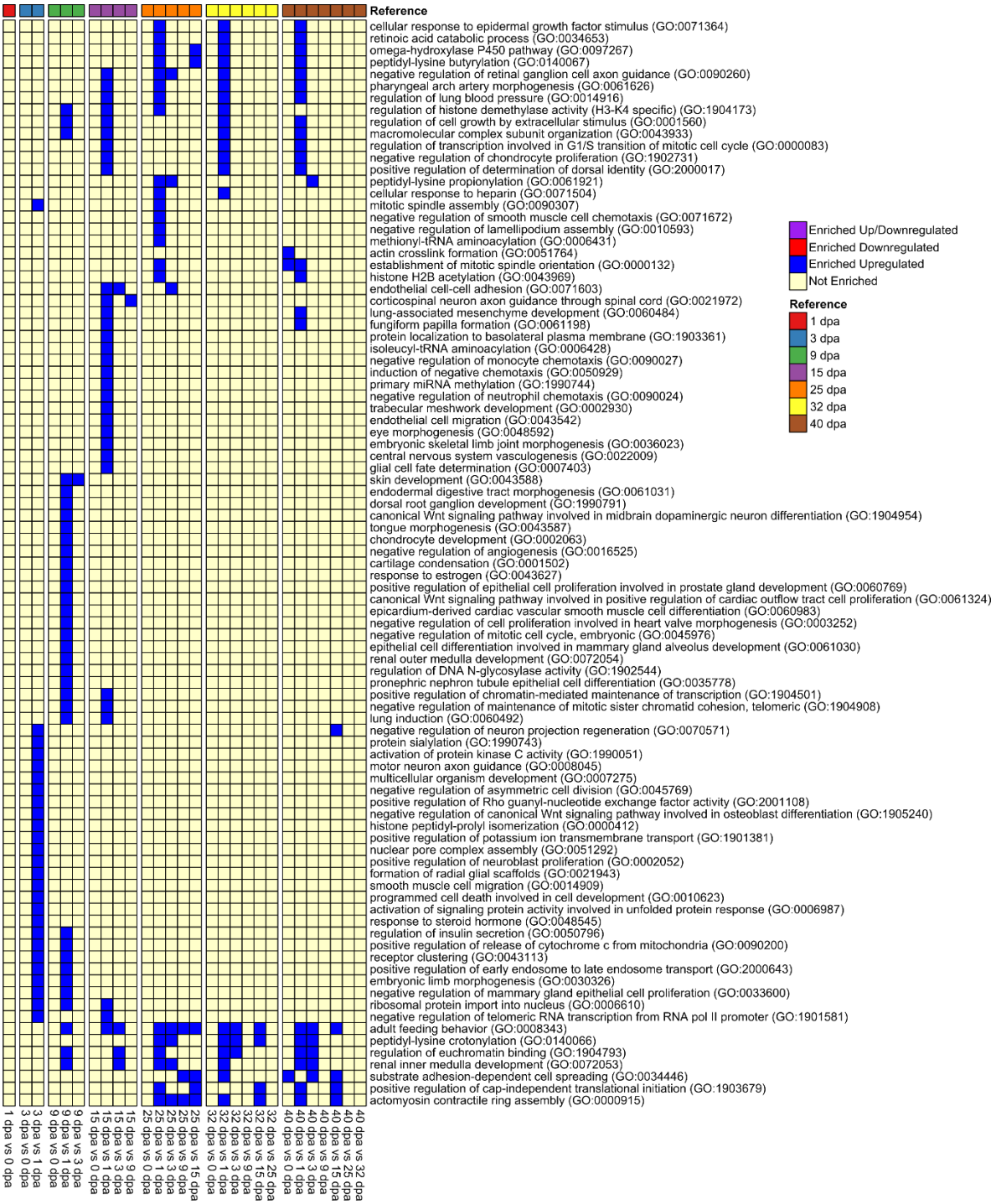
Reference
cellular response to epidermal growth factor stimulus (GO:0071364)
retinoic acid catabolic process (GO:0034653)
omega-hydroxylase P450 pathway (GO:0097267)
peptidyl-lysine butyrylation (GO:0140067)
negative regulation of retinal ganglion cell axon guidance (GO:0090260)
pharyngeal arch artery morphogenesis (GO:0061626)
regulation of lung blood pressure (GO:0014916)
regulation of histone demethylase activity (H3-K4 specific) (GO:1904173)
regulation of cell growth by extracellular stimulus (GO:0001560)
macromolecular complex subunit organization (GO:0043933)
regulation of transcription involved in G1/S transition of mitotic cell cycle (GO:0000083)
negative regulation of chondrocyte proliferation (GO:1902731)
positive regulation of determination of dorsal identity (GO:2000017)
peptidyl-lysine propionylation (GO:0061921)
cellular response to heparin (GO:0071504)
mitotic spindle assembly (GO:0090307)
negative regulation of smooth muscle cell chemotaxis (GO:0071672)
negative regulation of lamellipodium assembly (GO:0010593)
methionyl-tRNA aminoacylation (GO:0006431)
actin crosslink formation (GO:0051764)
establishment of mitotic spindle orientation (GO:0000132)
histone H2B acetylation (GO:0043969)
endothelial cell-cell adhesion (GO:0071603)
corticospinal neuron axon guidance through spinal cord (GO:0021972)
lung-associated mesenchyme development (GO:0060484)
fungiform papilla formation (GO:0061198)
protein localization to basolateral plasma membrane (GO:1903361)
isoleucyl-tRNA aminoacylation (GO:0006428)
negative regulation of monocyte chemotaxis (GO:0090027)
induction of negative chemotaxis (GO:0050929)
primary miRNA methylation (GO:1990744)
negative regulation of neutrophil chemotaxis (GO:0090024)
trabecular meshwork development (GO:0002930)
endothelial cell migration (GO:0043542)
eye morphogenesis (GO:0048592)
embryonic skeletal limb joint morphogenesis (GO:0036023)
central nervous system vasculogenesis (GO:0022009)
glial cell fate determination (GO:0007403)
skin development (GO:0043588)
endodermal digestive tract morphogenesis (GO:0061031)
dorsal root ganglion development (GO:1990791)
canonical Wnt signaling pathway involved in midbrain dopaminergic neuron differentiation (GO:1904954)
tongue morphogenesis (GO:0043587)
chondrocyte development (GO:0002063)
negative regulation of angiogenesis (GO:0016525)
cartilage condensation (GO:0001502)
response to estrogen (GO:0043627)
positive regulation of epithelial cell proliferation involved in prostate gland development (GO:0060769)
canonical Wnt signaling pathway involved in positive regulation of cardiac outflow tract cell proliferation (GO:0061324)
epicardium-derived cardiac vascular smooth muscle cell differentiation (GO:0060983)
negative regulation of cell proliferation involved in heart valve morphogenesis (GO:0003252)
negative regulation of mitotic cell cycle, embryonic (GO:0045976)
epithelial cell differentiation involved in mammary gland alveolus development (GO:0061030)
renal outer medulla development (GO:0072054)
regulation of DNA N-glycosylase activity (GO:1902544)
pronephric nephron tubule epithelial cell differentiation (GO:0035778)
positive regulation of chromatin-mediated maintenance of transcription (GO:1904501)
negative regulation of maintenance of mitotic sister chromatid cohesion, telomeric (GO:1904908)
lung induction (GO:0060492)
negative regulation of neuron projection regeneration (GO:0070571)
protein sialylation (GO:1990743)
activation of protein kinase C activity (GO:1990051)
motor neuron axon guidance (GO:0008045)
multicellular organism development (GO:0007275)
negative regulation of asymmetric cell division (GO:0045769)
positive regulation of Rho guanyl-nucleotide exchange factor activity (GO:2001108)
negative regulation of canonical Wnt signaling pathway involved in osteoblast differentiation (GO:1905240)
histone peptidyl-prolyl isomerization (GO:0000412)
positive regulation of potassium ion transmembrane transport (GO:1901381)
nuclear pore complex assembly (GO:0051292)
positive regulation of neuroblast proliferation (GO:0002052)
formation of radial glial scaffolds (GO:0021943)
smooth muscle cell migration (GO:0014909)
programmed cell death involved in cell development (GO:0010623)
activation of signaling protein activity involved in unfolded protein response (GO:0006987)
response to steroid hormone (GO:0048545)
regulation of insulin secretion (GO:0050796)
positive regulation of release of cytochrome c from mitochondria (GO:0090200)
receptor clustering (GO:0043113)
positive regulation of early endosome to late endosome transport (GO:2000643)
embryonic limb morphogenesis (GO:0030326)
negative regulation of mammary gland epithelial cell proliferation (GO:0033600)
ribosomal protein import into nucleus (GO:0006610)
negative regulation of telomeric RNA transcription from RNA pol II promoter (GO:1901581)
adult feeding behavior (GO:0008343)
peptidyl-lysine crotonylation (GO:0140066)
regulation of euchromatin binding (GO:1904793)
renal inner medulla development (GO:0072053)
substrate adhesion-dependent cell spreading (GO:0034446)
positive regulation of cap-independent translational initiation (GO:1903679)
actomyosin contractile ring assembly (GO:0000915)
Enriched Up/Downregulated
Enriched Downregulated
Enriched Upregulated
Not Enriched
Reference
1 dpa
3 dpa
9 dpa
15 dpa
25 dpa
32 dpa
40 dpa
1 dpa vs 0 dpa
3 dpa vs 0 dpa
3 dpa vs 1 dpa
9 dpa vs 0 dpa
9 dpa vs 1 dpa
9 dpa vs 3 dpa
15 dpa vs 0 dpa
15 dpa vs 1 dpa
15 dpa vs 3 dpa
15 dpa vs 9 dpa
25 dpa vs 0 dpa
25 dpa vs 1 dpa
25 dpa vs 3 dpa
25 dpa vs 9 dpa
25 dpa vs 15 dpa
32 dpa vs 0 dpa
32 dpa vs 1 dpa
32 dpa vs 3 dpa
32 dpa vs 9 dpa
32 dpa vs 15 dpa
32 dpa vs 25 dpa
40 dpa vs 0 dpa
40 dpa vs 1 dpa
40 dpa vs 3 dpa
40 dpa vs 9 dpa
40 dpa vs 15 dpa
40 dpa vs 25 dpa
40 dpa vs 32 dpa

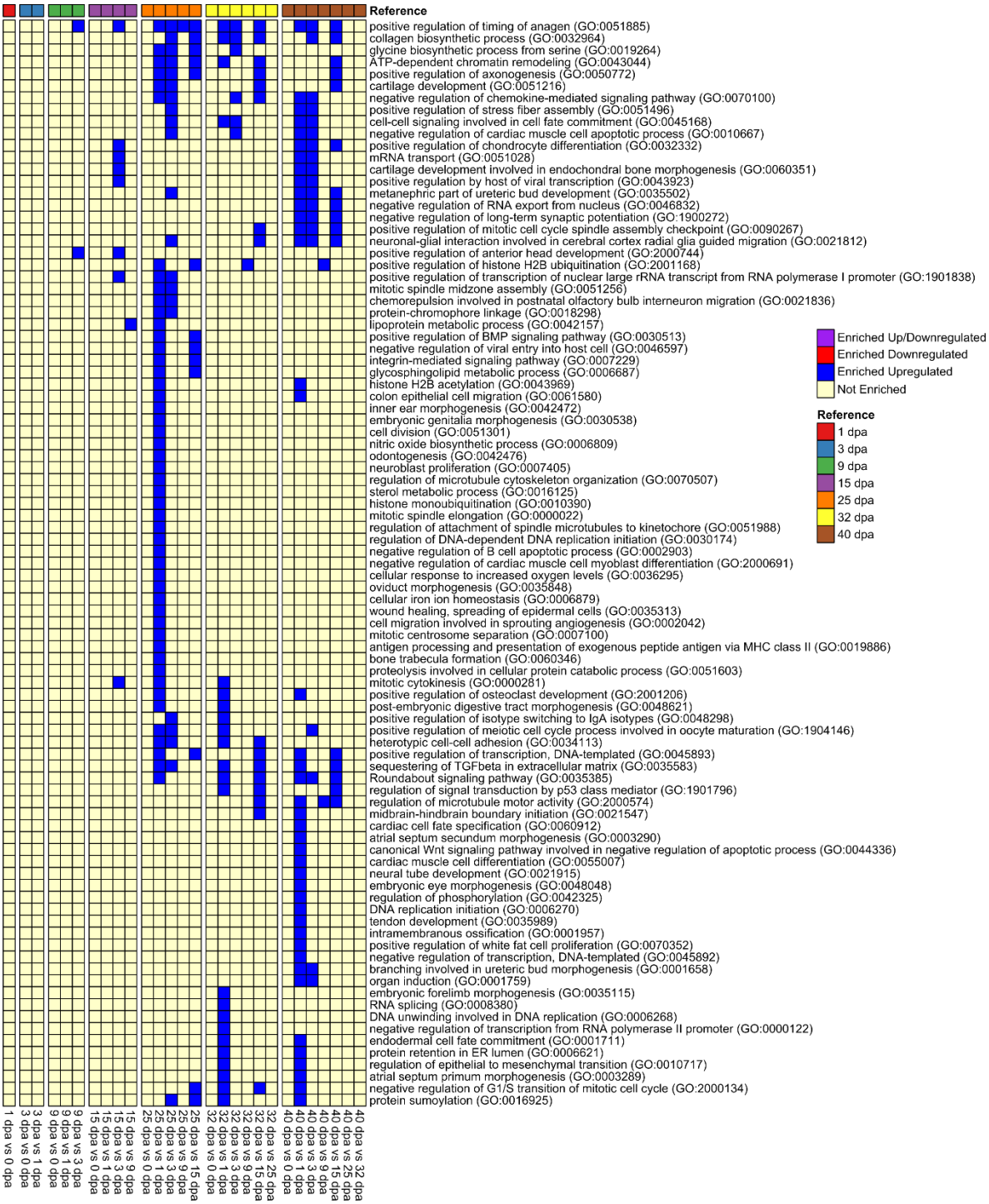
Reference
positive regulation of timing of anagen (GO:0051885)
collagen biosynthetic process (GO:0032964)
glycine biosynthetic process from serine (GO:0019264)
ATP-dependent chromatin remodeling (GO:0043044)
positive regulation of axonogenesis (GO:0050772)
cartilage development (GO:0051216)
negative regulation of chemokine-mediated signaling pathway (GO:0070100)
positive regulation of stress fiber assembly (GO:0051496)
cell-cell signaling involved in cell fate commitment (GO:0045168)
negative regulation of cardiac muscle cell apoptotic process (GO:0010667)
positive regulation of chondrocyte differentiation (GO:0032332)
mRNA transport (GO:0051028)
cartilage development involved in endochondral bone morphogenesis (GO:0060351)
positive regulation by host of viral transcription (GO:0043923)
metanephric part of ureteric bud development (GO:0035502)
negative regulation of RNA export from nucleus (GO:0046832)
negative regulation of long-term synaptic potentiation (GO:1900272)
positive regulation of mitotic cell cycle spindle assembly checkpoint (GO:0090267)
neuronal-glial interaction involved in cerebral cortex radial glia guided migration (GO:0021812)
positive regulation of anterior head development (GO:2000744)
positive regulation of histone H2B ubiquitination (GO:2001168)
positive regulation of transcription of nuclear large rRNA transcript from RNA polymerase I promoter (GO:1901838)
mitotic spindle midzone assembly (GO:0051256)
chemorepulsion involved in postnatal olfactory bulb interneuron migration (GO:0021836)
protein-chromophore linkage (GO:0018298)
lipoprotein metabolic process (GO:0042157)
positive regulation of BMP signaling pathway (GO:0030513)
negative regulation of viral entry into host cell (GO:0046597)
integrin-mediated signaling pathway (GO:0007229)
glycosphingolipid metabolic process (GO:0006687)
histone H2B acetylation (GO:0043969)
colon epithelial cell migration (GO:0061580)
inner ear morphogenesis (GO:0042472)
embryonic genitalia morphogenesis (GO:0030538)
cell division (GO:0051301)
nitric oxide biosynthetic process (GO:0006809)
odontogenesis (GO:0042476)
neuroblast proliferation (GO:0007405)
regulation of microtubule cytoskeleton organization (GO:0070507)
sterol metabolic process (GO:0016125)
histone monoubiquitination (GO:0010390)
mitotic spindle elongation (GO:0000022)
regulation of attachment of spindle microtubules to kinetochore (GO:0051988)
regulation of DNA-dependent DNA replication initiation (GO:0030174)
negative regulation of B cell apoptotic process (GO:0002903)
negative regulation of cardiac muscle cell myoblast differentiation (GO:2000691)
cellular response to increased oxygen levels (GO:0036295)
oviduct morphogenesis (GO:0035848)
cellular iron ion homeostasis (GO:0006879)
wound healing, spreading of epidermal cells (GO:0035313)
cell migration involved in sprouting angiogenesis (GO:0002042)
mitotic centrosome separation (GO:0007100)
antigen processing and presentation of exogenous peptide antigen via MHC class II (GO:0019886)
bone trabecula formation (GO:0060346)
proteolysis involved in cellular protein catabolic process (GO:0051603)
mitotic cytokinesis (GO:0000281)
positive regulation of osteoclast development (GO:2001206)
post-embryonic digestive tract morphogenesis (GO:0048621)
positive regulation of isotype switching to IgA isotypes (GO:0048298)
positive regulation of meiotic cell cycle process involved in oocyte maturation (GO:1904146)
heterotypic cell-cell adhesion (GO:0034113)
positive regulation of transcription, DNA-templated (GO:0045893)
sequestering of TGFbeta in extracellular matrix (GO:0035583)
Roundabout signaling pathway (GO:0035385)
regulation of signal transduction by p53 class mediator (GO:1901796)
regulation of microtubule motor activity (GO:2000574)
midbrain-hindbrain boundary initiation (GO:0021547)
cardiac cell fate specification (GO:0060912)
atrial septum secundum morphogenesis (GO:0003290)
canonical Wnt signaling pathway involved in negative regulation of apoptotic process (GO:0044336)
cardiac muscle cell differentiation (GO:0055007)
neural tube development (GO:0021915)
embryonic eye morphogenesis (GO:0048048)
regulation of phosphorylation (GO:0042325)
DNA replication initiation (GO:0006270)
tendon development (GO:0035989)
intramembranous ossification (GO:0001957)
positive regulation of white fat cell proliferation (GO:0070352)
negative regulation of transcription, DNA-templated (GO:0045892)
branching involved in ureteric bud morphogenesis (GO:0001658)
organ induction (GO:0001759)
embryonic forelimb morphogenesis (GO:0035115)
RNA splicing (GO:0008380)
DNA unwinding involved in DNA replication (GO:0006268)
negative regulation of transcription from RNA polymerase II promoter (GO:0000122)
endodermal cell fate commitment (GO:0001711)
protein retention in ER lumen (GO:0006621)
regulation of epithelial to mesenchymal transition (GO:0010717)
atrial septum primum morphogenesis (GO:0003289)
negative regulation of G1/S transition of mitotic cell cycle (GO:2000134)
protein sumoylation (GO:0016925)
Enriched Up/Downregulated
Enriched Downregulated
Enriched Upregulated
Not Enriched
Reference
1 dpa
3 dpa
9 dpa
15 dpa
25 dpa
32 dpa
40 dpa
1 dpa vs 0 dpa
3 dpa vs 0 dpa
3 dpa vs 1 dpa
9 dpa vs 0 dpa
9 dpa vs 1 dpa
9 dpa vs 3 dpa
15 dpa vs 0 dpa
15 dpa vs 1 dpa
15 dpa vs 3 dpa
15 dpa vs 9 dpa
25 dpa vs 0 dpa
25 dpa vs 1 dpa
25 dpa vs 3 dpa
25 dpa vs 9 dpa
25 dpa vs 15 dpa
32 dpa vs 0 dpa
32 dpa vs 1 dpa
32 dpa vs 3 dpa
32 dpa vs 9 dpa
32 dpa vs 15 dpa
32 dpa vs 25 dpa
40 dpa vs 0 dpa
40 dpa vs 1 dpa
40 dpa vs 3 dpa
40 dpa vs 9 dpa
40 dpa vs 15 dpa
40 dpa vs 25 dpa
40 dpa vs 32 dpa

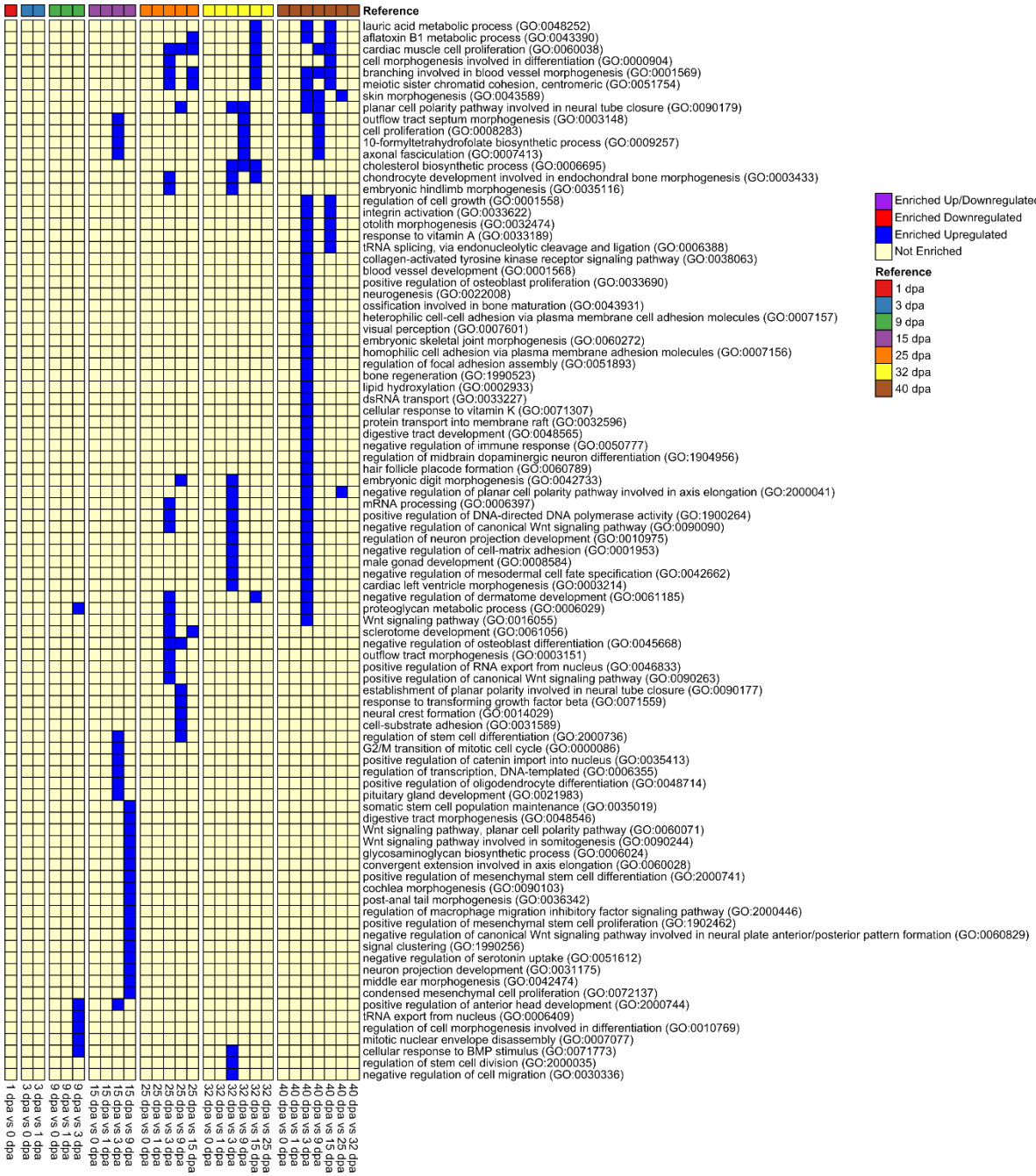
Reference
lauric acid metabolic process (GO:0048252)
aflatoxin B1 metabolic process (GO:0043390)
cardiac muscle cell proliferation (GO:0060038)
cell morphogenesis involved in differentiation (GO:0000904)
branching involved in blood vessel morphogenesis (GO:0001569)
meiotic sister chromatid cohesion, centromeric (GO:0051754)
skin morphogenesis (GO:0043589)
planar cell polarity pathway involved in neural tube closure (GO:0090179)
outflow tract septum morphogenesis (GO:0003148)
cell proliferation (GO:0008283)
10-formyltetrahydrofolate biosynthetic process (GO:0009257)
axonal fasciculation (GO:0007413)
cholesterol biosynthetic process (GO:0006695)
chondrocyte development involved in endochondral bone morphogenesis (GO:0003433)
embryonic hindlimb morphogenesis (GO:0035116)
regulation of cell growth (GO:0001558)
integrin activation (GO:0033622)
otolith morphogenesis (GO:0032474)
response to vitamin A (GO:0033189)
tRNA splicing, via endonucleolytic cleavage and ligation (GO:0006388)
collagen-activated tyrosine kinase receptor signaling pathway (GO:0038063)
blood vessel development (GO:0001568)
positive regulation of osteoblast proliferation (GO:0033690)
neurogenesis (GO:0022008)
ossification involved in bone maturation (GO:0043931)
heterophilic cell-cell adhesion via plasma membrane cell adhesion molecules (GO:0007157)
visual perception (GO:0007601)
embryonic skeletal joint morphogenesis (GO:0060272)
homophilic cell adhesion via plasma membrane adhesion molecules (GO:0007156)
regulation of focal adhesion assembly (GO:0051893)
bone regeneration (GO:1990523)
lipid hydroxylation (GO:0002933)
dsRNA transport (GO:0033227)
cellular response to vitamin K (GO:0071307)
protein transport into membrane raft (GO:0032596)
digestive tract development (GO:0048565)
negative regulation of immune response (GO:0050777)
regulation of midbrain dopaminergic neuron differentiation (GO:1904956)
hair follicle placode formation (GO:0060789)
embryonic digit morphogenesis (GO:0042733)
negative regulation of planar cell polarity pathway involved in axis elongation (GO:2000041)
mRNA processing (GO:0006397)
positive regulation of DNA-directed DNA polymerase activity (GO:1900264)
negative regulation of canonical Wnt signaling pathway (GO:0090090)
regulation of neuron projection development (GO:0010975)
negative regulation of cell-matrix adhesion (GO:0001953)
male gonad development (GO:0008584)
negative regulation of mesodermal cell fate specification (GO:0042662)
cardiac left ventricle morphogenesis (GO:0003214)
negative regulation of dermatome development (GO:0061185)
proteoglycan metabolic process (GO:0006029)
Wnt signaling pathway (GO:0016055)
sclerotome development (GO:0061056)
negative regulation of osteoblast differentiation (GO:0045668)
outflow tract morphogenesis (GO:0003151)
positive regulation of RNA export from nucleus (GO:0046833)
positive regulation of canonical Wnt signaling pathway (GO:0090263)
establishment of planar polarity involved in neural tube closure (GO:0090177)
response to transforming growth factor beta (GO:0071559)
neural crest formation (GO:0014029)
cell-substrate adhesion (GO:0031589)
regulation of stem cell differentiation (GO:2000736)
G2/M transition of mitotic cell cycle (GO:0000086)
positive regulation of catenin import into nucleus (GO:0035413)
regulation of transcription, DNA-templated (GO:0006355)
positive regulation of oligodendrocyte differentiation (GO:0048714)
pituitary gland development (GO:0021983)
somatic stem cell population maintenance (GO:0035019)
digestive tract morphogenesis (GO:0048546)
Wnt signaling pathway, planar cell polarity pathway (GO:0060071)
Wnt signaling pathway involved in somitogenesis (GO:0090244)
glycosaminoglycan biosynthetic process (GO:0006024)
convergent extension involved in axis elongation (GO:0060028)
positive regulation of mesenchymal stem cell differentiation (GO:2000741)
cochlea morphogenesis (GO:0090103)
post-anal tail morphogenesis (GO:0036342)
regulation of macrophage migration inhibitory factor signaling pathway (GO:2000446)
positive regulation of mesenchymal stem cell proliferation (GO:1902462)
negative regulation of canonical Wnt signaling pathway involved in neural plate anterior/posterior pattern formation (GO:0060829)
signal clustering (GO:1990256)
negative regulation of serotonin uptake (GO:0051612)
neuron projection development (GO:0031175)
middle ear morphogenesis (GO:0042474)
condensed mesenchymal cell proliferation (GO:0072137)
positive regulation of anterior head development (GO:2000744)
tRNA export from nucleus (GO:0006409)
regulation of cell morphogenesis involved in differentiation (GO:0010769)
mitotic nuclear envelope disassembly (GO:0007077)
cellular response to BMP stimulus (GO:0071773)
regulation of stem cell division (GO:2000035)
negative regulation of cell migration (GO:0030336)
Enriched Up/Downregulated
Enriched Downregulated
Enriched Upregulated
Not Enriched
Reference
1 dpa
3 dpa
9 dpa
15 dpa
25 dpa
32 dpa
40 dpa
1 dpa vs 0 dpa
3 dpa vs 0 dpa
3 dpa vs 1 dpa
9 dpa vs 0 dpa
9 dpa vs 1 dpa
9 dpa vs 3 dpa
15 dpa vs 0 dpa
15 dpa vs 1 dpa
15 dpa vs 3 dpa
15 dpa vs 9 dpa
25 dpa vs 0 dpa
25 dpa vs 1 dpa
25 dpa vs 3 dpa
25 dpa vs 9 dpa
25 dpa vs 15 dpa
32 dpa vs 0 dpa
32 dpa vs 1 dpa
32 dpa vs 3 dpa
32 dpa vs 9 dpa
32 dpa vs 15 dpa
32 dpa vs 25 dpa
40 dpa vs 0 dpa
40 dpa vs 1 dpa
40 dpa vs 3 dpa
40 dpa vs 9 dpa
40 dpa vs 15 dpa
40 dpa vs 25 dpa
40 dpa vs 32 dpa

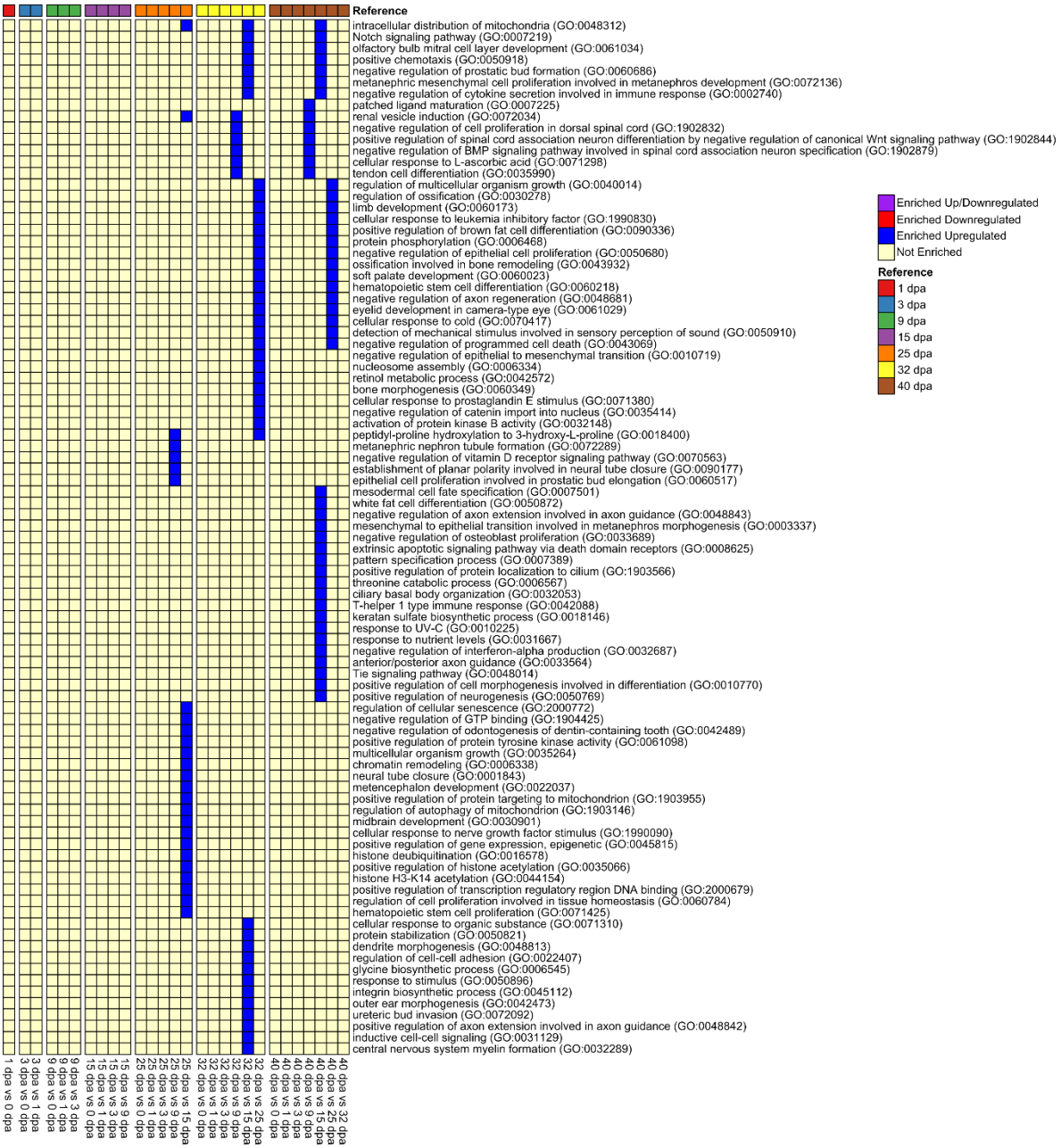
Reference
intracellular distribution of mitochondria (GO:0048312)
Notch signaling pathway (GO:0007219)
olfactory bulb mitral cell layer development (GO:0061034)
positive chemotaxis (GO:0050918)
negative regulation of prostatic bud formation (GO:0060686)
metanephric mesenchymal cell proliferation involved in metanephros development (GO:0072136)
negative regulation of cytokine secretion involved in immune response (GO:0002740)
patched ligand maturation (GO:0007225)
renal vesicle induction (GO:0072034)
negative regulation of cell proliferation in dorsal spinal cord (GO:1902832)
positive regulation of spinal cord association neuron differentiation by negative regulation of canonical Wnt signaling pathway (GO:1902844)
negative regulation of BMP signaling pathway involved in spinal cord association neuron specification (GO:1902879)
cellular response to L-ascorbic acid (GO:0071298)
tendon cell differentiation (GO:0035990)
regulation of multicellular organism growth (GO:0040014)
regulation of ossification (GO:0030278)
limb development (GO:0060173)
cellular response to leukemia inhibitory factor (GO:1990830)
positive regulation of brown fat cell differentiation (GO:0090336)
protein phosphorylation (GO:0006468)
negative regulation of epithelial cell proliferation (GO:0050680)
ossification involved in bone remodeling (GO:0043932)
soft palate development (GO:0060023)
hematopoietic stem cell differentiation (GO:0060218)
negative regulation of axon regeneration (GO:0048681)
eyelid development in camera-type eye (GO:0061029)
cellular response to cold (GO:0070417)
detection of mechanical stimulus involved in sensory perception of sound (GO:0050910)
negative regulation of programmed cell death (GO:0043069)
negative regulation of epithelial to mesenchymal transition (GO:0010719)
nucleosome assembly (GO:0006334)
retinol metabolic process (GO:0042572)
bone morphogenesis (GO:0060349)
cellular response to prostaglandin E stimulus (GO:0071380)
negative regulation of catenin import into nucleus (GO:0035414)
activation of protein kinase B activity (GO:0032148)
peptidyl-proline hydroxylation to 3-hydroxy-L-proline (GO:0018400)
metanephric nephron tubule formation (GO:0072289)
negative regulation of vitamin D receptor signaling pathway (GO:0070563)
establishment of planar polarity involved in neural tube closure (GO:0090177)
epithelial cell proliferation involved in prostatic bud elongation (GO:0060517)
mesodermal cell fate specification (GO:0007501)
white fat cell differentiation (GO:0050872)
negative regulation of axon extension involved in axon guidance (GO:0048843)
mesenchymal to epithelial transition involved in metanephros morphogenesis (GO:0003337)
negative regulation of osteoblast proliferation (GO:0033689)
extrinsic apoptotic signaling pathway via death domain receptors (GO:0008625)
pattern specification process (GO:0007389)
positive regulation of protein localization to cilium (GO:1903566)
threonine catabolic process (GO:0006567)
ciliary basal body organization (GO:0032053)
T-helper 1 type immune response (GO:0042088)
keratan sulfate biosynthetic process (GO:0018146)
response to UV-C (GO:0010225)
response to nutrient levels (GO:0031667)
negative regulation of interferon-alpha production (GO:0032687)
anterior/posterior axon guidance (GO:0033564)
Tie signaling pathway (GO:0048014)
positive regulation of cell morphogenesis involved in differentiation (GO:0010770)
positive regulation of neurogenesis (GO:0050769)
regulation of cellular senescence (GO:2000772)
negative regulation of GTP binding (GO:1904425)
negative regulation of odontogenesis of dentin-containing tooth (GO:0042489)
positive regulation of protein tyrosine kinase activity (GO:0061098)
multicellular organism growth (GO:0035264)
chromatin remodeling (GO:0006338)
neural tube closure (GO:0001843)
metencephalon development (GO:0022037)
positive regulation of protein targeting to mitochondrion (GO:1903955)
regulation of autophagy of mitochondrion (GO:1903146)
midbrain development (GO:0030901)
cellular response to nerve growth factor stimulus (GO:1990090)
positive regulation of gene expression, epigenetic (GO:0045815)
histone deubiquitination (GO:0016578)
positive regulation of histone acetylation (GO:0035066)
histone H3-K14 acetylation (GO:0044154)
positive regulation of transcription regulatory region DNA binding (GO:2000679)
regulation of cell proliferation involved in tissue homeostasis (GO:0060784)
hematopoietic stem cell proliferation (GO:0071425)
cellular response to organic substance (GO:0071310)
protein stabilization (GO:0050821)
dendrite morphogenesis (GO:0048813)
regulation of cell-cell adhesion (GO:0022407)
glycine biosynthetic process (GO:0006545)
response to stimulus (GO:0050896)
integrin biosynthetic process (GO:0045112)
outer ear morphogenesis (GO:0042473)
ureteric bud invasion (GO:0072092)
positive regulation of axon extension involved in axon guidance (GO:0048842)
inductive cell-cell signaling (GO:0031129)
central nervous system myelin formation (GO:0032289)
Enriched Up/Downregulated
Enriched Downregulated
Enriched Upregulated
Not Enriched
Reference
1 dpa
3 dpa
9 dpa
15 dpa
25 dpa
32 dpa
40 dpa
1 dpa vs 0 dpa
3 dpa vs 0 dpa
3 dpa vs 1 dpa
9 dpa vs 0 dpa
9 dpa vs 1 dpa
9 dpa vs 3 dpa
15 dpa vs 0 dpa
15 dpa vs 1 dpa
15 dpa vs 3 dpa
15 dpa vs 9 dpa
25 dpa vs 0 dpa
25 dpa vs 1 dpa
25 dpa vs 3 dpa
25 dpa vs 9 dpa
25 dpa vs 15 dpa
32 dpa vs 0 dpa
32 dpa vs 1 dpa
32 dpa vs 3 dpa
32 dpa vs 9 dpa
32 dpa vs 15 dpa
32 dpa vs 25 dpa
40 dpa vs 0 dpa
40 dpa vs 1 dpa
40 dpa vs 3 dpa
40 dpa vs 9 dpa
40 dpa vs 15 dpa
40 dpa vs 25 dpa
40 dpa vs 32 dpa

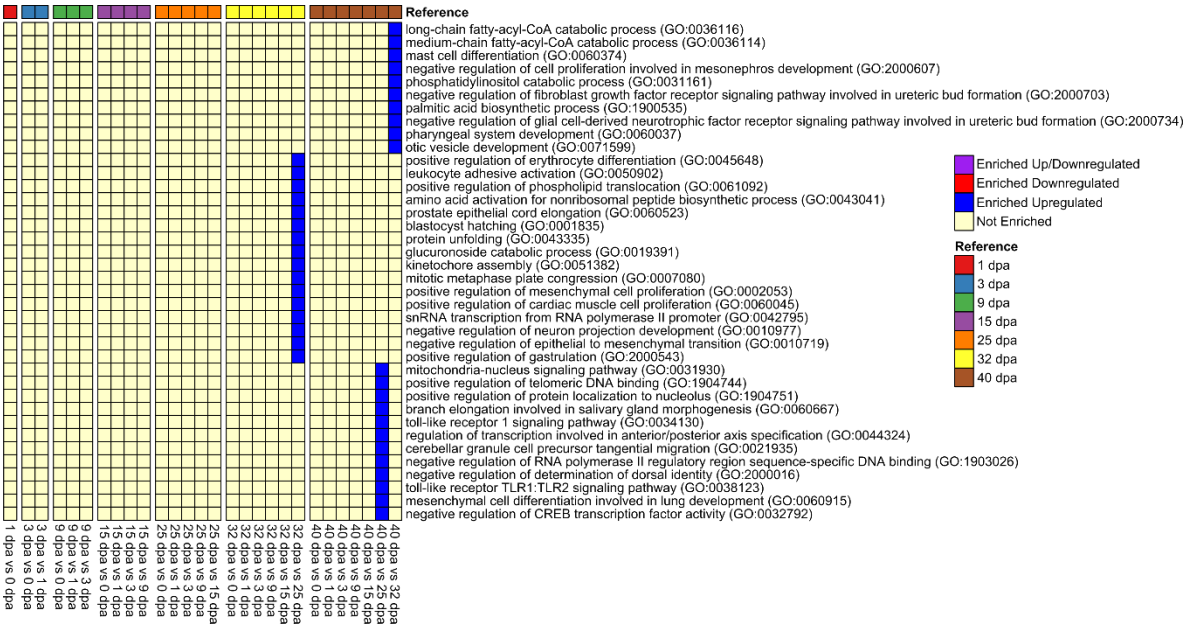
Reference
long-chain fatty-acyl-CoA catabolic process (GO:0036116)
medium-chain fatty-acyl-CoA catabolic process (GO:0036114)
mast cell differentiation (GO:0060374)
negative regulation of cell proliferation involved in mesonephros development (GO:2000607)
phosphatidylinositol catabolic process (GO:0031161)
negative regulation of fibroblast growth factor receptor signaling pathway involved in ureteric bud formation (GO:2000703)
palmitic acid biosynthetic process (GO:1900535)
negative regulation of glial cell-derived neurotrophic factor receptor signaling pathway involved in ureteric bud formation (GO:2000734)
pharyngeal system development (GO:0060037)
otic vesicle development (GO:0071599)
positive regulation of erythrocyte differentiation (GO:0045648)
leukocyte adhesive activation (GO:0050902)
positive regulation of phospholipid translocation (GO:0061092)
amino acid activation for nonribosomal peptide biosynthetic process (GO:0043041)
prostate epithelial cord elongation (GO:0060523)
blastocyst hatching (GO:0001835)
protein unfolding (GO:0043335)
glucuronoside catabolic process (GO:0019391)
kinetochore assembly (GO:0051382)
mitotic metaphase plate congression (GO:0007080)
positive regulation of mesenchymal cell proliferation (GO:0002053)
positive regulation of cardiac muscle cell proliferation (GO:0060045)
snRNA transcription from RNA polymerase II promoter (GO:0042795)
negative regulation of neuron projection development (GO:0010977)
negative regulation of epithelial to mesenchymal transition (GO:0010719)
positive regulation of gastrulation (GO:2000543)
mitochondria-nucleus signaling pathway (GO:0031930)
positive regulation of telomeric DNA binding (GO:1904744)
positive regulation of protein localization to nucleolus (GO:1904751)
branch elongation involved in salivary gland morphogenesis (GO:0060667)
toll-like receptor 1 signaling pathway (GO:0034130)
regulation of transcription involved in anterior/posterior axis specification (GO:0044324)
cerebellar granule cell precursor tangential migration (GO:0021935)
negative regulation of RNA polymerase II regulatory region sequence-specific DNA binding (GO:1903026)
negative regulation of determination of dorsal identity (GO:2000016)
toll-like receptor TLR1:TLR2 signaling pathway (GO:0038123)
mesenchymal cell differentiation involved in lung development (GO:0060915)
negative regulation of CREB transcription factor activity (GO:0032792)
1 dpa vs 0 dpa
3 dpa vs 0 dpa
3 dpa vs 1 dpa
9 dpa vs 0 dpa
9 dpa vs 1 dpa
9 dpa vs 3 dpa
15 dpa vs 0 dpa
15 dpa vs 1 dpa
15 dpa vs 3 dpa
15 dpa vs 9 dpa
25 dpa vs 0 dpa
25 dpa vs 1 dpa
25 dpa vs 3 dpa
25 dpa vs 9 dpa
25 dpa vs 15 dpa
32 dpa vs 0 dpa
32 dpa vs 1 dpa
32 dpa vs 3 dpa
32 dpa vs 9 dpa
32 dpa vs 15 dpa
32 dpa vs 25 dpa
40 dpa vs 0 dpa
40 dpa vs 1 dpa
40 dpa vs 3 dpa
40 dpa vs 9 dpa
40 dpa vs 15 dpa
40 dpa vs 25 dpa
40 dpa vs 32 dpa
Enriched Up/Downregulated
Enriched Downregulated
Enriched Upregulated
Not Enriched
Reference
1 dpa
3 dpa
9 dpa
15 dpa
25 dpa
32 dpa
40 dpa

10.3 KEGG enriched terms

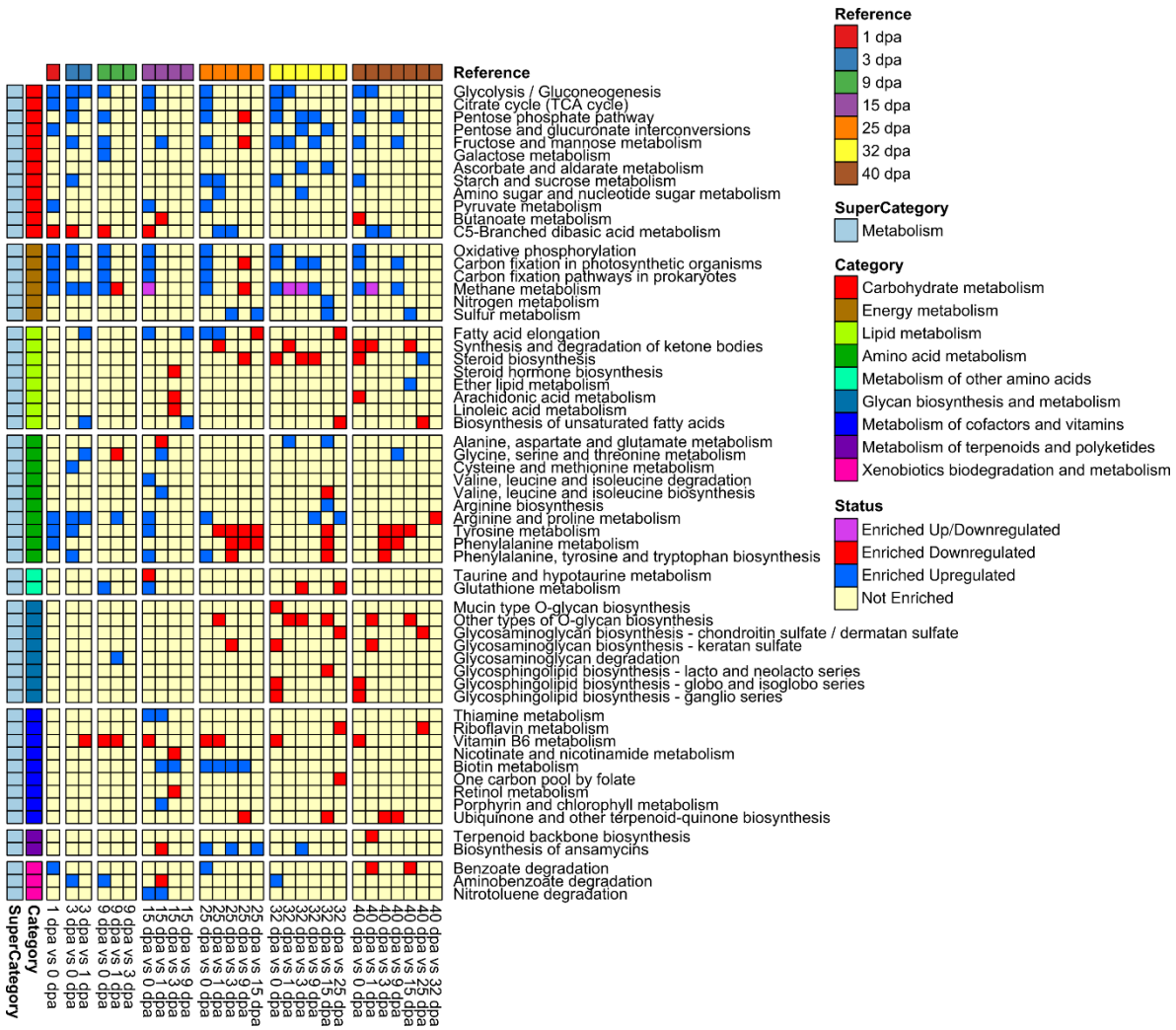

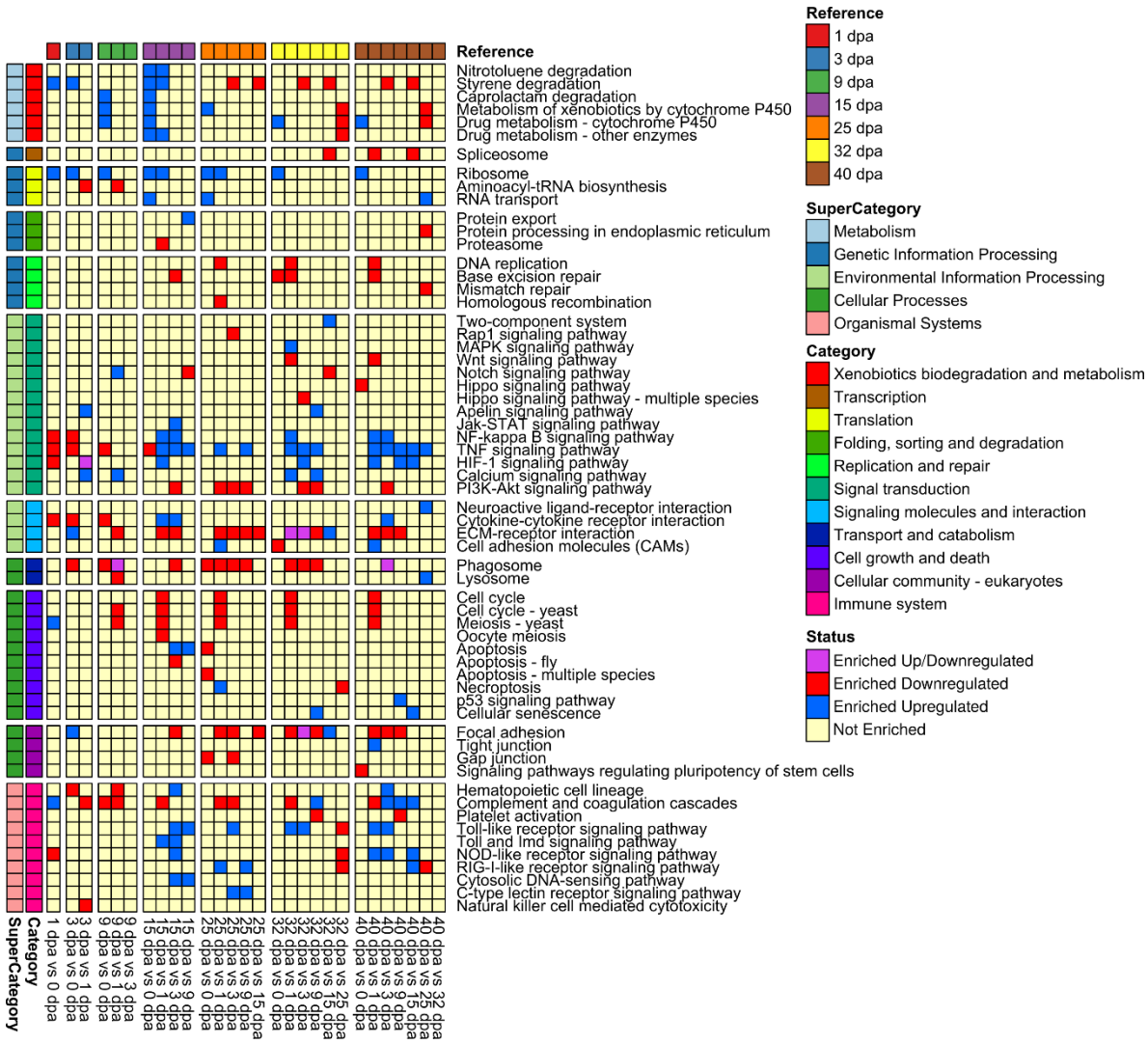
Reference
Nitrotoluene degradation
Styrene degradation
Caprolactam degradation
Metabolism of xenobiotics by cytochrome P450
Drug metabolism - cytochrome P450
Drug metabolism - other enzymes
Spliceosome
Ribosome
Aminoacyl-tRNA biosynthesis
RNA transport
Protein export
Protein processing in endoplasmic reticulum
Proteasome
DNA replication
Base excision repair
Mismatch repair
Homologous recombination
Two-component system
Rap1 signaling pathway
MAPK signaling pathway
Wnt signaling pathway
Notch signaling pathway
Hippo signaling pathway
Hippo signaling pathway - multiple species
Apelin signaling pathway
Jak-STAT signaling pathway
NF-kappa B signaling pathway
TNF signaling pathway
HIF-1 signaling pathway
Calcium signaling pathway
PI3K-Akt signaling pathway
Neuroactive ligand-receptor interaction
Cytokine-cytokine receptor interaction
ECM-receptor interaction
Cell adhesion molecules (CAMs)
Phagosome
Lysosome
Cell cycle
Cell cycle - yeast
Meiosis - yeast
Oocyte meiosis
Apoptosis
Apoptosis - fly
Apoptosis - multiple species
Necroptosis
p53 signaling pathway
Cellular senescence
Focal adhesion
Tight junction
Gap junction
Signaling pathways regulating pluripotency of stem cells
Hematopoietic cell lineage
Complement and coagulation cascades
Platelet activation
Toll-like receptor signaling pathway
Toll and Imd signaling pathway
NOD-like receptor signaling pathway
RIG-I-like receptor signaling pathway
Cytosolic DNA-sensing pathway
C-type lectin receptor signaling pathway
Natural killer cell mediated cytotoxicity
SuperCategory
Category
1 dpa vs 0 dpa
3 dpa vs 0 dpa
3 dpa vs 1 dpa
9 dpa vs 0 dpa
9 dpa vs 1 dpa
9 dpa vs 3 dpa
15 dpa vs 0 dpa
15 dpa vs 1 dpa
15 dpa vs 3 dpa
15 dpa vs 9 dpa
25 dpa vs 0 dpa
25 dpa vs 1 dpa
25 dpa vs 3 dpa
25 dpa vs 9 dpa
25 dpa vs 15 dpa
32 dpa vs 0 dpa
32 dpa vs 1 dpa
32 dpa vs 3 dpa
32 dpa vs 9 dpa
32 dpa vs 15 dpa
32 dpa vs 25 dpa
40 dpa vs 0 dpa
40 dpa vs 1 dpa
40 dpa vs 3 dpa
40 dpa vs 9 dpa
40 dpa vs 15 dpa
40 dpa vs 25 dpa
40 dpa vs 32 dpa
Reference
1 dpa
3 dpa
9 dpa
15 dpa
25 dpa
32 dpa
40 dpa
SuperCategory
Metabolism
Genetic Information Processing
Environmental Information Processing
Cellular Processes
Organismal Systems
Category
Xenobiotics biodegradation and metabolism
Transcription
Translation
Folding, sorting and degradation
Replication and repair
Signal transduction
Signaling molecules and interaction
Transport and catabolism
Cell growth and death
Cellular community - eukaryotes
Immune system
Status
Enriched Up/Downregulated
Enriched Downregulated
Enriched Upregulated
Not Enriched

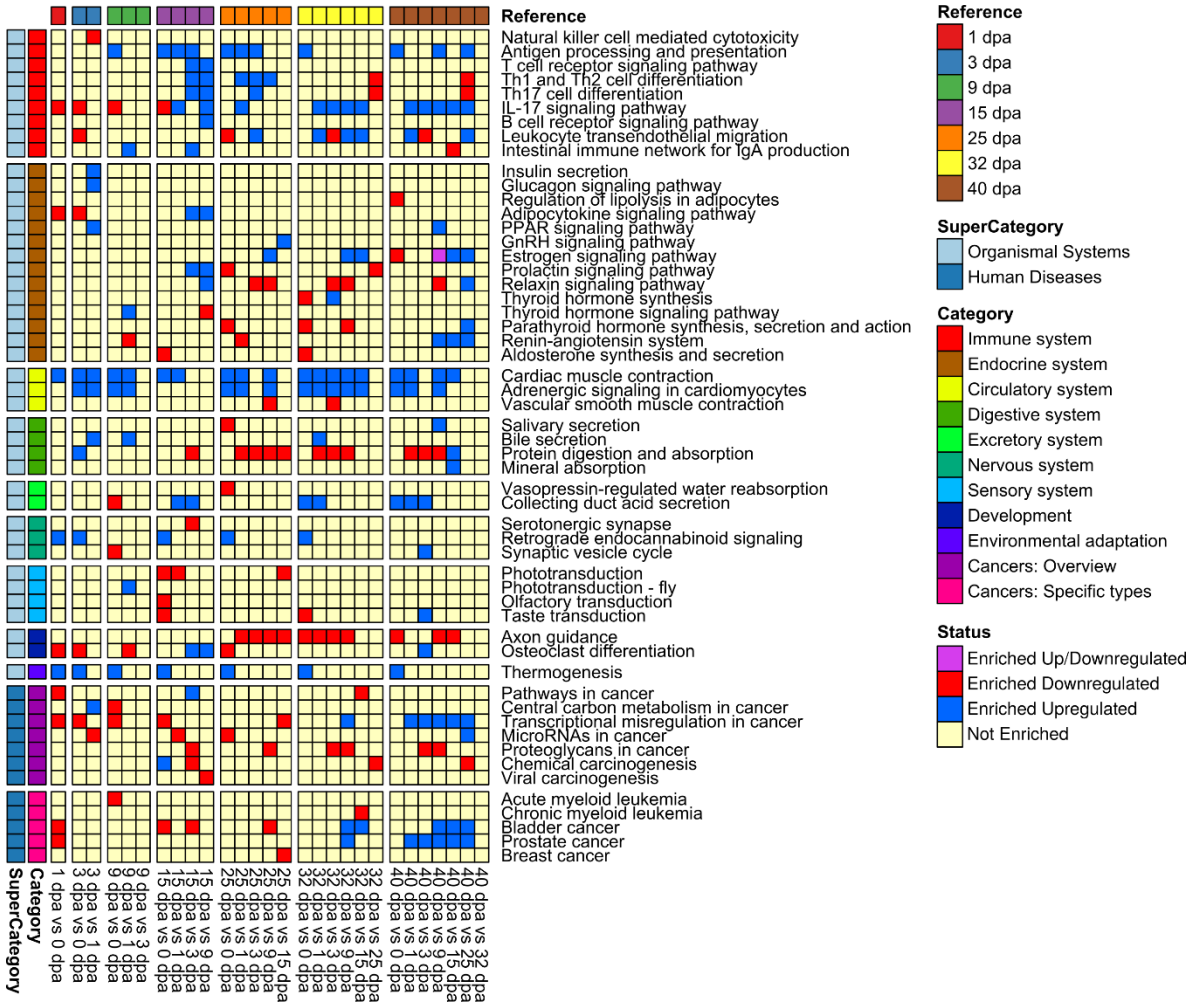
Reference
Natural killer cell mediated cytotoxicity
Antigen processing and presentation
T cell receptor signaling pathway
Th1 and Th2 cell differentiation
Th17 cell differentiation
IL-17 signaling pathway
B cell receptor signaling pathway
Leukocyte transendothelial migration
Intestinal immune network for IgA production
Insulin secretion
Glucagon signaling pathway
Regulation of lipolysis in adipocytes
Adipocytokine signaling pathway
PPAR signaling pathway
GnRH signaling pathway
Estrogen signaling pathway
Prolactin signaling pathway
Relaxin signaling pathway
Thyroid hormone synthesis
Thyroid hormone signaling pathway
Parathyroid hormone synthesis, secretion and action
Renin-angiotensin system
Aldosterone synthesis and secretion
Cardiac muscle contraction
Adrenergic signaling in cardiomyocytes
Vascular smooth muscle contraction
Salivary secretion
Bile secretion
Protein digestion and absorption
Mineral absorption
Vasopressin-regulated water reabsorption
Collecting duct acid secretion
Serotonergic synapse
Retrograde endocannabinoid signaling
Synaptic vesicle cycle
Phototransduction
Phototransduction - fly
Olfactory transduction
Taste transduction
Axon guidance
Osteoclast differentiation
Thermogenesis
Pathways in cancer
Central carbon metabolism in cancer
Transcriptional misregulation in cancer
MicroRNAs in cancer
Proteoglycans in cancer
Chemical carcinogenesis
Viral carcinogenesis
Acute myeloid leukemia
Chronic myeloid leukemia
Bladder cancer
Prostate cancer
Breast cancer
SuperCategory
Category
1 dpa vs 0 dpa
3 dpa vs 0 dpa
3 dpa vs 1 dpa
9 dpa vs 0 dpa
9 dpa vs 1 dpa
9 dpa vs 3 dpa
15 dpa vs 0 dpa
15 dpa vs 1 dpa
15 dpa vs 3 dpa
15 dpa vs 9 dpa
25 dpa vs 0 dpa
25 dpa vs 1 dpa
25 dpa vs 3 dpa
25 dpa vs 9 dpa
25 dpa vs 15 dpa
32 dpa vs 0 dpa
32 dpa vs 1 dpa
32 dpa vs 3 dpa
32 dpa vs 9 dpa
32 dpa vs 15 dpa
32 dpa vs 25 dpa
40 dpa vs 0 dpa
40 dpa vs 1 dpa
40 dpa vs 3 dpa
40 dpa vs 9 dpa
40 dpa vs 15 dpa
40 dpa vs 25 dpa
40 dpa vs 32 dpa
Reference
1 dpa
3 dpa
9 dpa
15 dpa
25 dpa
32 dpa
40 dpa
SuperCategory
Organismal Systems
Human Diseases
Category
Immune system
Endocrine system
Circulatory system
Digestive system
Excretory system
Nervous system
Sensory system
Development
Environmental adaptation
Cancers: Overview
Cancers: Specific types
Status
Enriched Up/Downregulated
Enriched Downregulated
Enriched Upregulated
Not Enriched

10.4 TF expression patterns

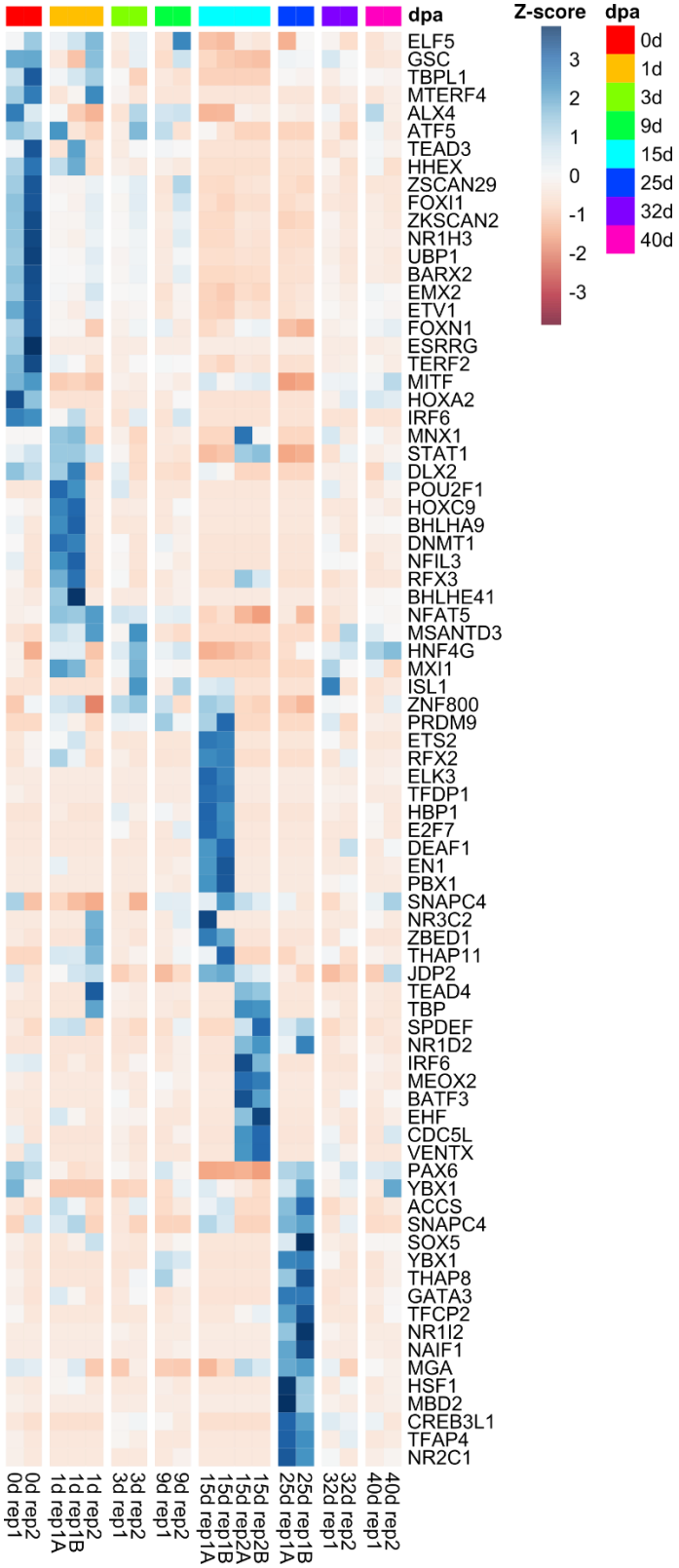

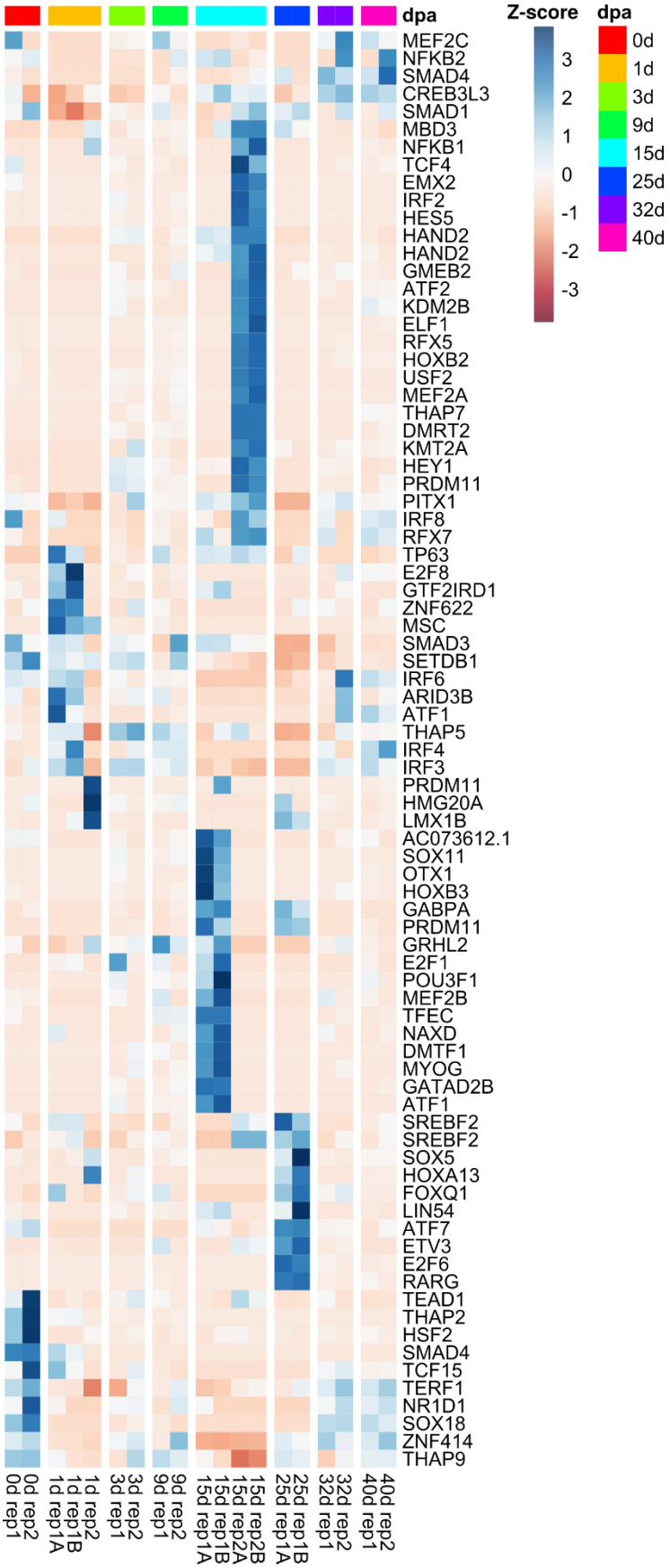
dpa
Z-score
dpa
3
2
1
0
-1
-2
-3
0d
1d
3d
9d
15d
25d
32d
40d
MEF2C
NFKB2
SMAD4
CREB3L3
SMAD1
MBD3
NFKB1
TCF4
EMX2
IRF2
HES5
HAND2
HAND2
GMEB2
ATF2
KDM2B
ELF1
RFX5
HOXB2
USF2
MEF2A
THAP7
DMRT2
KMT2A
HEY1
PRDM11
PITX1
IRF8
RFX7
TP63
E2F8
GTF2IRD1
ZNF622
MSC
SMAD3
SETDB1
IRF6
ARID3B
ATF1
THAP5
IRF4
IRF3
PRDM11
HMG20A
LMX1B
AC073612.1
SOX11
OTX1
HOXB3
GABPA
PRDM11
GRHL2
E2F1
POU3F1
MEF2B
TFEC
NAXD
DMTF1
MYOG
GATAD2B
ATF1
SREBF2
SREBF2
SOX5
HOXA13
FOXQ1
LIN54
ATF7
ETV3
E2F6
RARG
TEAD1
THAP2
HSF2
SMAD4
TCF15
TERF1
NR1D1
SOX18
ZNF414
THAP9
0d rep2
0d rep1
1d rep1A
1d rep1B
1d rep2
3d rep1
3d rep2
9d rep1
9d rep2
15d rep1A
15d rep1B
15d rep2A
15d rep2B
25d rep1A
25d rep1B
32d rep1
32d rep2
40d rep1
40d rep2

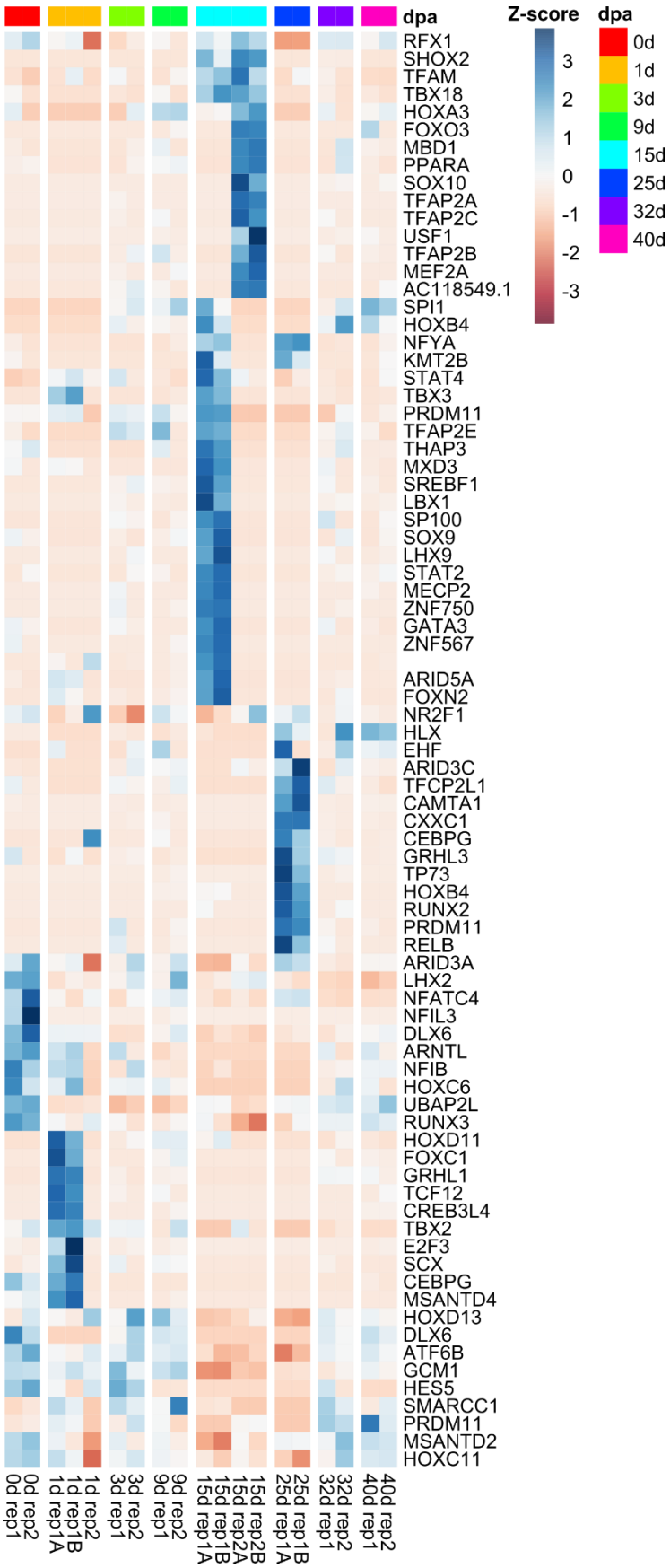
dpa
RFX1
SHOX2
TFAM
TBX18
HOXA3
FOXO3
MBD1
PPARA
SOX10
TFAP2A
TFAP2C
USF1
TFAP2B
MEF2A
AC118549.1
SPI1
HOXB4
NFYA
KMT2B
STAT4
TBX3
PRDM11
TFAP2E
THAP3
MXD3
SREBF1
LBX1
SP100
SOX9
LHX9
STAT2
MECP2
ZNF750
GATA3
ZNF567
ARID5A
FOXN2
NR2F1
HLX
EHF
ARID3C
TFCP2L1
CAMTA1
CXXC1
CEBPG
GRHL3
TP73
HOXB4
RUNX2
PRDM11
RELB
ARID3A
LHX2
NFATC4
NFIL3
DLX6
ARNTL
NFIB
HOXC6
UBAP2L
RUNX3
HOXD11
FOXC1
GRHL1
TCF12
CREB3L4
TBX2
E2F3
SCX
CEBPG
MSANTD4
HOXD13
DLX6
ATF6B
GCM1
HES5
SMARCC1
PRDM11
MSANTD2
HOXC11
0d rep1
0d rep2
1d rep1A
1d rep1B
1d rep2
3d rep1
3d rep2
9d rep1
9d rep2
15d rep1A
15d rep1B
15d rep2A
15d rep2B
25d rep1A
25d rep1B
32d rep1
32d rep2
40d rep1
40d rep2
Z-score
3
2
1
0
-1
-2
-3
dpa
0d
1d
3d
9d
15d
25d
32d
40d

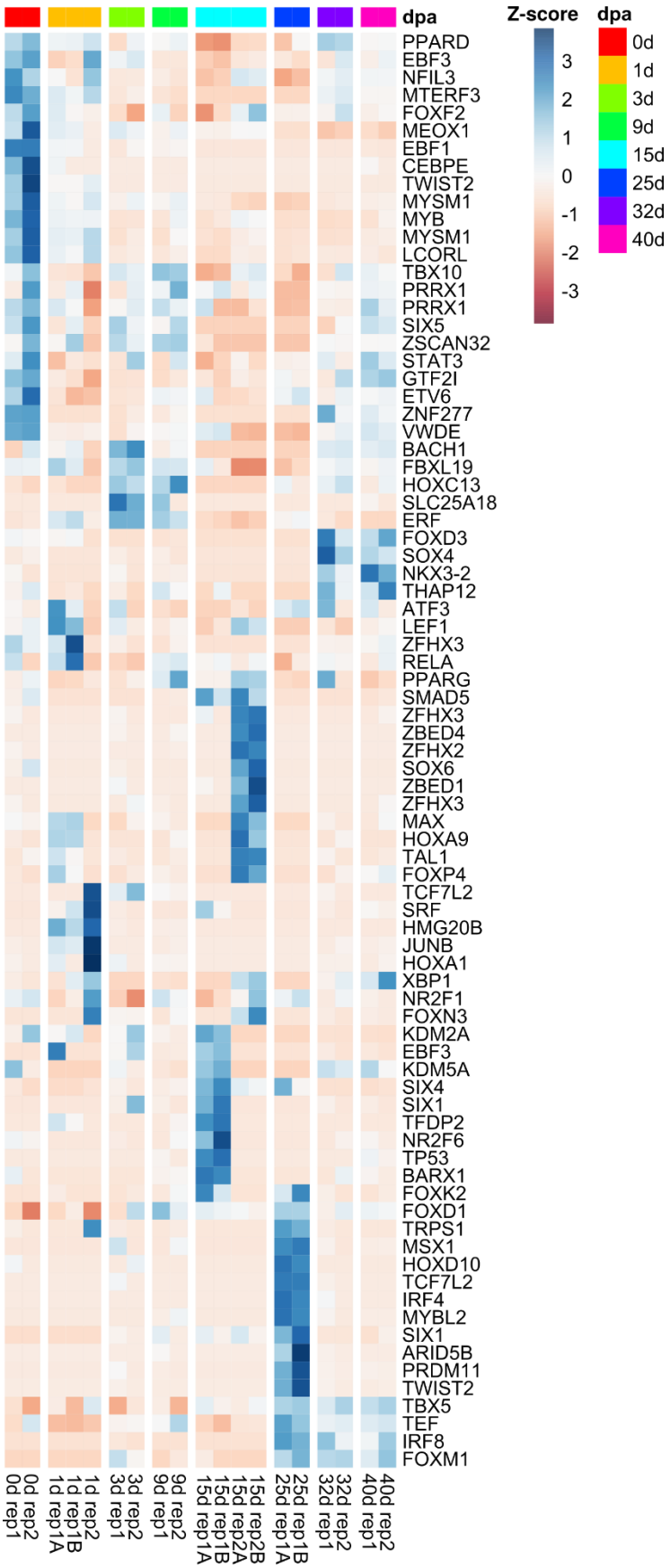
dpa
PPARD
EBF3
NFIL3
MTERF3
FOXF2
MEOX1
EBF1
CEBPE
TWIST2
MYSM1
MYB
MYSM1
LCORL
TBX10
PRRX1
PRRX1
SIX5
ZSCAN32
STAT3
GTF2I
ETV6
ZNF277
VWDE
BACH1
FBXL19
HOXC13
SLC25A18
ERF
FOXD3
SOX4
NKX3-2
THAP12
ATF3
LEF1
ZFHX3
RELA
PPARG
SMAD5
ZFHX3
ZBED4
ZFHX2
SOX6
ZBED1
ZFHX3
MAX
HOXA9
TAL1
FOXP4
TCF7L2
SRF
HMG20B
JUNB
HOXA1
XBP1
NR2F1
FOXN3
KDM2A
EBF3
KDM5A
SIX4
SIX1
TFDP2
NR2F6
TP53
BARX1
FOXK2
FOXD1
TRPS1
MSX1
HOXD10
TCF7L2
IRF4
MYBL2
SIX1
ARID5B
PRDM11
TWIST2
TBX5
TEF
IRF8
FOXM1
0d rep2
0d rep1
1d rep2
1d rep1B
1d rep1A
3d rep2
3d rep1
9d rep2
9d rep1
15d rep2B
15d rep2A
15d rep1B
15d rep1A
25d rep1B
25d rep1A
32d rep2
32d rep1
40d rep2
40d rep1
Z-score
3
2
1
0
-1
-2
-3
dpa
0d
1d
3d
9d
15d
25d
32d
40d

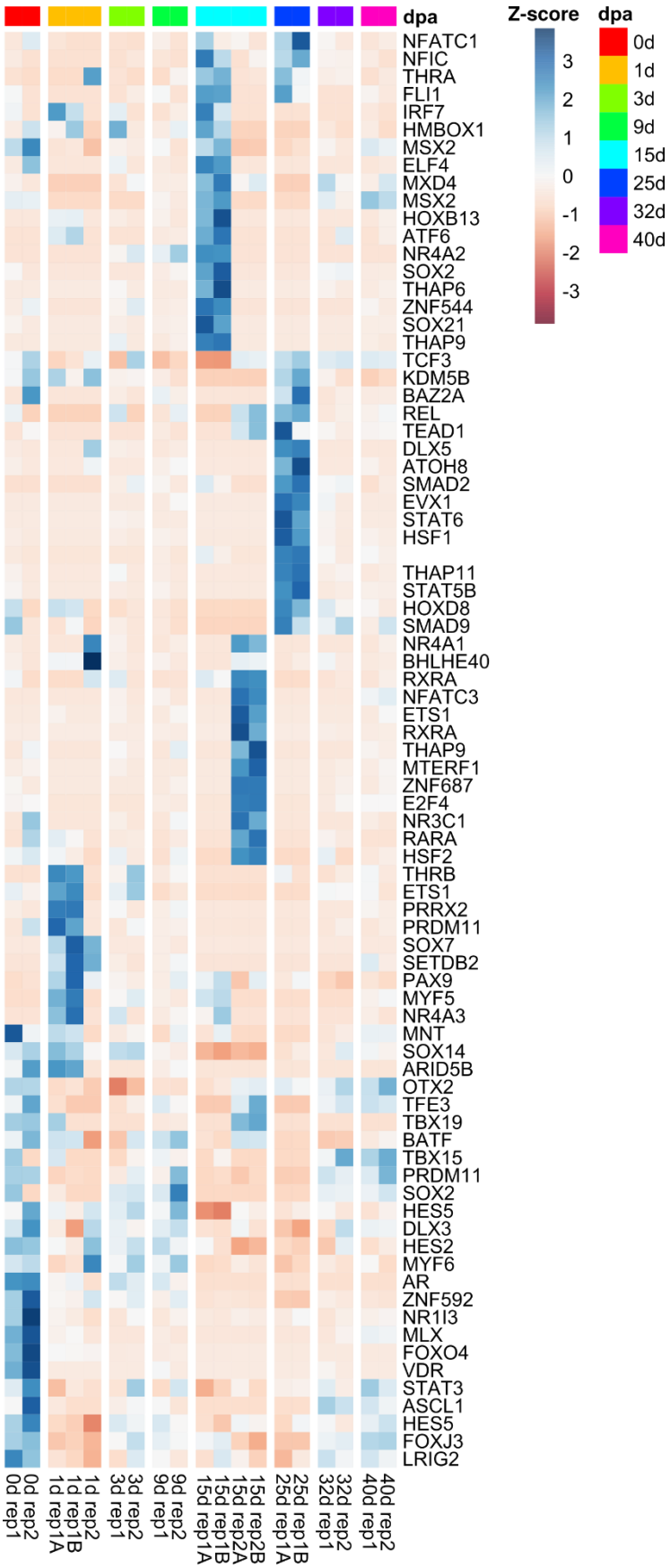
dpa
NFATC1
NFIC
THRA
FLI1
IRF7
HMBOX1
MSX2
ELF4
MXD4
MSX2
HOXB13
ATF6
NR4A2
SOX2
THAP6
ZNF544
SOX21
THAP9
TCF3
KDM5B
BAZ2A
REL
TEAD1
DLX5
ATOH8
SMAD2
EVX1
STAT6
HSF1
THAP11
STAT5B
HOXD8
SMAD9
NR4A1
BHLHE40
RXRA
NFATC3
ETS1
RXRA
THAP9
MTERF1
ZNF687
E2F4
NR3C1
RARA
HSF2
THRB
ETS1
PRRX2
PRDM11
SOX7
SETDB2
PAX9
MYF5
NR4A3
MNT
SOX14
ARID5B
OTX2
TFE3
TBX19
BATF
TBX15
PRDM11
SOX2
HES5
DLX3
HES2
MYF6
AR
ZNF592
NR1I3
MLX
FOXO4
VDR
STAT3
ASCL1
HES5
FOXJ3
LRIG2
0d rep1
0d rep2
1d rep1A
1d rep1B
1d rep2
3d rep1
3d rep2
9d rep1
9d rep2
15d rep1A
15d rep1B
15d rep2A
15d rep2B
25d rep1A
25d rep1B
32d rep1
32d rep2
40d rep1
40d rep2
Z-score
3
2
1
0
-1
-2
-3
dpa
0d
1d
3d
9d
15d
25d
32d
40d

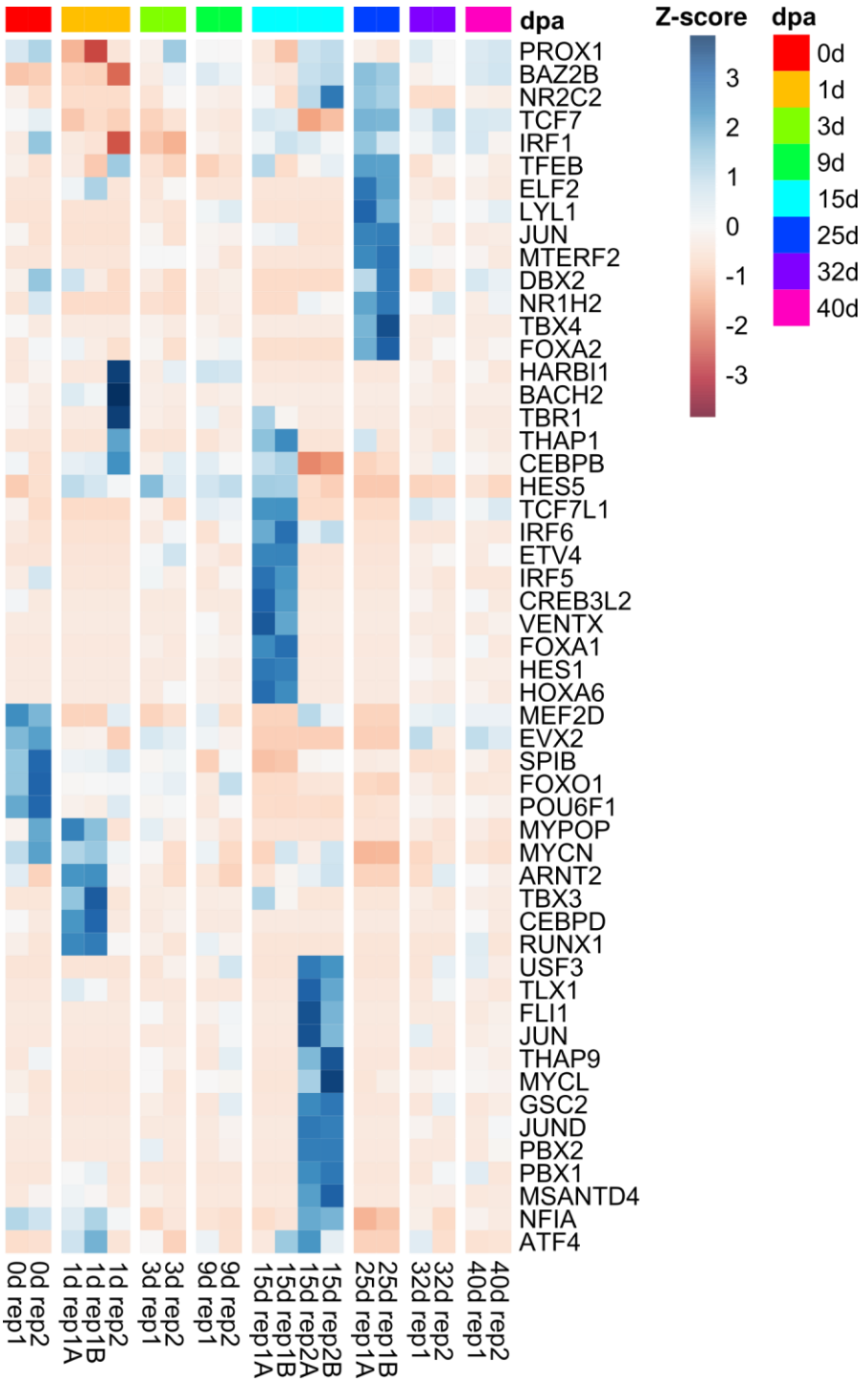
dpa
PROX1
BAZ2B
NR2C2
TCF7
IRF1
TFEB
ELF2
LYL1
JUN
MTERF2
DBX2
NR1H2
TBX4
FOXA2
HARBI1
BACH2
TBR1
THAP1
CEBPB
HES5
TCF7L1
IRF6
ETV4
IRF5
CREB3L2
VENTX
FOXA1
HES1
HOXA6
MEF2D
EVX2
SPIB
FOXO1
POU6F1
MYPOP
MYCN
ARNT2
TBX3
CEBPD
RUNX1
USF3
TLX1
FLI1
JUN
THAP9
MYCL
GSC2
JUND
PBX2
PBX1
MSANTD4
NFIA
ATF4
0d rep1
0d rep2
1d rep1A
1d rep1B
1d rep2
3d rep1
3d rep2
9d rep1
9d rep2
15d rep1A
15d rep1B
15d rep2A
15d rep2B
25d rep1A
25d rep1B
32d rep1
32d rep2
40d rep1
40d rep2
Z-score
3
2
1
0
-1
-2
-3
dpa
0d
1d
3d
9d
15d
25d
32d
40d

10.5 Stage Enriched Genes

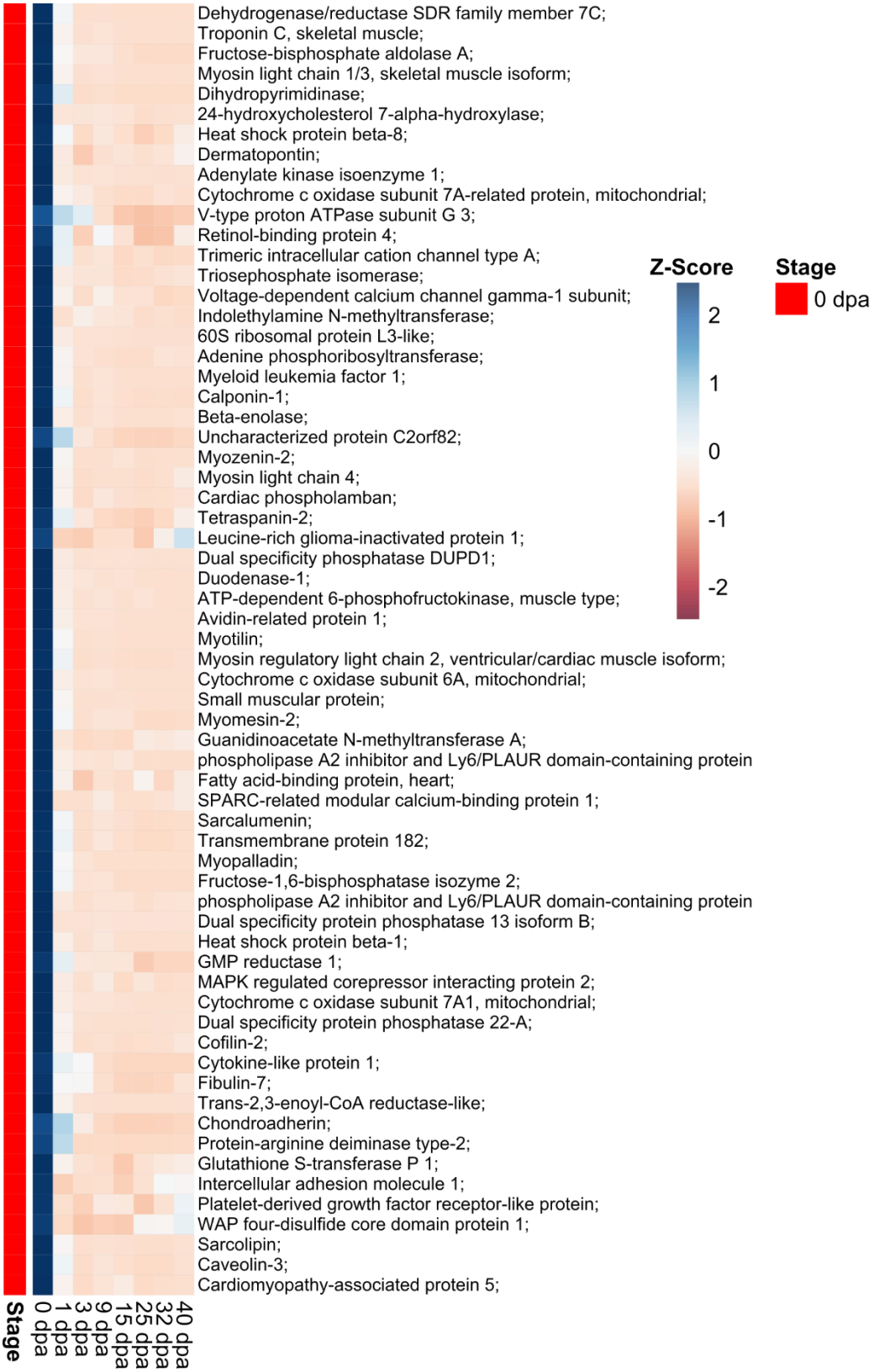

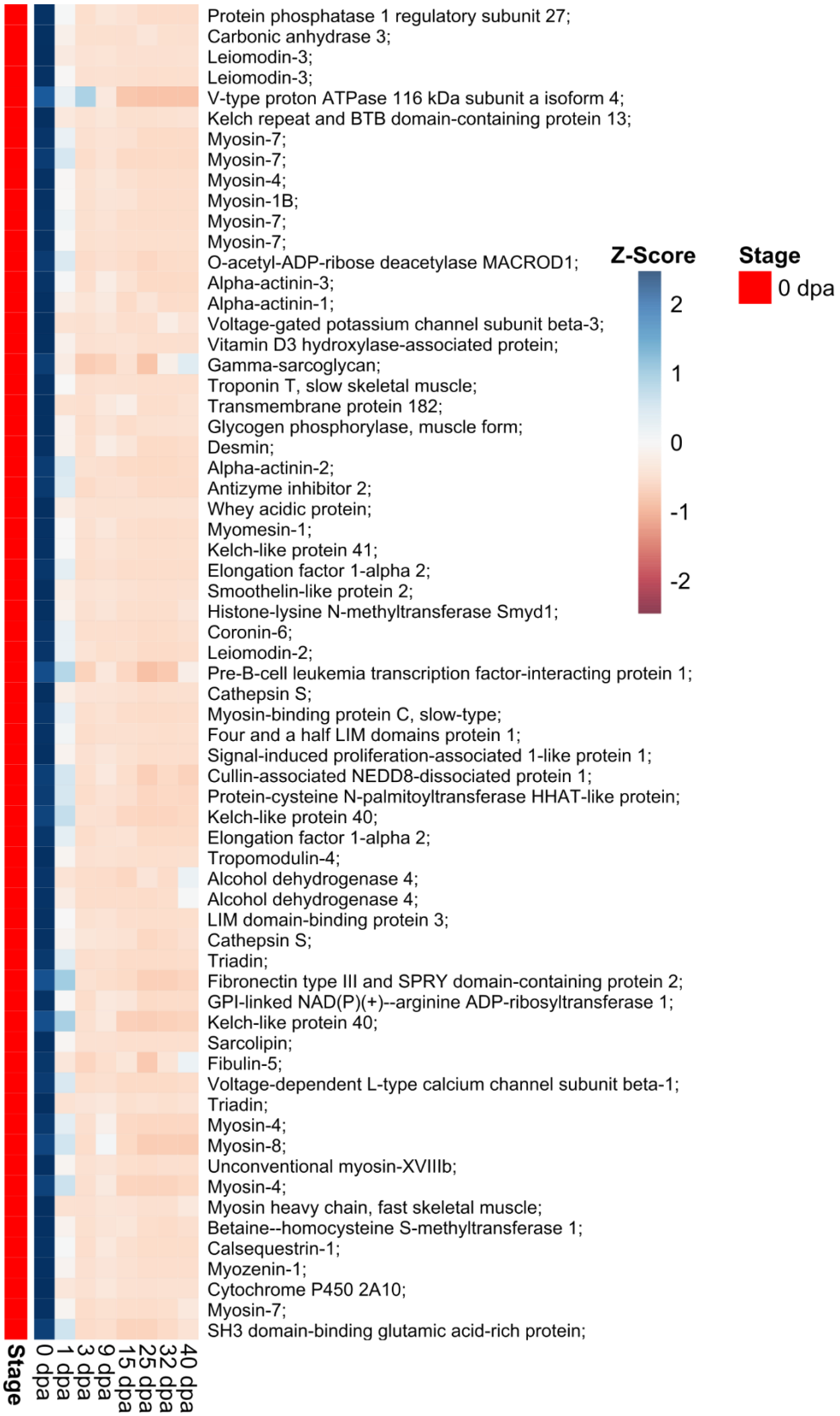
Protein phosphatase 1 regulatory subunit 27;
Carbonic anhydrase 3;
Leiomodin-3;
Leiomodin-3;
V-type proton ATPase 116 kDa subunit a isoform 4;
Kelch repeat and BTB domain-containing protein 13;
Myosin-7;
Myosin-7;
Myosin-4;
Myosin-1B;
Myosin-7;
Myosin-7;
O-acetyl-ADP-ribose deacetylase MACROD1;
Alpha-actinin-3;
Alpha-actinin-1;
Voltage-gated potassium channel subunit beta-3;
Vitamin D3 hydroxylase-associated protein;
Gamma-sarcoglycan;
Troponin T, slow skeletal muscle;
Transmembrane protein 182;
Glycogen phosphorylase, muscle form;
Desmin;
Alpha-actinin-2;
Antizyme inhibitor 2;
Whey acidic protein;
Myomesin-1;
Kelch-like protein 41;
Elongation factor 1-alpha 2;
Smoothelin-like protein 2;
Histone-lysine N-methyltransferase Smyd1;
Coronin-6;
Leiomodin-2;
Pre-B-cell leukemia transcription factor-interacting protein 1;
Cathepsin S;
Myosin-binding protein C, slow-type;
Four and a half LIM domains protein 1;
Signal-induced proliferation-associated 1-like protein 1;
Cullin-associated NEDD8-dissociated protein 1;
Protein-cysteine N-palmitoyltransferase HHAT-like protein;
Kelch-like protein 40;
Elongation factor 1-alpha 2;
Tropomodulin-4;
Alcohol dehydrogenase 4;
Alcohol dehydrogenase 4;
LIM domain-binding protein 3;
Cathepsin S;
Triadin;
Fibronectin type III and SPRY domain-containing protein 2;
GPI-linked NAD(P)(+)--arginine ADP-ribosyltransferase 1;
Kelch-like protein 40;
Sarcolipin;
Fibulin-5;
Voltage-dependent L-type calcium channel subunit beta-1;
Triadin;
Myosin-4;
Myosin-8;
Unconventional myosin-XVIIIb;
Myosin-4;
Myosin heavy chain, fast skeletal muscle;
Betaine--homocysteine S-methyltransferase 1;
Calsequestrin-1;
Myozenin-1;
Cytochrome P450 2A10;
Myosin-7;
SH3 domain-binding glutamic acid-rich protein;
Z-Score
2
1
0
-1
-2
Stage
0 dpa
Stage
0 dpa
1 dpa
3 dpa
9 dpa
15 dpa
25 dpa
32 dpa
40 dpa

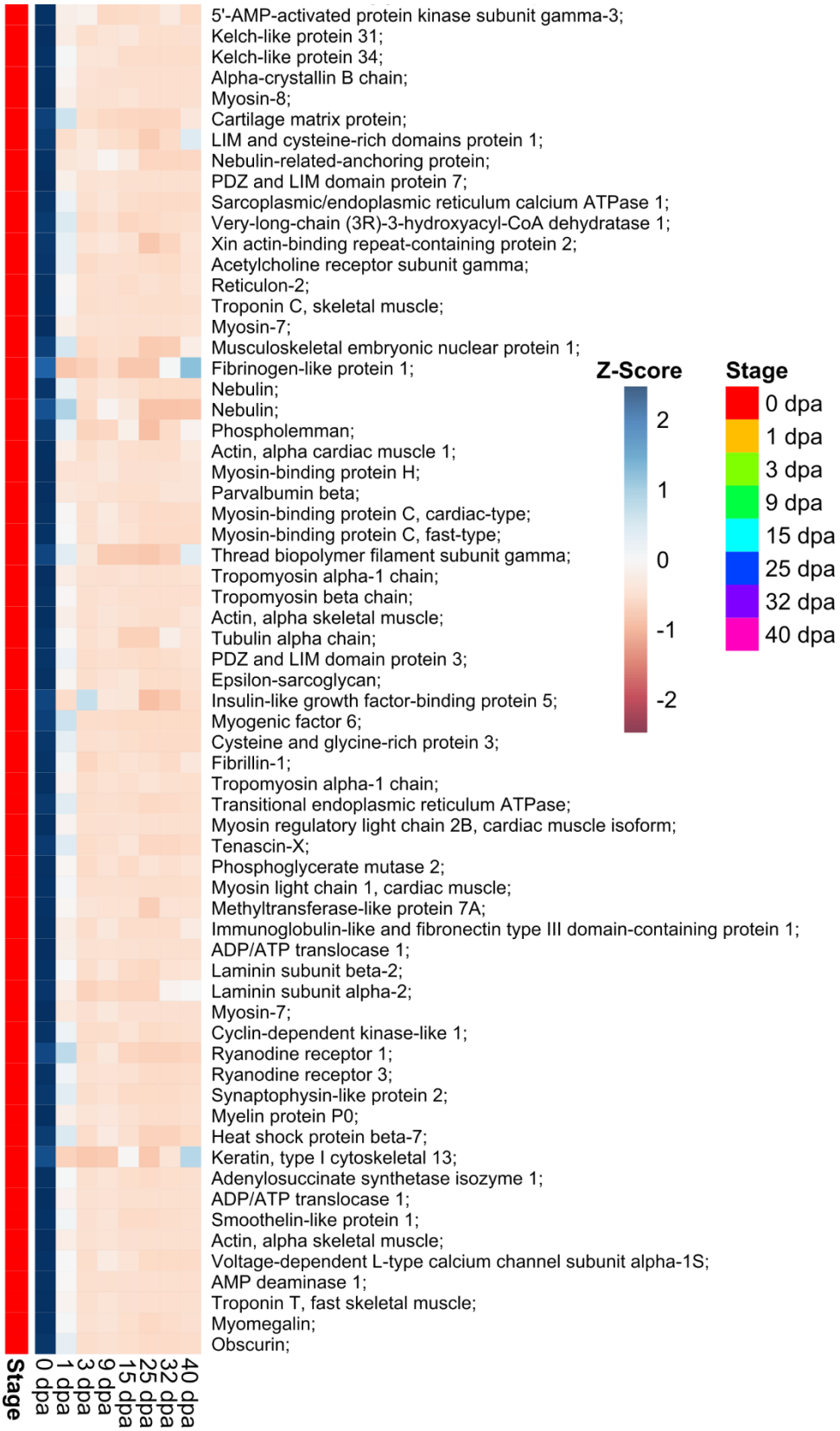
5'-AMP-activated protein kinase subunit gamma-3;
Kelch-like protein 31;
Kelch-like protein 34;
Alpha-crystallin B chain;
Myosin-8;
Cartilage matrix protein;
LIM and cysteine-rich domains protein 1;
Nebulin-related-anchoring protein;
PDZ and LIM domain protein 7;
Sarcoplasmic/endoplasmic reticulum calcium ATPase 1;
Very-long-chain (3R)-3-hydroxyacyl-CoA dehydratase 1;
Xin actin-binding repeat-containing protein 2;
Acetylcholine receptor subunit gamma;
Reticulon-2;
Troponin C, skeletal muscle;
Myosin-7;
Musculoskeletal embryonic nuclear protein 1;
Fibrinogen-like protein 1;
Nebulin;
Nebulin;
Phospholemman;
Actin, alpha cardiac muscle 1;
Myosin-binding protein H;
Parvalbumin beta;
Myosin-binding protein C, cardiac-type;
Myosin-binding protein C, fast-type;
Thread biopolymer filament subunit gamma;
Tropomyosin alpha-1 chain;
Tropomyosin beta chain;
Actin, alpha skeletal muscle;
Tubulin alpha chain;
PDZ and LIM domain protein 3;
Epsilon-sarcoglycan;
Insulin-like growth factor-binding protein 5;
Myogenic factor 6;
Cysteine and glycine-rich protein 3;
Fibrillin-1;
Tropomyosin alpha-1 chain;
Transitional endoplasmic reticulum ATPase;
Myosin regulatory light chain 2B, cardiac muscle isoform;
Tenascin-X;
Phosphoglycerate mutase 2;
Myosin light chain 1, cardiac muscle;
Methyltransferase-like protein 7A;
Immunoglobulin-like and fibronectin type III domain-containing protein 1;
ADP/ATP translocase 1;
Laminin subunit beta-2;
Laminin subunit alpha-2;
Myosin-7;
Cyclin-dependent kinase-like 1;
Ryanodine receptor 1;
Ryanodine receptor 3;
Synaptophysin-like protein 2;
Myelin protein P0;
Heat shock protein beta-7;
Keratin, type I cytoskeletal 13;
Adenylosuccinate synthetase isozyme 1;
ADP/ATP translocase 1;
Smoothelin-like protein 1;
Actin, alpha skeletal muscle;
Voltage-dependent L-type calcium channel subunit alpha-1S;
AMP deaminase 1;
Troponin T, fast skeletal muscle;
Myomegalin;
Obscurin;
Z-Score
2
1
0
-1
-2
Stage
0 dpa
1 dpa
3 dpa
9 dpa
15 dpa
25 dpa
32 dpa
40 dpa
Stage
0 dpa
1 dpa
3 dpa
9 dpa
15 dpa
25 dpa
32 dpa
40 dpa

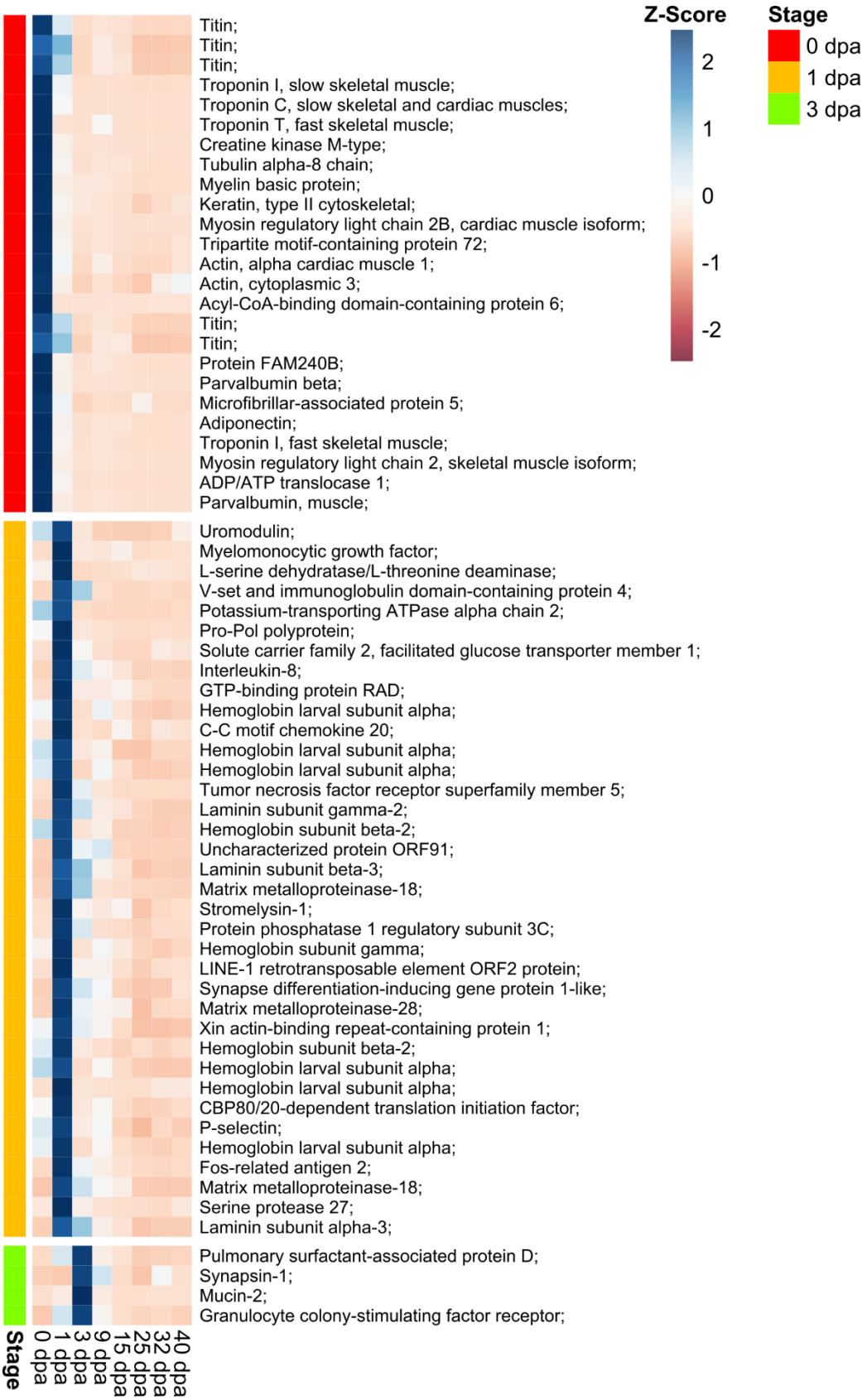
Z-Score
2
1
0
-1
-2
Stage
0 dpa
1 dpa
3 dpa
Titin;
Titin;
Titin;
Troponin I, slow skeletal muscle;
Troponin C, slow skeletal and cardiac muscles;
Troponin T, fast skeletal muscle;
Creatine kinase M-type;
Tubulin alpha-8 chain;
Myelin basic protein;
Keratin, type II cytoskeletal;
Myosin regulatory light chain 2B, cardiac muscle isoform;
Tripartite motif-containing protein 72;
Actin, alpha cardiac muscle 1;
Actin, cytoplasmic 3;
Acyl-CoA-binding domain-containing protein 6;
Titin;
Titin;
Protein FAM240B;
Parvalbumin beta;
Microfibrillar-associated protein 5;
Adiponectin;
Troponin I, fast skeletal muscle;
Myosin regulatory light chain 2, skeletal muscle isoform;
ADP/ATP translocase 1;
Parvalbumin, muscle;
Uromodulin;
Myelomonocytic growth factor;
L-serine dehydratase/L-threonine deaminase;
V-set and immunoglobulin domain-containing protein 4;
Potassium-transporting ATPase alpha chain 2;
Pro-Pol polyprotein;
Solute carrier family 2, facilitated glucose transporter member 1;
Interleukin-8;
GTP-binding protein RAD;
Hemoglobin larval subunit alpha;
C-C motif chemokine 20;
Hemoglobin larval subunit alpha;
Hemoglobin larval subunit alpha;
Tumor necrosis factor receptor superfamily member 5;
Laminin subunit gamma-2;
Hemoglobin subunit beta-2;
Uncharacterized protein ORF91;
Laminin subunit beta-3;
Matrix metalloproteinase-18;
Stromelysin-1;
Protein phosphatase 1 regulatory subunit 3C;
Hemoglobin subunit gamma;
LINE-1 retrotransposable element ORF2 protein;
Synapse differentiation-inducing gene protein 1-like;
Matrix metalloproteinase-28;
Xin actin-binding repeat-containing protein 1;
Hemoglobin subunit beta-2;
Hemoglobin larval subunit alpha;
Hemoglobin larval subunit alpha;
CBP80/20-dependent translation initiation factor;
P-selectin;
Hemoglobin larval subunit alpha;
Fos-related antigen 2;
Matrix metalloproteinase-18;
Serine protease 27;
Laminin subunit alpha-3;
Pulmonary surfactant-associated protein D;
Synapsin-1;
Mucin-2;
Granulocyte colony-stimulating factor receptor;
Stage
0 dpa
1 dpa
3 dpa
9 dpa
15 dpa
25 dpa
32 dpa
40 dpa

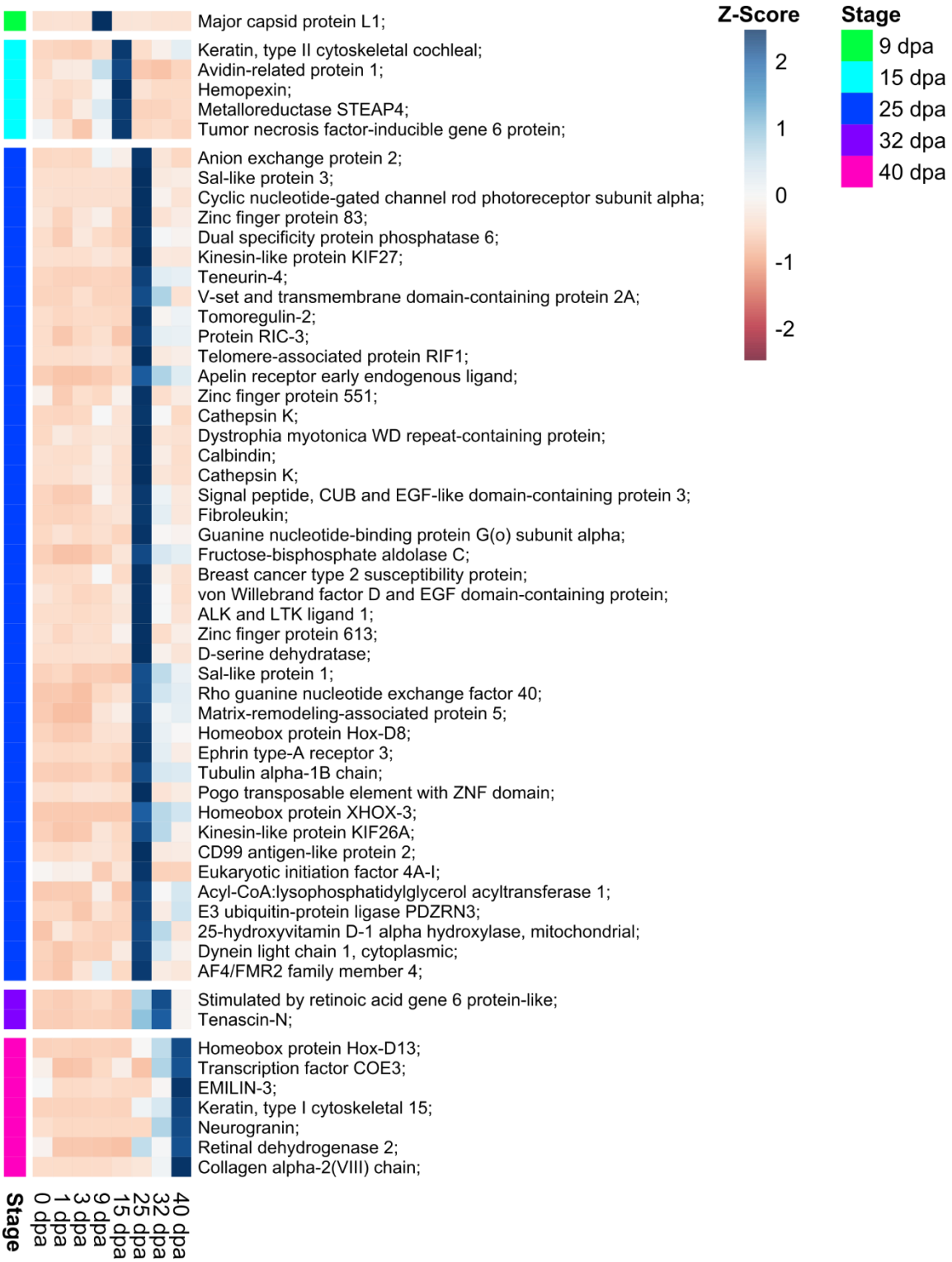
Major capsid protein L1;
Keratin, type II cytoskeletal cochleal;
Avidin-related protein 1;
Hemopexin;
Metalloreductase STEAP4;
Tumor necrosis factor-inducible gene 6 protein;
Anion exchange protein 2;
Sal-like protein 3;
Cyclic nucleotide-gated channel rod photoreceptor subunit alpha;
Zinc finger protein 83;
Dual specificity protein phosphatase 6;
Kinesin-like protein KIF27;
Teneurin-4;
V-set and transmembrane domain-containing protein 2A;
Tomoregulin-2;
Protein RIC-3;
Telomere-associated protein RIF1;
Apelin receptor early endogenous ligand;
Zinc finger protein 551;
Cathepsin K;
Dystrophia myotonica WD repeat-containing protein;
Calbindin;
Cathepsin K;
Signal peptide, CUB and EGF-like domain-containing protein 3;
Fibroleukin;
Guanine nucleotide-binding protein G(o) subunit alpha;
Fructose-bisphosphate aldolase C;
Breast cancer type 2 susceptibility protein;
von Willebrand factor D and EGF domain-containing protein;
ALK and LTK ligand 1;
Zinc finger protein 613;
D-serine dehydratase;
Sal-like protein 1;
Rho guanine nucleotide exchange factor 40;
Matrix-remodeling-associated protein 5;
Homeobox protein Hox-D8;
Ephrin type-A receptor 3;
Tubulin alpha-1B chain;
Pogo transposable element with ZNF domain;
Homeobox protein XHOX-3;
Kinesin-like protein KIF26A;
CD99 antigen-like protein 2;
Eukaryotic initiation factor 4A-I;
Acyl-CoA:lysophosphatidylglycerol acyltransferase 1;
E3 ubiquitin-protein ligase PDZRN3;
25-hydroxyvitamin D-1 alpha hydroxylase, mitochondrial;
Dynein light chain 1, cytoplasmic;
AF4/FMR2 family member 4;
Stimulated by retinoic acid gene 6 protein-like;
Tenascin-N;
Homeobox protein Hox-D13;
Transcription factor COE3;
EMILIN-3;
Keratin, type I cytoskeletal 15;
Neurogranin;
Retinal dehydrogenase 2;
Collagen alpha-2(VIII) chain;
Stage
0 dpa
1 dpa
3 dpa
9 dpa
15 dpa
25 dpa
32 dpa
40 dpa
Z-Score
2
1
0
-1
-2
Stage
9 dpa
15 dpa
25 dpa
32 dpa
40 dpa